European Journal of Medicinal Chemistry 222 (2021) 113560

Contents lists available at ScienceDirect

European Journal of Medicinal Chemistry

journal homepage: http://www.elsevier.com/locate/ejmech

HTS-based discovery and optimization of novel positive allosteric modulators of the α7 nicotinic acetylcholine receptor

István Ledneczki [a, *], Anita Horváth [a], Pál Tapolcsányi [a], János Éles [a], Katalin Dudás Molnár [a], István Vágó [a], András Visegrády [b], László Kiss [b], Áron Szigetvári [c], János Kóti [c], Balázs Krámos [c], Sándor Mahó [a], Patrik Holm [d], Sándor Kolok [b], László Fodor [b], Márta Thán [b], Diána Kostyalik [b], Ottilia Balázs [b], Mónika Vastag [b], István Greiner [e], György Lévay [b], Balázs Lendvai [b], Zsolt Némethy [b]

[a] Department of Chemistry, Gedeon Richter Plc., Budapest, Hungary
[b] Pharmacological and Drug Safety Research, Gedeon Richter Plc., Budapest, Hungary
[c] Spectroscopic Research Department, Gedeon Richter Plc., Budapest, Hungary
[d] Orion Corporation, Turku, Finland
[e] Research Management, Gedeon Richter Plc., Budapest, Hungary

ARTICLE INFO

Article history:
Received 26 February 2021
Received in revised form
26 April 2021
Accepted 18 May 2021
Available online 29 May 2021

Keywords:
Alpha 7 nicotinic acetylcholine receptor
Positive allosteric modulation
High-throughput screening
Structure-activity relationship
Cognitive enhancement

ABSTRACT

HTS campaign of the corporate compound collection resulted in a novel, oxalic acid diamide scaffold of α7 nACh receptor positive allosteric modulators. During the hit expansion, several derivatives, such as **4**, **11**, **17** demonstrated not only high *in vitro* potency, but also *in vivo* efficacy in the mouse place recognition test. The advanced hit molecule **11** was further optimized by the elimination of the putatively mutagenic aromatic-amine building block that resulted in a novel, aminomethylindole compound family. The most balanced physico-chemical and pharmacological profile was found in case of compound **55.** Docking study revealed an intersubunit binding site to be the most probable for our compounds. **55** demonstrated favorable cognitive enhancing profile not only in scopolamine-induced amnesia (place recognition test in mice) but also in natural forgetting (novel object recognition test in rats). Compound **55** was, furthermore, active in a cognitive paradigm of high translational value, namely in the rat touch screen visual discrimination test. Therefore, **55** was selected as a lead compound for further optimization. Based on the obtained favorable results, the invented aminomethylindole cluster may provide a viable approach for cognitive enhancement through positive allosteric modulation of α7 nAChRs.

1. Introduction

Cognition is a highly complex function of the central nervous system (CNS). Acetylcholine (ACh) is essential for the proper functioning of various domains of cognition (*e.g.* memory, attention or executive processes such as cognitive control or flexibility). Cognitive impairment is prevalent in many neurological (*e.g.* Alzheimer's disease, Parkinson's disease) and psychiatric (*e.g.* schizophrenia, depression) diseases, as well as in general aging. Due to its central role in the cognitive processes, cholinergic neurotransmission was intensively investigated by academic and industrial research groups in the past two decades. Despite the increasing efforts, symptomatic treatment options for cognitive disturbances are still limited to acetylcholinesterase inhibitors (AChEi; *e.g.* donepezil, rivastigmine, galantamine) and the NMDA receptor antagonist memantine. ACh exerts its beneficial effects through the activation of cholinergic receptors. Two types of ACh receptors (muscarinic and nicotinic receptors) exist, as shown by the different agonist activities of muscarine and nicotine. Nicotinic ACh receptors (nAChRs) are pentameric ligand-gated ion channels formed by α- and β-subunits [1]. Various α- and β-subunit compositions result in distinct nAChR subtypes, the most predominant nAChR subtypes in the CNS being the heteromeric $(\alpha4)_2(\beta2)_3$ and the homomeric $(\alpha7)_5$ nAChRs [2]. The α7 nAChR is considered as the most common nicotinic receptor subtype in the rat [3] and human [4] brain, expressed in high densities in "areas of cognition", *e.g.* in

* Corresponding author.
E-mail address: ledneczki@richter.hu (I. Ledneczki).

https://doi.org/10.1016/j.ejmech.2021.113560
0223-5234/

the prefrontal cortex [5], hippocampus and various subcortical limbic structures [6,7]. Lower expression levels of α7 nAChRs were detected in the thalamic regions and basal ganglia [8,9]. α7 nAChRs occur pre-, post and extrasynaptically in various neuronal cells. Extrasynaptic localization of α7 nAChRs [10] may constitute the main target of nicotinic ligands arriving from the extracellular space [11]. However, ACh may also enter the synapse and activates synaptic nAChRs even at very low concentrations [12].

Activation of nAChRs yields local excitation of the host cells mainly by increasing the permeability for Ca^{2+} ions, which, in turn, leads to the modulation of key neurotransmitter levels [13]. Orthosteric agonists of the α7 nAChR bind to the conventional agonist binding site located at the interface between two adjacent subunits distinct from the transmembrane ion-channel pore [14]. Unique features of the α7 nAChR activation include the low probability of channel opening, fast activation kinetics, high permeability to Na^{+}, K^{+} and Ca^{2+} compared to other nAChR subtypes [15,16], as well as the extremely fast desensitization [17,18], which limits the efficacy of α7 nAChR agonists, and leads to reduced responsiveness (under extreme conditions, α7 nAChR agonists may even behave as antagonists). Suboptimal *in vivo* efficacy of ligands binding to the orthosteric site may well be attributed to desensitization. The problem of fast receptor inactivation and the limited agonist efficacy may be circumvented by using positive allosteric modulators (PAMs). In the absence of endogenous ligands, prototypical PAMs normally lack any intrinsic activity, however, they can enhance the effect of the orthosteric agonists. One extreme PAM phenotype (generally described as "Type I") predominantly affects the peak current upon α7 nAChR activation with little or no effect on desensitization kinetics [19,20] while the so called "Type II" PAMs modulate not only the peak current but also the speed of current decay due to the inhibition of desensitization [21]. This terminology proved to be as an oversimplification as several PAMs were described with intermediate characteristics. Positive modulation of α7 nAChRs has been shown to have cognitive benefits in various preclinical models [22,23]using both rodents [24,25] and non-human primates [26]. Agonists were investigated extensively in clinical trials [27,28]. Distribution of α7 nAChRs across brain areas associated with cognition and the association of CHRNA7 gene with inhibitory sensory gating deficit in schizophrenic patients suggest that nAChR activation may have benefits in the treatment of schizophrenia. Some clinical observations in the past two decades also point to this direction [29]. For representative structures, see Fig. 1 (see Refs. [20,21,23,30–40]).

In our previous paper [41] a scaffold hopping approach to identify α7 nAChR positive modulator compounds with procognitive potential was reported. Hereinafter we present the results of a separate approach based on new chemical starting points emerging from a high throughput screening (HTS) campaign. Modification of an initial HTS hit series resulted in an advanced chemotype, that, after further optimization, provided a novel, benzylic amine type of α7 nAChR positive modulator lead compound with improved physico-chemical characteristics, favorable *in vitro* properties and procognitive potential [42]. General formulas of the investigated chemotypes and the main phases of the optimization process can be seen in Fig. 2.

2. Results and discussion

2.1. Chemistry

2.1.1. The synthesis of new indole-amine intermediates *27e* and *22e*

Indolamine and aminomethyl-indole building blocks were purchased from commercially available sources or their synthesis was based either on the chemical literature (in case of **21**, **24**) or on newly invented synthetic methods (Scheme 1). Indolamine building blocks **22e** (6-fluoro-1-methyl-1*H*-indol-5-amine) and **27e** (3-fluoro-1-methyl-1*H*-pyrrolo[2,3-*b*]pyridin-5-amine) were synthesized according to newly invented synthetic methods depicted in Scheme 1. 6-Fluoro-1*H*-indole-2,3-dione (**22a**) was nitrated with the "mixed acid" system and subsequently in **22b** the dioxo functionality was reduced with borane-THF complex to obtain **22c**. Afterwards it was *N*-methylated and the nitro group of the resulting **22d** was reduced to amine moiety (**22e**). 5-Bromo-7-azaindole (**27a)** was fluorinated at position 3 with Selectfluor. The resulted 3-fluoroindole (**27b**) was *N*-methylated to obtain **27c**, which was then substituted with benzylamine to **27d** in a Buchwald-Hartwig reaction and finally the benzyl group was cleaved by catalytic hydrogenation to obtain **27e**.

2.1.2. The synthesis for secondary amine intermediates *5d*, *9c* and *10c*

In Scheme 2 the synthesis of the non-purchasable amine intermediates was exemplified in case of the azetidinemethyl intermediate **5d** (for compounds **5**–**8**, **44**, **48**–**55**). *tert*-Butyl 3-(hydroxymethyl)azetidine-1-carboxylate (**5a**) was mesylated (**5b**) and then reacted with *p*-cresol (**5c**) and finally the BOC protecting group was removed under acidic conditions to obtain the azetidinemethyl intermediate **5d**. The amine intermediates for the pyrrolidine (**6**), the azepane (**7**) and the azetidine (**8**) compounds were synthesized in an analogous way.

Piperidine and piperazine secondary amine intermediates (for compounds **1**–**4** and **11**) were purchased from commercially available sources. The syntheses of the non-purchasable **9c** and **10c** intermediates are depicted in Scheme 2. *N*-BOC-nortropine (**9a**) was arylated in a Mitsunobu reaction while **10a** was alkylated with 4-methylbenzyl bromide and in both cases the BOC protecting group was removed under acidic media resulting in derivatives **9c** or **10c**, respectively.

2.1.3. The synthesis of oxoacetic acid intermediates *11c*, *12d*, *13g*, *14b*, *15h*, *16b*, *17b* and *18e*

The synthesis of the oxoacetic acid intermediates was exemplified in the piperazine derivative **11c** depicted in Scheme 3. The amine intermediate **11a** was reacted with ethyl chlorooxoacetate to gain the oxoacetic ester derivative **11b**. It was then hydrolyzed under basic conditions to yield the oxoacid compound **11c**. This synthetic methodology was applied for the oxoacetic intermediates of compounds **1**–**11** and **19**–**30**.

Different syntheses of the oxoacetic acid intermediates for compounds **12**–**18** are also depicted in Scheme 3. 4-Piperidone (**12a**) was *N*-alkylated with 1-bromomethyl-4-methylbenzene and the resulted **12b** was added to a solution of NaH and ethyl isocyanoacetate yielding **12c**. It was subjected first to acidic and subsequently basic hydrolysis to obtain **12d**. 6-Methylpyridin-3-ol (**13a)** was reacted in a Mitsunobu reaction with cyclohexanol intermediate **13b**. The ester functionality in **13c** was hydrolyzed (**13d**), followed by the reaction with cyano-phosphorane reagent **13e**. The resulted **13f** cyanoketo phosphorane was heated with oxone to gain the methyl ester derivative **13g**. For the synthesis of **14b,** pyrazole was *N*-alkylated with *p*-chlorobenzyl bromide, then the formed intermediate **14a** was *C*-alkylated with ethyl 2-chloro-2-oxoacetate. The synthesis of **15h** started with the bromination of ethyl 2-aminothiazole-4-carboxylate (**15a**) in a Sandmeyer reaction. **15b** was reacted with 4-chlorophenol and the ester function of **15c** was reduced to aldehyde **15d** with DIBAL-H. Cyanohydrin **15e** was formed in the reaction with methylmorpholine-*N*-oxide and trimethylsilyl cyanide (TMSCN). The nitrile moiety in **15e** was subsequently hydrolyzed with cc. HCl to 2-hydroxycarboxylic acid derivative **15f**, which was then transformed to a methyl ester **15g**.

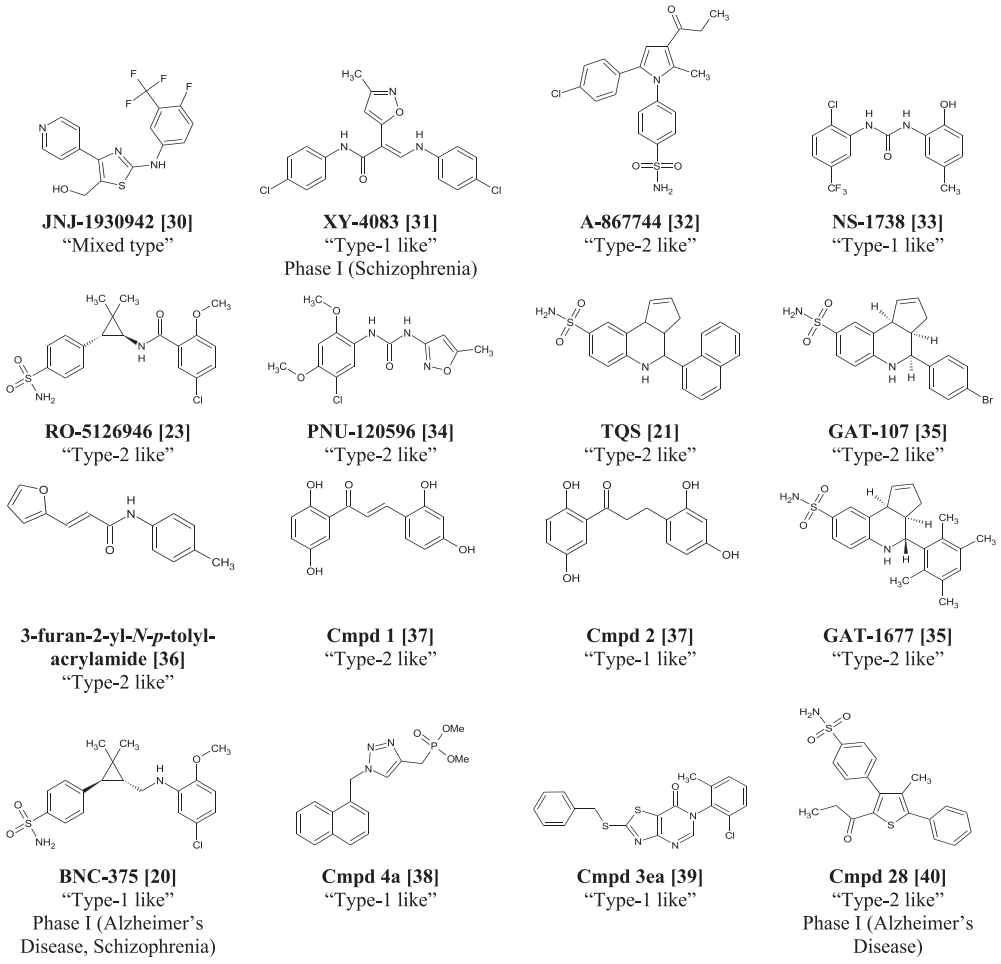

Fig. 1. Selected positive allosteric modulators of α7 nAChR with highly variable degree of inhibition of the agonist-evoked channel desensitization. If available, the clinical status and indication of the compounds are also indicated.

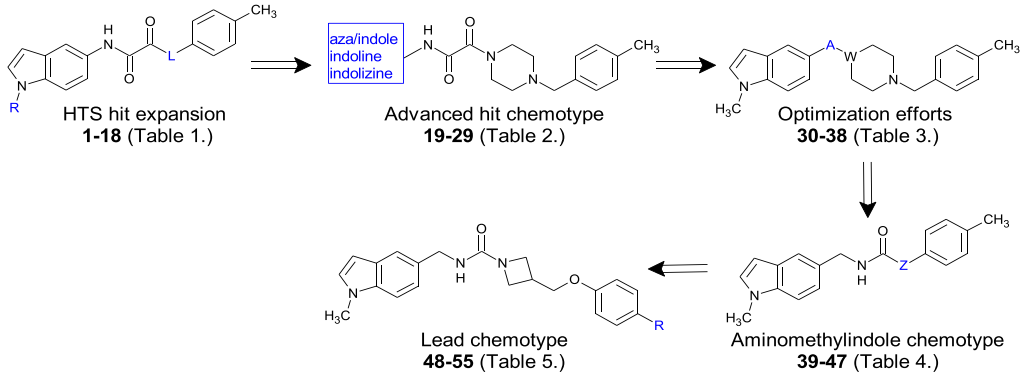

Fig. 2. The optimization process from the HTS hits to the Lead molecule with general and representative formulas of the investigated chemotypes.

Using Dess-Martin periodinane the desired 2-oxocarboxylic acid methyl ester **15h** was isolated. To have intermediate **16b**, **16a** was Friedel-Crafts acylated with ethylchlorooxoacetate, while in case of **17b,** the pyridine derivative **17a** was lithiated and then reacted with diethyloxalate to isolate **17b**. The necessary hydrolysis of **13g**, **14b**, **15h**, **16b** and **17b** was accomplished in an analogous way as described in case of **11c**. For the synthesis of **18e,** dibromopyrazine **18a** was reacted with *p*-cresol and then **18b** was further reacted with 1-ethoxy-1-(tributhylstannylethylene) (**18c)** using palladium catalysis to obtain the acetyl derivative **18d**. It was further oxidized with SeO_2 to yield the desired derivative.

*2.1.4. Amide couplings for the synthesis of oxalic acid diamide products (**1**–**30**)*

The applied four different methods for the amide coupling to obtain the desired, oxalic acid diamide final products (**1**–**30**) are shown in Scheme 4. The synthesis of compounds **1**–**4**, **9**–**12**, **17**–**20** was achieved in an analogous way as it was exemplified via the

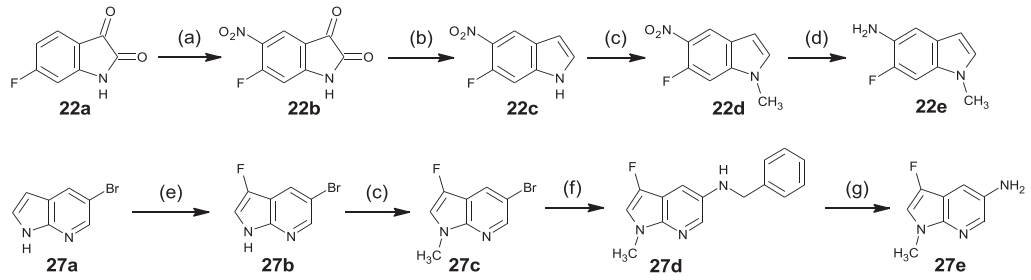

Scheme 1. The synthesis of non-purchasable, novel indole-amine intermediates **22e** and **27e**. Reagents and conditions: (a) $NaNO_3$, cc. H_2SO_4, 0 °C; (b) Borane-THF, THF, 0 °C to rt; (c) MeI, NaH, dry THF, 0 °C to rt.; (d) H_2, Pd/C, MeOH, rt (e) Selectfluor, MeCN, cc. CH_3COOH, 80 °C; (f) benzylamine, NaO*t*Bu, RuPhos, $Pd_2(dba)_3$, dry toluene, rfx.; (g) H_2, Pd/C, MeOH, EtOAc, rt.

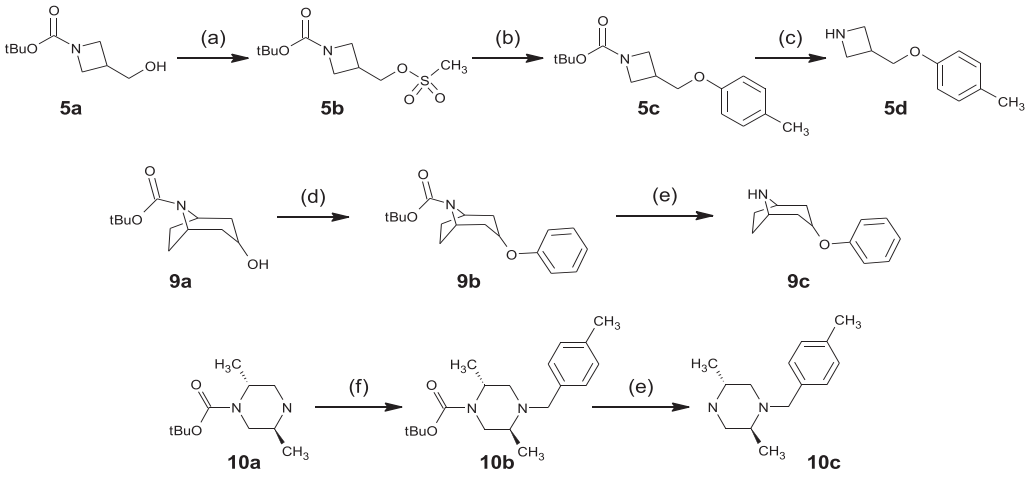

Scheme 2. The synthesis for secondary amine intermediates **5d**, **9c** and **10c**. Reagents and conditions: (a) methanesulfonyl chloride, Et_3N, CH_2Cl_2, rt.; (b) *p*-cresol, Cs_2CO_3, DMF, 110 °C; (c) TFA, CH_2Cl_2, 0 °C; (d) *p*-cresol, PPh_3, DIAD, THF, rt.; (e) HCl in 1,4-dioxane, 1,4-dioxane, rt; (f) 4-methylbenzyl bromide, MeCN, Et_3N, 0 °C to rt.

synthesis of **11**. Its oxoacetic acid intermediate **11c** was amidated with the corresponding indole-amine **11d** in the presence of 1-hydroxybenzotriazole hydrate (HOBt·H_2O) and of *N*-(3-dimethylaminopropyl)-*N*′-ethylcarbodiimide hydrochloride (EDC. HCl) with Et_3N base.

The synthesis of compounds **6**–**7**, **13**–**16**, **21**–**26**, **28**–**30** was achieved in an analogous way as it was exemplified by the synthesis of compound **23**. The corresponding aryl-amine (**23a**) and the oxoacetic acid derivative (**11c**) were reacted with the help of HATU (Hexafluorophosphate Azabenzotriazole Tetramethyl Uronium) coupling agent in the presence of DIPEA base.

Compounds **5** and **8** were synthesized starting from the indole-amine **11d**, which was amidated with ethyl oxalyl chloride and the isolated intermediate **8a** was hydrolyzed to **8b**. In this compound the newly formed carboxylic acid functionality was amidated with the corresponding azetidine or azetidinemethyl (**5d**) intermediates in the presence of HBTU (*N*,*N*,*N*′,*N*′-tetramethyl-*O*-(1*H*-benzotriazol-1-yl)uronium hexafluorophosphate) and Et_3N. For the synthesis of compound **27** intermediate **11c** was transformed into an acid chloride with 1-chloro-*N*,*N*,2-trimethyl-1-propenylamine (Ghosez's reagent) and the obtained activated derivative was coupled with indole-amine (**27e**).

*2.1.5. The syntheses of final compounds with modified linker region (**31**–**37**)*

The syntheses of compounds with modified linker region (**31**–**37**) are depicted in Scheme 5. In a Suzuki reaction, 3-bromo-2-propenoate **31a** was reacted with indoleboronic acid **31b** and the resulted **31c** was hydrolyzed under basic conditions to obtain **31d**. For the synthesis of compound **31** intermediates **31d** and **11a** were coupled with HATU/DIPEA system. Compound **32** was synthesized from indole-carbonitrile **32a**, which was first *N*-methylated to **32b** followed by conversion to carboxamide **32c** with H_2O_2 and then reacting with oxalyl chloride the crude benzoyl isocyanate derivative (**32d**) was yielded. Compound **32** was obtained in the reaction of **32d** with 4-(4-methylbenzyl)piperidine hydrochloride. Compound **33** was synthesized from indole-carboxylic acid **33a**, which was transformed to the ester **33b** which was then *N*-methylated with dimethyl sulphate. Intermediate **33c** was then converted to hydrazide **33d** and was further reacted with ethyl piperazine-oxoacetate **11b** to oxoacetohydrazide **33e** in the presence of HBTU as the coupling agent. The final compound **33** was yielded in a cyclization reaction of **33e** with thionyl chloride. The synthesis of compound **34** started with the condensation reaction of 5-acetylindole **34a** with diethyl oxalate and then **34b** was cyclized with methylhydrazine to the pyrazole derivative **34c**. The ester functionality was hydrolyzed and the carboxylic acid **34d** was coupled with 1-(4-chlorobenzyl)piperazine in the presence of 1-propanephosphonic acid cyclic anhydride (PPAA) to **34**. For the synthesis of compound **35,** ethyl piperidine-4-carboxylate (**35a**) was *N*-alkylated with the corresponding benzyl bromide and **35b** was transformed to hydrazide **35c**. This derivative was then reacted with ethyl oxalyl chloride to form the oxadiazole core in **35d** and after ester hydrolysis (using the same methodology as in case of **11b**) carboxylic acid **35e** was obtained. The amide coupling with **11d** was accomplished with *N*,*N*,*N*′,*N*′-tetramethyl-*O*-(1*H*-

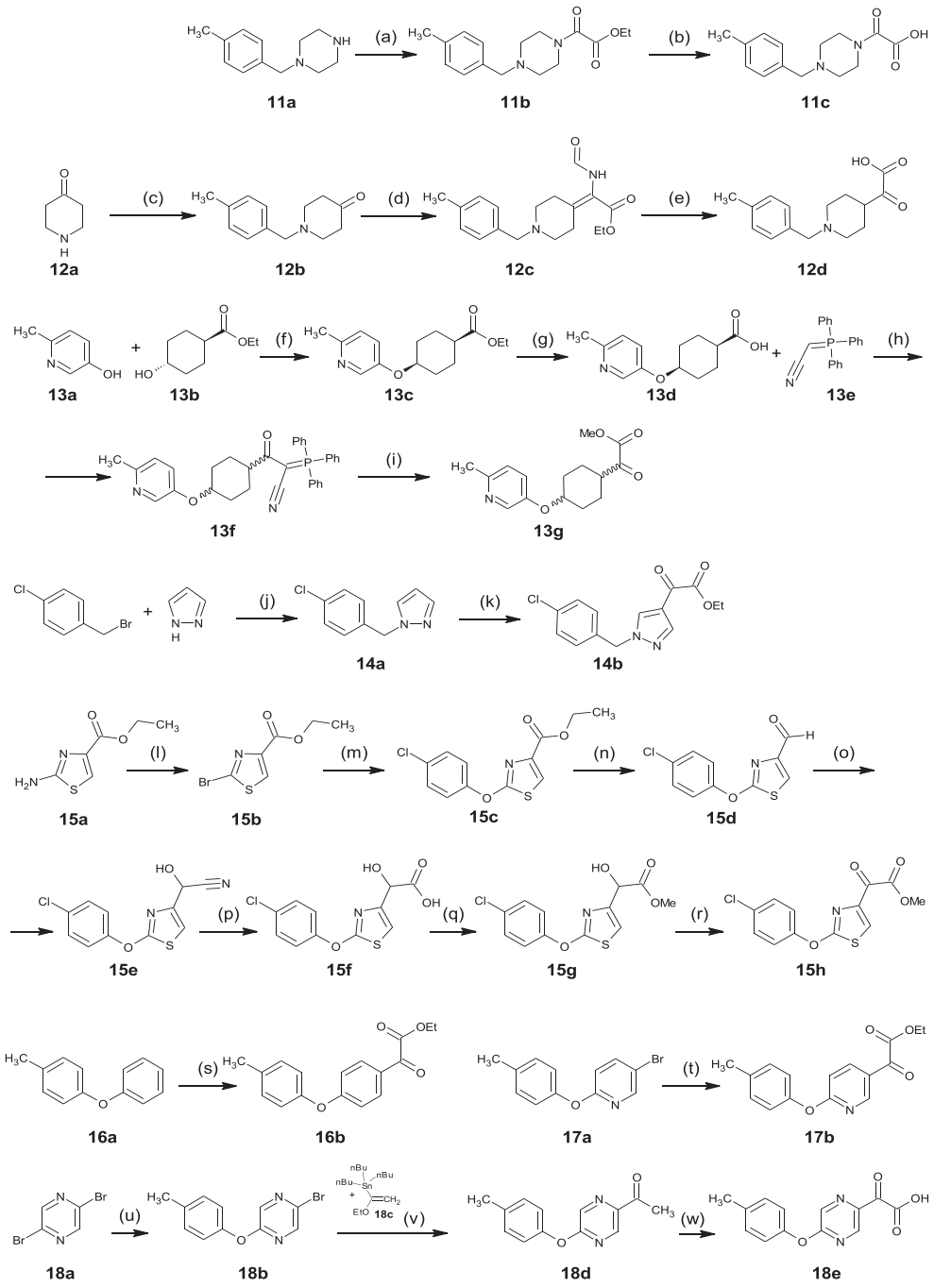

Scheme 3. The synthesis of oxoacetic acid intermediates **11c**, **12d**, **13g**, **14b**, **15h**, **16b**, **17b** and **18e**. Reagents and conditions: (a) ethyl chlorooxoacetate, Et_3N, CH_2Cl_2, rt.; (b) NaOH, EtOH, 0 °C to rt; (c) DMF, K_2CO_3, 1-bromomethyl-4-methlybenzene, rt.; (d) NaH, dry THF, ethyl-isocyanoacetate, 0−5 °C to rt.; (e) 1. EtOH, 10% HCl, 0−5 °C to rt. 2. KOH, EtOH, water, rt; (f) PPh_3, DIAD, THF, 0 °C; (g) MeOH, K_2CO_3, 70 °C; (h) EDC, DMAP, CH_2Cl_2, 0 °C; (i) oxone, CH_2Cl_2, MeOH, 40 °C; (j) K_2CO_3, DMF, 0−80 °C; (k) 2-chloro-2-oxoacetate, MeCN, 0 °C to rfx.; (l) MeCN, $CuBr_2$, *t*BuONO, 0 °C to rt.; (m) 1. 4-chlorophenol, THF, *t*BuOK, 0 °C, 2. DMSO, 85 °C; (n) CH_2Cl_2, DIBAL-H, citric acid, −70 °C to rt.; (o) CH_2Cl_2, methylmorpholine-*N*-oxide, TMSCN, 0 °C to rt; (p) cc. HCl, rfx.; (q) MeOH, cc. H_2SO_4, 0 °C to rt; (r) CH_2Cl_2, Dess-Martin periodinane, 0 °C to rt; (s) ethylchlorooxoacetate, $AlCl_3$, $CHCl_3$, 0 °C to rt; (t) toluene, BuLi in hexane, diethyloxalate, −78 °C; (u) *p*-cresol, K_2CO_3, DMF, rfx.; (v) toluene, $Pd(PPh_3)_4$, rfx; (w) SeO_2, pyridine, 70 °C.

benzotriazol-1-yl)uronium hexafluorophosphate (HBTU) and Et_3N to isolate **35**. Compound **36** was synthesized from methyl 2-bromo-3-methoxypropanoate (**36a**) with 4-(4-methylphenoxy)piperidine. The resulted methyl ester **36b** was hydrolyzed to the acid compound **36c**, which was subsequently amidated with **11d** in the presence of HATU/DIPEA system to yield compound **36**. Compound **37** was synthesized in the reaction of 1-methyl-1*H*-indole-5-carbonyl azide (**37a**) and 1-[(4-methylphenyl)methyl]piperidin-4-amine (**37b**). The syntheses of the aminomethylindole derivatives **38, 45**−**47** were exemplified in case of **38**. The aminomethylindole derivative **38a** was coupled with the carboxylic acid **38b** using the corresponding coupling agent. The synthesis of derivatives **39**−**44** and **48**−**55** were exemplified in case of compound **44**. The aminomethylindole derivative **38a** was activated with 4-nitrophenyl chloroformate and the resulted active carbamate was one-pot further reacted with 3-{[4-(trifluoromethyl)phenoxy]methyl}

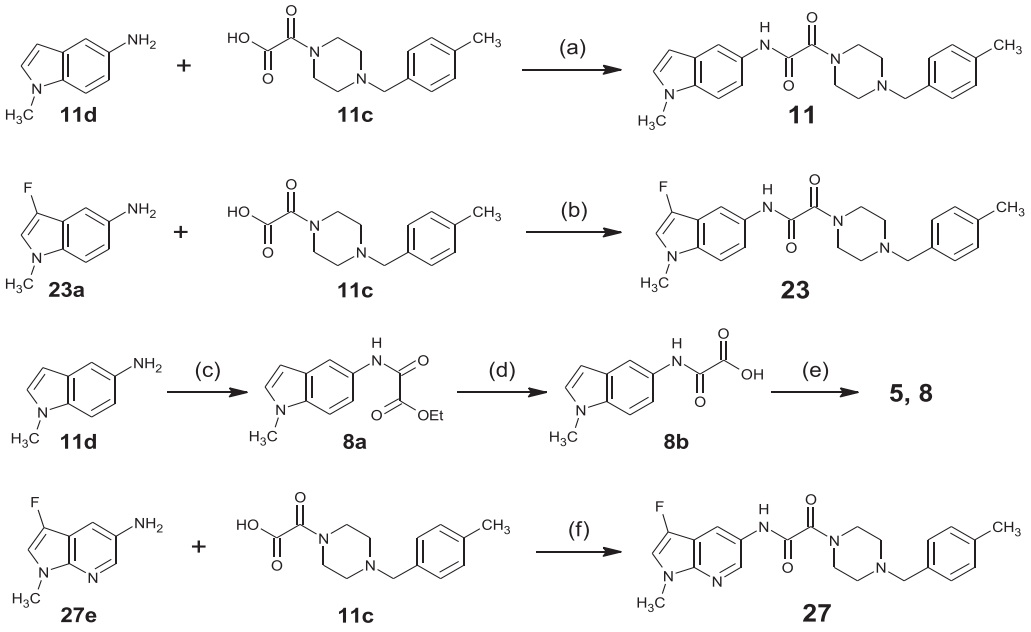

Scheme 4. Amide couplings for the synthesis of oxalic acid diamide derivatives (**1**–**30**). Reagents and conditions: (a) 1-hydroxybenzotriazole hydrate (HOBt·H_2O), *N*-(3-dimethylaminopropyl)-*N*′-ethylcarbodiimide hydrochloride (EDC. HCl), DMF, Et_3N; (b) 1-[Bis(dimethylamino)methylene]-1*H*-1,2,3-triazolo[4,5-*b*]pyridinium 3-oxide hexafluorophosphate (HATU), DMF, DIPEA, rt., (c) DIPEA, CH_2Cl_2, ethyl oxalyl chloride, 0 °C to rt; (d) LiOH·H_2O, water, MeOH, rt.; (e) amine, CH_2Cl_2, *N*,*N*,*N*′,*N*′-tetramethyl-*O*-(1*H*-benzotriazol-1-yl)uronium hexafluorophosphate (HBTU), Et_3N, rt.; (f) DMF, 1-chloro-*N*,*N*, 2-trimethyl-1-propenylamine (Ghosez's reagent), rt.

azetidine (**5d**).

2.2. Identification of the oxalic acid diamide scaffold

In order to identify structurally novel positive modulators of the human α7 nAChR, a HTS campaign of our corporate compound collection was undertaken utilizing a highly sensitive *in vitro* functional $[Ca^{2+}]_i$ assay. Multiple hit series were identified, in particular the presence of HTS hits **1**, **2** lead to robust $[Ca^{2+}]_i$ responses upon agonist addition in the primary assay (Table 1.). During hit expansion two structurally close, methylated analogues were also identified as active. Though the 2-methyl derivative **3** showed complete inactivity, the nitrogen methylation in compound **4** exerted beneficial impact on the activity. Furthermore, the *in vivo* evaluation of this compound revealed procognitive effects in the mouse place recognition test at 3 mg/kg with appropriate brain penetration, indicating optimization potential (Fig. 3).

Based on these promising initial findings comprehensive SAR evaluation of the central core was initiated and versatile saturated and aromatic rings were applied. Basic physico-chemical and *in vitro* characteristics of the synthesized derivatives are presented in Table 1. In case of the azetidinemethyl (**5**) analogue, moderate activity was detected. Unfortunately, introduction of the pyrrolidine (**6**), azepine (**7**) and azetidine (**8**) structural elements resulted in suboptimal activity while the usage of nortropine (**9**) or a dimethylated piperazine building blocks (**10**) led to complete inactivity. Interestingly, the non-substituted piperazine derivative (**11**) proved to be very potent. The *in vitro* metabolic stabilities characterized with intrinsic clearance (CL_{int}) values in human and mouse microsomes remained in the acceptable range, while the metabolic stability in rat microsomes was rather low. While searching for "metabolic soft points", we found that certain inactive derivatives lacking the nitrogen on right-hand side amide part showed higher metabolic stability (data not shown). Therefore, the piperazine central ring was attempted to be replaced with several 5- and 6-membered aromatic and saturated rings not having a nitrogen in the connection point. In certain cases – such as the saturated reversed piperidine (**12**) and cyclohexyl (**13**) derivatives – moderate, while in the case of the 5-membered heteroaromatic analogues (**14**, **15**), suboptimal or even complete lack of activity was found. On the other hand, the aromatic phenyl, pyridyl and pyrazine derivatives (**16**, **17**, **18**) showed significant activity. Furthermore, the pyridyl analogue **17** was active not just *in vitro* but also showed *in vivo* efficacy in the mouse place recognition test (Fig. 3). Unfortunately, drug-likeness of these planar structures with four aromatic rings seemed to be suboptimal as they had low solubility, high logP with no improvement in metabolic stability. Therefore, the less planar piperazine-based compound **11** seemed the most favorable choice. It showed a considerably balanced profile and fulfilled the criteria of an advanced hit molecule and it was subjected to further characterization.

2.3. Biological characterization of the advanced hit molecule *11*

The piperazine-centered chemotype's chemical accessibility was excellent, and **11** showed proper physicochemical parameters with appropriate kinetic solubility and experimental logP values (41.6 μM and 3.7, respectively). Compound **11** showed robust activity in the functional assay with an EC_{50} value of 90 nM. Using patch clamp a considerable inhibition of the choline-evoked current desensitization and enhancement of peak current amplitude was observed with an EC_{50} value of 710 nM (Fig. 4., upper panel).

The compound proved to be highly selective in a set of displacement binding assays for 68 molecular targets, showing affinity to 5-HT_{2B} and sigma-1 receptors (98 and 55% displacement at 10 μM, respectively). Importantly, **11** did not show >15% displacement at 10 μM in binding assays relevant for ligand affinity to 5-HT_3 receptors (human [^{3}H] GR-65630 binding in recombinant HEK-293 cells), NMDA receptors ([^{3}H]kainic acid, [^{3}H]MDL105,519, [^{3}H]CGP-39653 or [^{3}H]TCP binding in Wistar rat cerebral cortex preparations) or $GABA_A$ receptors ([^{3}H]flunitrazepam or [^{3}H]muscimol binding in Wistar Rat brain preparations minus cerebellum).

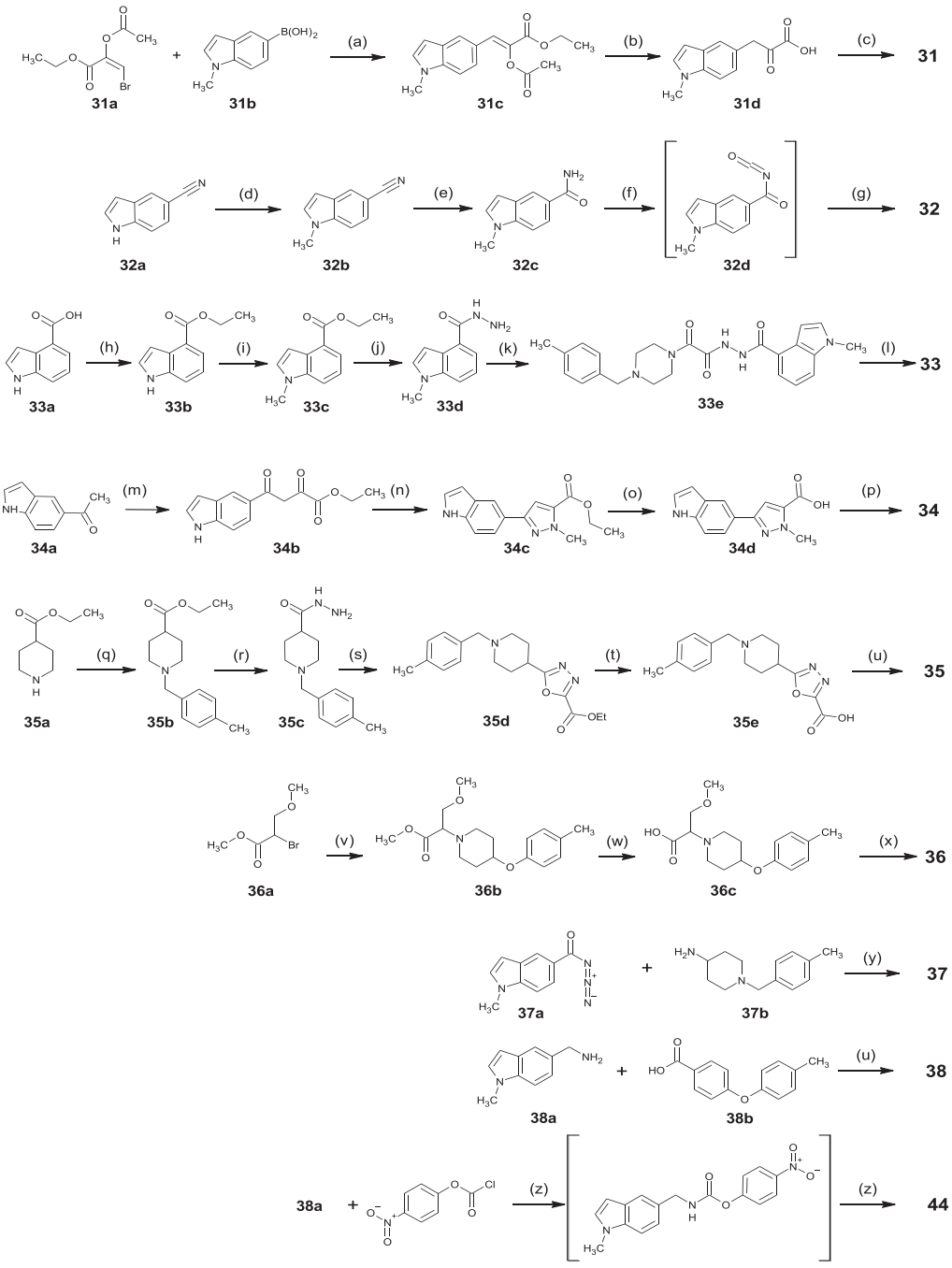

Scheme 5. The syntheses of compounds with modified linker region (**31**–**37** and **44**). Reagents and conditions: (a) K_2CO_3, $Pd(PPh_3)_4$, 1,4-dioxane, 90 °C; (b) EtOH, 1,4-dioxane, sat. $NaHCO_3$, rfx.; (c) **11a**, HATU, DIPEA, DMF, rt.; (d) MeI, NaH, dry THF, 0 °C to rt.; (e) 30% aq. H_2O_2 sol., K_2CO_3, DMSO, rt.; (f) oxalyl chloride, CH_2Cl_2, 0 °C to rfx., (g) 4-(4-methylbenzyl) piperidine hydrochloride, Et_3N, 1,2-dichloroethane, rt.; (h) EtOH, cc. H_2SO_4, rfx., (i) MeCN, K_2CO_3, Me_2SO_4, 95 °C; (j) EtOH, hydrazine hydrate, rfx., (k) **11b**, CH_2Cl_2, Et_3N, HBTU, rt.; (l) 1,4-dioxane, Et_3N, $SOCl_2$, 100 °C; (m) Na, EtOH, 0–5 °C, diethyl oxalate, rfx., (n) EtOH, methylhydrazine, rfx., (o) EtOH, water, KOH, rt., (p) 1-(4-chlorobenzyl)piperazine, CH_2Cl_2, Et_3N, 1-propanephosphonic acid cyclic anhydride 50% in EtOAc, rt., (q) DMF, K_2CO_3, 1-(bromomethyl)-4-methylbenzene, 80 °C, (r) hydrazine hydrate, 120 °C, (s) 1. CH_2Cl_2, Et_3N, ethyl oxalyl chloride, rt., (t) NaOH, EtOH, 0 °C to rt.; (u) **11d** (in case of **35**) or **38a** (in case of **38**), CH_2Cl_2, Et_3N, HBTU, rt.; (v) 4-(4-methylphenoxy)piperidine hydrochloride, K_2CO_3, DMF, 90 °C; (w) MeOH, water, $LiOH \cdot H_2O$, rt., (x) **11d**, HATU, DIPEA, DMF, rt.; (y) toluene, rfx; (z) 1. CH_2Cl_2, DIPEA, 0 °C, 2. **5d**, CH_2Cl_2, rt.

To further characterize the effects of **11** with respect to functional selectivity, electrophysiological measurements were done in cells expressing recombinant human α1 and α5 $GABA_A$ receptors that revealed no effect. **11** exhibited neither inhibition nor enhancement of the 1 μM GABA-evoked currents (effects were <7% in 1 or 10 μM) in HEK-293 cells expressing α1β3γ2 or α5β3γ2 $GABA_A$Rs (n = 5–9). In addition, **11** showed no agonism (up to 30 μM) or PAM activity (up to 10 μM) in α3β4 nACh-expressing cells in QPatch experiments (Dr. Hugh Chapman, personal communication. For further details, see Table S4. in the Supplementary Materials. Metabolic stability remained in the medium-to-low range both in human and rodent microsomes (with CL_{int} of 15, 158 and 55 μL/min/mg protein in human, rat and mouse microsome preparations, respectively, while its penetration through vinblastine-selected Caco-2 (VB-Caco-2) monolayers expressing high level of P-gp [43] was excellent with a PDR value of 0.7 and $Papp_{A-B}$ of 30.7×10^{-6} cm s^{-1} (tested @10 μM),

Table 1
The piperidine-based HTS hits and derivatives with modified central core (aromatic and aliphatic central rings).

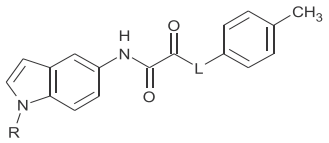

Cmpd	R	L	Kin. sol.[a] (μM)	cx_logP	$[Ca^{2+}]_i$ EC_{50} (nM) or % response at 1* or 10 μM	CL_{int}[a] μL/min/mg protein)
1	H	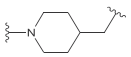	14.8	4.2	910	23/148/242
2	H	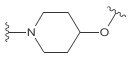	43.5	3.1	260	18/138/184
3[b]	H	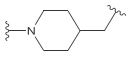	2.8	4.6	inact.	19/160/112
4	Me	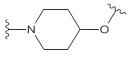	8.7	3.4	120	19/74/78
5	Me	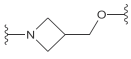	1.8	3.4	3000	–
6	Me	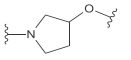	6.7	3.3	25%	–
7	Me	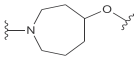	7.7	3.8	13%*	–
8	Me	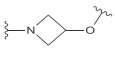	0.1	3.3	47%	–
9	H	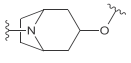	8.1	3.6	inact.	12/61/40
10	H	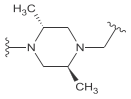	14.9	3.9	inact.	2/–/–
11 Advanced hit	Me	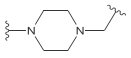	41.6	3.3	90	15/158/55
12	Me	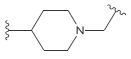	24.8	4.8	600	28/42/169
13[c]	Me	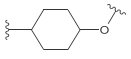	–	3.9	670	133/65/64
14[d]	Me	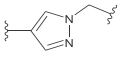	3.0	4.4	52%	–
15[d]	Me	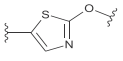	0.1	5.5	inact.	–
16	Me	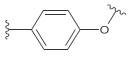	2.0	5.5	60	34/48/46
17	Me	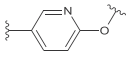	3.0	4.9	130	51/59/33
18	Me	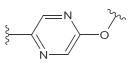	10.0	3.9	650	90/127/156

[a] Kin. sol.: kinetic solubility; cx_logP: calculated logP; $CL_{int.}$: intrinsic clearance measured in isolated microsomes; h: human; r: rat; m: mouse.
[b] On the indole ring position 2 was methylated.
[c] On the right-hand side of the molecule, 6-methyl-pyridin-4-yl was used, instead of the 4-methylphenyl moiety.
[d] On the right-hand side of the molecule, 4-chlorophenyl was used, instead of the 4-methylphenyl moiety. (Since the chlorine substitution provided equipotency with the methyl one (44 vs 49 in Table 5.), in case of the 4-methyl substituted derivatives the activities most probably would still not be high enough.).

respectively. Inhibitory activity of **11** on the hERG channel activity remained also in the acceptable range with an IC_{50} value of 7.5 μM. The compound, furthermore, resulted in significant alleviation of the scopolamine-induced amnesia in the mouse place recognition test in the dose range of 1–10 mg/kg, but remained ineffective in the rat novel object recognition paradigm (Fig. 4., middle panel). Brain-to-plasma ratios were favorable (above 1.2 and 3.8 in mice and rats, respectively), as revealed by pharmacokinetic analysis of

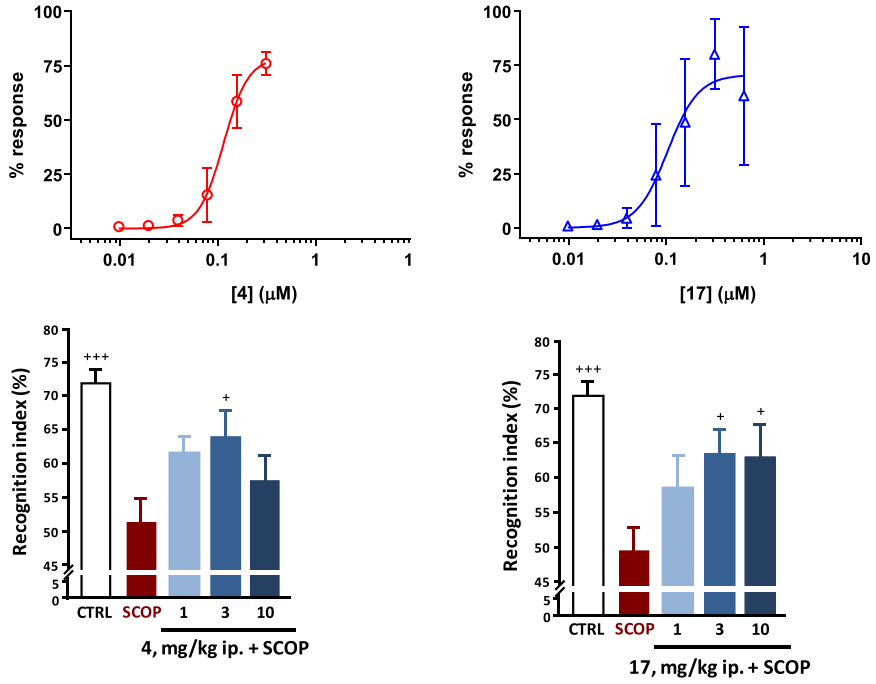

Dose (mg/kg)	4				
	Brain		*Plasma*		B/P
	ng/g	nM	ng/mL	nM	
1	47.1	120	24.5	63	1.95
3	116	297	66.5	170	1.74
10	506	1291	256	653	1.96

Dose (mg/kg)	17				
	Brain		*Plasma*		B/P
	ng/g	nM	ng/mL	nM	
1	41.8	108	40.2	104	1.05
3	190	492	161	417	1.17
10	744	1931	486	1262	1.53

Fig. 3. *Upper panel:* Effect of **4** and **17** on $[Ca^{2+}]_i$ in the presence of an agonists. *Middle panel:* Impact on recognition index of the ip. administration of **4** and **17** on the 1 mg/kg (ip.) scopolamine-induced amnesia in the mouse place recognition test. + $p < 0.05$ (ANOVA, followed by post-hoc Dunnett-test). *Lower panel:* results of the pilot pharmacokinetic measurement from brain and plasma samples taken from the experimental animals.

the samples taken from the experimental animals in both cognitive tests (Fig. 4., lower panel).

2.4. Optimization in the selected structural regions

However, besides the mixed cognitive profile, another disadvantageous feature also emerged. Despite the fact that **11** did not show any genotoxic liability in the Ames test and the presence of the corresponding indole-amine building block was never experienced *in vitro* during the stability measurements, putative *in vivo* formation of this aromatic amine metabolite could not be excluded (according to the Benigni/Bossa rulebase there was some risk for mutagenicity and carcinogenicity [44]). However, numerous ethical, biological, and technical difficulties dissuaded us from the demonstration of the formation of this metabolite *in vivo*. Another problematic feature identified was the chemically reactive nature of the indole motif. Therefore, the focus of the hit-to-lead optimization campaign was put on either the modification/replacement of the non-druglike, indole structural element (*Region I.*) or the total omission of the problematic aromatic-amine (indole-amine) moiety through modification of the oxalic acid diamide structural element (*Region II.*). (Fig. 5.). These approaches were mapped with focused libraries using conventional and parallel syntheses.

2.4.1. Optimization in region I

2.4.1.1. The usage of modified indole building blocks. First, versatile substitution patterns were applied on the indole ring with the aim of identifying indole-amines with improved metabolic stability and with no genotoxic liability. According to the initial hypothesis, the different substituents may differently affect the electron density both on the indole ring and the amine moiety, consequently they may differently influence the resulting compounds' behavior in these regards. Several, non-purchasable, substituted amino-indole/azaindole derivatives were synthesized, however only few active ones (**19**–**27**) were found due to the steep SAR. Table 2 summarizes only the active derivatives of this synthetic campaign, where $[Ca^{2+}]_i$ responses were ≥10% at 10 μM or higher.

Contrary to the results of monomethylation in position R^1 (**11**), the dimethylated analogues (R^1, R^3, as well as R^1, R^2: **19** and **20**, respectively), along with the 6-aminoindole (**21**) and 6-fluoroindole derivatives (**22**) showed suboptimal functional activity. However, substitution of the indole at position 3 (R^3) or 7 (R^7) with halogens – especially with fluorine – resulted in compounds of robust activity (**23**, **24, 25**): their activity proved to be comparable with the lead (**11**) itself. In contrast, however, no improvement in metabolic stability was achieved with these modifications. In addition to that the *in silico* evaluation of the corresponding indolamine building blocks indicated some risk of mutagenic liability for all tested intermediates (using the Toxtree software [45], working with the Benigni/Bossa rules [44]. See results in Supplementary Material, in Table S1.)

Next, a diverse set of more druglike (less lipophilic, less reactive) azaindole-amine building blocks were synthesized and applied in coupling reactions (Fig. 6). Among them, only the 7-aza derivatives showed activity in the $[Ca^{2+}]_i$ assay that was accompanied with somewhat improved rodent metabolic stability (**26, 27**).

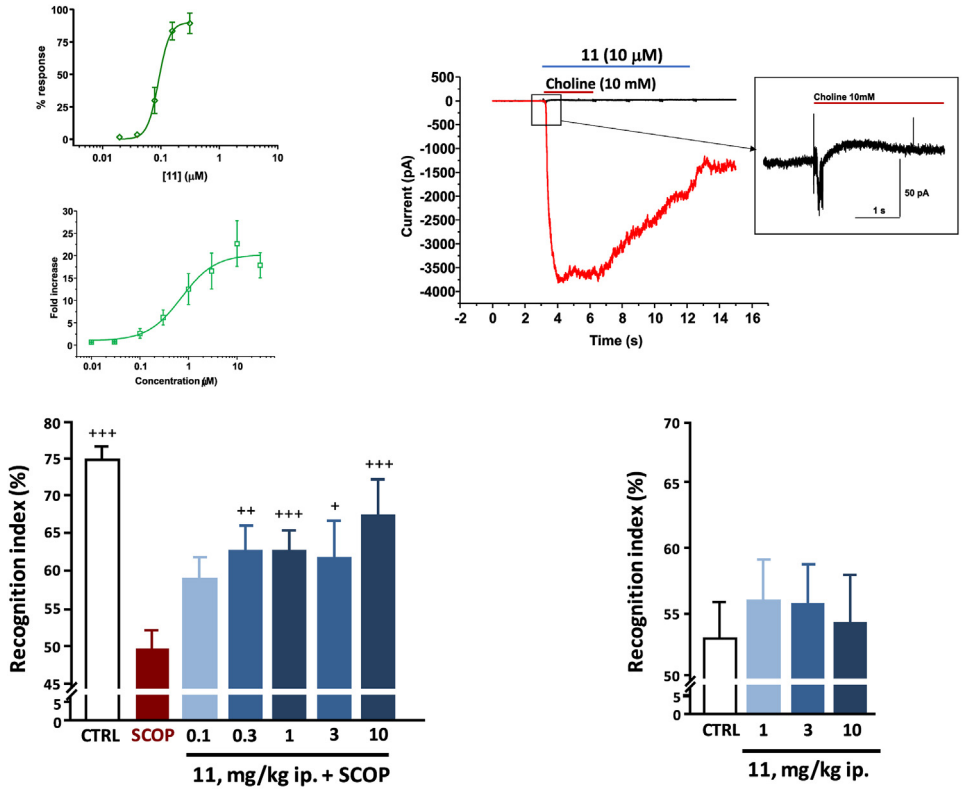

Dose (mg/kg)	11				
	Brain		*Plasma*		*B/P*
	ng/g	nM	ng/mL	nM	
0.1	1.23	3.1	0.83	2.1	1.32
0.3	2.14	5.5	1.69	4.3	1.22
1	15.4	39	8.17	21	1.88
3	25.0	64	14.6	37	1.68
10	90.9	233	55.6	142	1.67

Dose (mg/kg)	11				
	Brain		*Plasma*		*B/P*
	ng/g	nM	ng/mL	nM	
1	52.6	135	11.1	28	4.93
3	81.0	207	21.2	54	3.80
10	257	657	76.7	196	4.01

Fig. 4. *Upper panel: In vitro* characterization of the effect of **11**. On the left side, concentration-response curves measured in the $[Ca^{2+}]_i$ assay (upper figure) or in electrophysiological experiments (lower figure) are depicted. On the right side, electrophysiological characterization of the effect of **11** on the choline-induced current is demonstrated. Note the robust potentiation of the small, choline-induced current by **11**. *Middle panel:* Impact on recognition index of the ip. administration of **11** on the 1 mg/kg (ip.) scopolamine-induced amnesia in the mouse place recognition test (left) and on the delay-induced natural forgetting in the rat novel object recognition paradigm (right). + $p < 0.05$; ++ $p < 0.01$; +++ $p < 0.001$ (ANOVA, followed by post-hoc Dunnett-test). *Lower panel:* results of the pilot pharmacokinetic measurement from brain and plasma samples taken from the experimental animals in place recognition (mouse) and novel object recognition (rat) models.

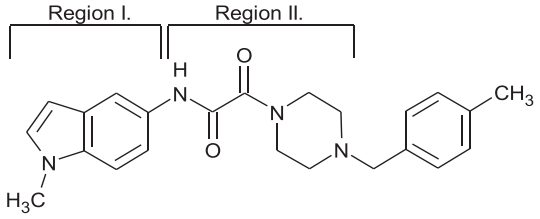

Fig. 5. The selected structural regions for optimization of the lead molecule **11**.

Unfortunately, the 4- and 5-azaindole derivatives showed no activity. Furthermore, significant amount of inactive substituted indole derivatives was also identified: their lack of activity highlighted the steepness of the observed SAR and lead us to abandon this approach.

2.4.1.2. The usage of non-indole aromatic and non-aromatic amine building blocks. Second, replacement of the entire indole moiety was attempted. Versatile non-aromatic and putatively (based on literature data) non-genotoxic aromatic amine building block libraries were applied in a parallel synthetic setup. Although the very steep SAR – and consequently, the low hit rate – is a widely known phenomenon in the field of allosteric modulators, it was still a surprise that only two of the approximately 200 synthesized derivatives (see a summary about the structures in the Supplementary Material, in Fig. S1.) exhibited significant *in vitro* activity. Compounds **28** (an indolizine analogue) and **29** (an indoline analogue) were identified as the most active ones, however, the activity remained in the non-acceptable (moderate) range ((See **28** and **29** in Table 2 and other 5 structures with subtle, however valid activity can be seen in Supplementary Material in Table S2.).

Summarizing the results of the optimization in Region I, it could be stated that the bioisoteric replacement of the indole building block seemed impossible, since only slight modifications of the substitution pattern were tolerated (and even in these cases the putative *in vivo* formation of mutagenic intermediates could not be excluded).

Table 2
Modification of Region I of the advanced hit 11. Active indole/azaindole and non-indole derivatives.

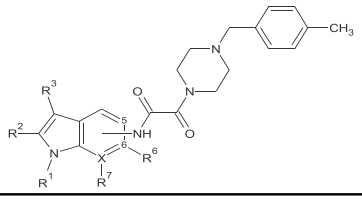

Cmpd	R^1	R^2	R^3	R^6	R^7	X	Connec. point	Kin.[a] sol. (μM)	cx_ logP[a]	$[Ca^{2+}]_i$ EC_{50} (nM) or % response at 10 μM	CL_{int}[a] μL/min/mg protein)
19	Me	H	Me	H	H	C	5	5.0	3.8	920	17/140/198
20	H	Me	Me	H	H	C	5	23.0	3.9	10%	13/56/151
21	Me	H	F	H	H	C	6	12.5	3.5	1400	–
22	Me	H	H	F	H	C	5	47.1	3.5	900	–
23	Me	H	F	H	H	C	5	16.5	3.5	85	21/192/214
24	Me	H	Cl	H	H	C	5	6.8	3.9	420	–
25	H	H	H	H	F	C	5	42.7	3.2	110	17/130/151
26	Me	H	H	H	H	N	5	47.4	2.4	400	0.3/56/46
27	Me	H	F	H	H	N	5	–	2.6	210	12/41/39
28	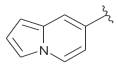							5.6	2.9	3300	–
29	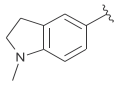							95.0	3.2	820	71/23/18

[a] Kin. sol.: kinetic solubility; cx_logP: calculated logP; CL_{int}.: intrinsic clearance measured in isolated microsomes; h: human; r: rat; m: mouse.

2.4.2. Optimization in region II. Trials to modify the oxalic acid diamide linker and the identification a benzylic-amine type chemotype

Omission of the problematic aromatic-amine (indole-amine) moiety through modification of the oxalic acid diamide linker was attempted via the synthesis of several interesting molecules (see the derivatives in Table 3.). Synthesis of the lengthier amino-methylindole derivative **30** was also accomplished, but it proved to be inactive. The replacement of the amine with a methylene (**31**) and the usage of the reversed-type amide (**32**) were attempted. As a result, significant activity loss was experienced in both cases. Furthermore, different amide bioisosteric heterocyclic rings were applied. Two of the resulting compounds – **33** (an oxadiazole derivative) and **34** (a methyl-pyrazole derivative) – showed moderate activity. Despite that these new chemotypes should have further extended the available chemical space, optimization of the structures led to inactivity in almost all cases (See in the Supplementary material in Table S3.). Replacement of the right-hand side amide moiety by an oxadiazole ring (**35**) resulted also inactivity. Finally, several oxo-group replacement methodologies were attempted, however, due to synthetic difficulties only two inactive analogues, a methoxymethyl (**36**) and a urea derivative (**37**) were successfully synthesized.

The experienced SAR in Region II proved to be so steep that the identification of the highly active benzyl-amine derivative **38** happened to be a serendipitous finding instead of the originally planned oxo-carboxylic acid derivative. **38** proved to be our first, *in vitro* active derivative lacking the problematic aromatic amine structural element. Evaluating compound **38** and the applied 1-(1-methylindol-5-yl)methanamine (**38a**) building block no structural

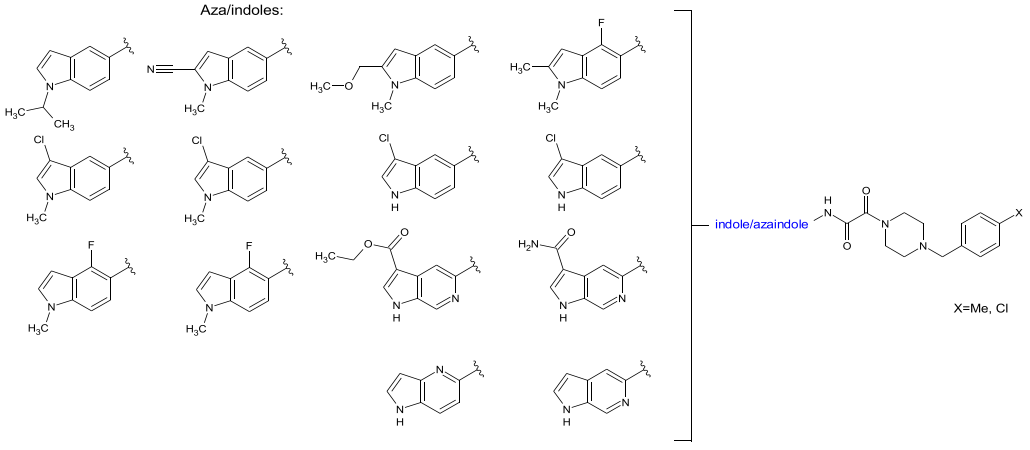

Fig. 6. Selected inactive substituted indole and azaindole derivatives (para-methyl/chlorine substituted piperazine analogues).

Table 3
Modifications of Region II. Trials for the elimination of aromatic amine building block.

Cmpd	Structure	$[Ca^{2+}]_i$ EC_{50} (nM) or % response at 10 μM
30	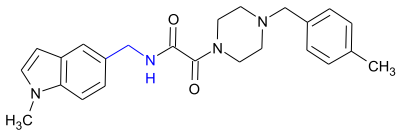	inact.
31	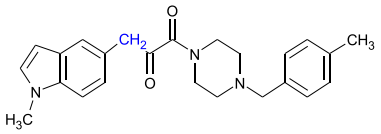	7%
32	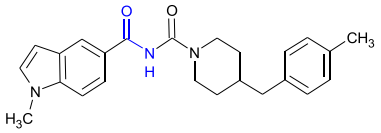	37%
33	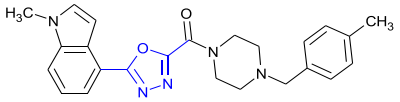	660
34	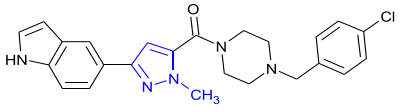	2500
35	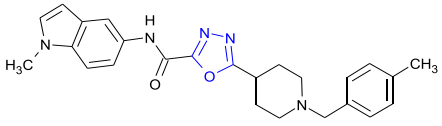	inact.
36	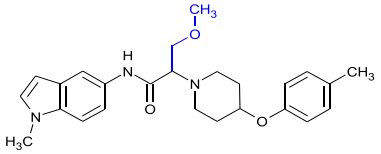	inact.
37	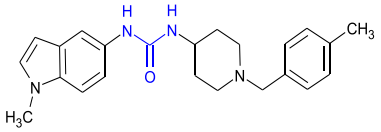	inact.
38	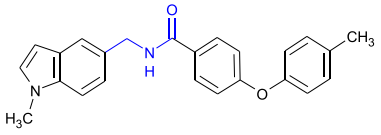	40

alerts were estimated by the Toxtree software (see results in Supplementary Material, in Table S1). According to this promising result, all further efforts were concentrated on the optimization of this newly identified chemotype.

2.5. Optimization of the newly identified, aminomethylindole cluster

Based on the high level of structural similarity between the new and the original chemotypes, it was hypothesized that the previously identified SAR (in Regions I and II) could at least partly be utilized in this new chemotype. Indeed, several new analogues – such as the piperidine (**39**), piperazine (**40**), azetidine (**41**), pyrrolidine (**42**), pyrrolidinemethyl (**43**) and azetidinemethyl (**44**) derivatives – were synthesized and found to be active (only a few analogues – namely the reversed piperidine (**45**), *trans*-cyclohexyl (**46**) and the nipecotic acid (**47**) derivatives – showed moderate or no activity). The results are summarized in Table 4.

Further optimization was performed using the most potent azetidinemethyl series, aiming at mainly the improvement of the metabolic stability. As the methyl substituent on the right-hand side phenyl ring seemed to be one of the "metabolic soft points" –, the evaluation of the phenyl substitution pattern was achieved. The *p*-fluorine (**48**), *p*-chlorine (**49**) *p*-methoxy (**50**), *p*-trifluoromethoxy (**51**) and even *p*-hydrogen (**52**) derivatives showed potent *in vitro* efficacy, however, their metabolic stabilities proved

Table 4
Derivatives of the new benzylic amine chemotype with versatile central cores.

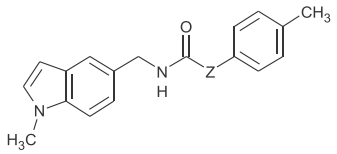

Cmpd	Z	Kin. sol.[a] (μM)	cx_logP[a]	$[Ca^{2+}]_i$ EC_{50} (nM) or % response at 1* or 10 μM	CL_{int}[a] μL/min/mg protein)
39	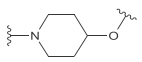	12.6	3.7	210	130/–/–
40	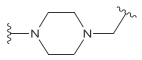	18.9	3.6	490	24/–/–
41	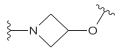	26.8	3.5	620	128/–/–
42	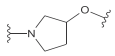	28.8	3.6	170	89/–/–
43	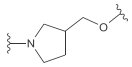	15.9	3.7	280	265/–/–
44	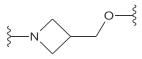	34.7	3.6	40	161/93/80
45	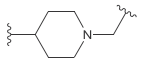	93.8	6.5	12%	–
46	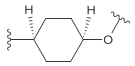	5.5	4.9	16%*	–
47	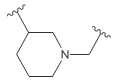	84.1	4.2	inact.	–

[a] Kin. sol.: kinetic solubility; cx_logP: calculated logP; CL_{int}.: intrinsic clearance measured in isolated microsomes; h: human; r: rat; m: mouse.

Table 5
Evaluation of the phenyl substitution pattern in derivatives with azetidinemethyl central core.

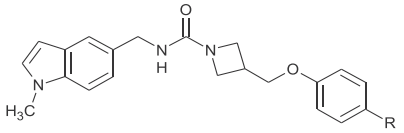

ID	R	Kin. Sol.[a] (μM)	cx_logP[a]	$[Ca^{2+}]_i$ EC_{50} (nM)	CL_{int}[a] μL/min/mg protein)
44	CH_3	34.7	3.6	40	161/93/80
48	F	1.6	3.2	220	43/–/–
49	Cl	0.7	3.6	55	72/–/–
50	OCH_3	42.3	2.8	60	348/–/–
51	OCF_3	0.4	4.8	25	23/100/109
52	H	18.0	3.1	180	19/134/91
53	CN	5.0	2.9	350	18/39/45
54	CF_3	0.1	4.0	80	19/42/45
55[b]	CF_3	18.4	3.7 4.3 (meas.)	160	22/56/58

[a] Kin. sol.: kinetic solubility; cx_logP: calculated logP; CL_{int}.: intrinsic clearance measured in isolated microsomes; h: human; r: rat; m: mouse.
[b] On the left-hand side of the structure the indole nitrogen was not methylated.

to be suboptimal. The highest metabolic stability was experienced with the *p*-nitrile derivative **53,** however with decreased activity. The usage of *p*-trifluororomethyl group (**54**) resulted in somewhat improved rodent metabolic stability with highly retained potency, but the compound had very poor solubility (Table 5.). Fortunately, the non-methylated (*N*—H) indole derivative provided enough balance between these two features: compound **55** showed improved kinetic solubility with retained activity and moderate metabolic stability. (In cases of **55** and its non-methylated 1-(1*H*-indol-5-yl)methanamine (**55a**) building block there were also no *in silico* toxicity alerts estimated (see results in Supplementary Material, in Table S1).

2.6. Docking study for the determination of the most probable binding site

The possible binding site of α7 nAChR PAMs is suggested to be in the transmembrane region of the homopentameric channel. However, it is not entirely clear whether the PAMs bind within a subunit or between two subunits of the ion-channel. Earlier studies based on site-directed mutagenesis complemented by homology modeling proposed an intrasubunit binding site located between the four transmembrane α-helices for both type I- and type II-like positive allosteric modulators [19,46]. On the other hand, another study [47] showed that a specific mutation of M260 to leucine only type II-like PAMs were converted into non-desensitizing agonists. These unexpected results pointed out that either the binding site and/or the binding modes of nAChR allosteric modulators needed to be revisited. It was also reported that different mutations could have different effect on the functional character of the ligands even in case of chemically similar type II-like PAMs [48]. The obtained results suggested that in the case of several of the investigated type II-like PAMs, the intersubunit site was more favored. In addition to that, in case of the ago-PAM GAT107, a second binding site (DAA site) located at the extracellular domain vestibule of the channel was proposed [35,49] with the assumption to be responsible for direct allosteric activation. Unfortunately, even the recently published results using the experimental cryo-EM structures of α7 nAChR (stabilized by the agonist epibatidine and the positive allosteric modulator PNU-120596) could not unequivocally clarify the location of the binding site [50]. To order to determine the most probable binding sites of our derivatives, the SiteMap module of the Schrödinger software package was applied (Schrödinger Release 2020−2: Schrödinger, LLC, New York, NY, 2020. Using the recently published open-state alpha-7 nicotinic acetylcholine receptor structure (PDB ID: 7KOX [50]), we were able to identify all above-mentioned allosteric binding sites (II-IV) and an additional external lipophilic site (V) was also found (see them in Fig. 7.). (It should be noted that other sites (mainly in the extracellular domain) were also found, however they had no relevance, either because of their size or their highly hydrophilic character.) Induced-fit docking [51] of compound **55** was carried out using the allosteric binding sites (II-IV). According to the obtained docking scores (III: −12.4 vs. II: −7.2, IV: −9.1, V: −10.8, see in Supplementary Material, in Figure S2.), the intersubunit binding site (III) seemed to be the most favorable. Furthermore, this binding site provided specific ligand-protein interactions such as a hydrogen bond between the carbonyl oxygen of 55 and the S248 residue and a π-π interaction between the ligand and the F252 residue. In parallel a lipophilic site formed by some apolar residues (*e.g.* L220, A223, I279 and L283) was found which was suitable to accommodate the substituted phenyl ring of the ligand. With these interactions, the molecule was complexed in a low energy elongated conformation. (For other binding sites, the best obtained poses can be seen in Supplementary Material, in Figure S2.) To gain further

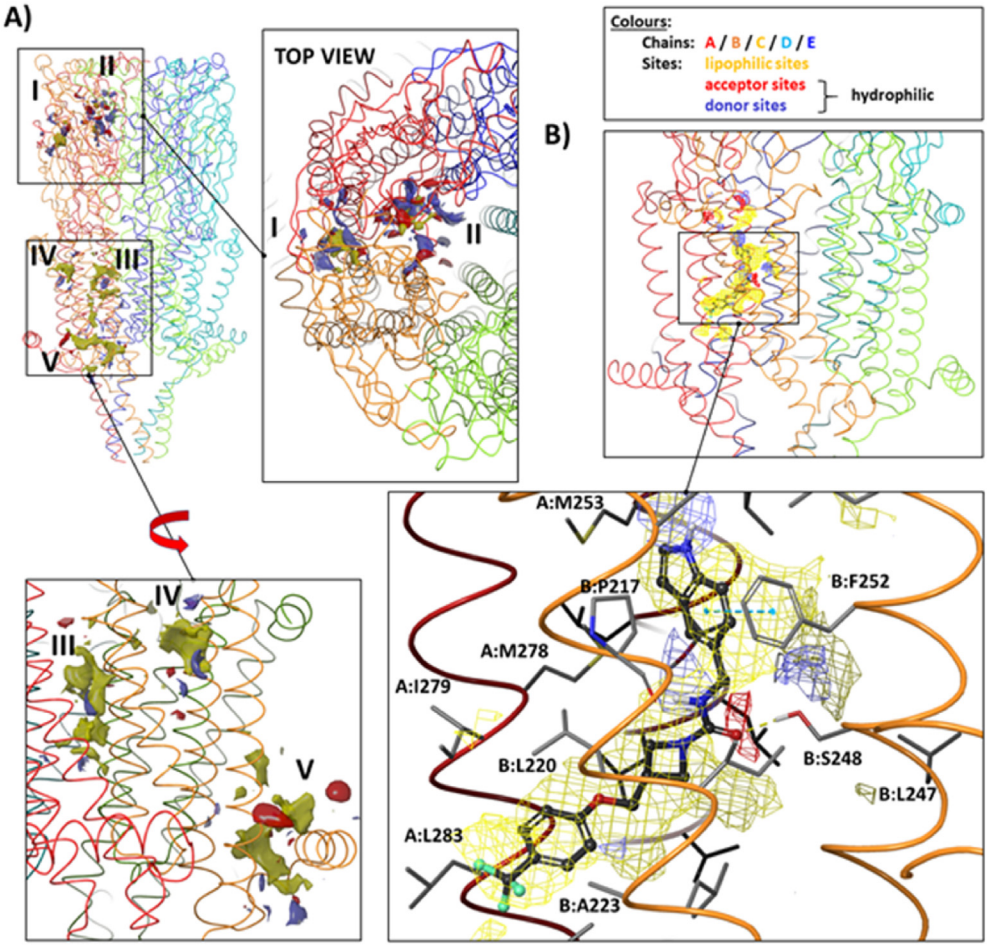

Fig. 7. Binding sites. A) The most relevant binding sites determined with SiteMap: I: Neurotransmitter site, II: DAA site [44], III: Intersubunit site, IV: Intrasubunit site, V: External lipophilic site; B) Refined intersubunit site (III): Compound **55** is placed with the induced-fit protocol.

confirmation, compounds **1**–**55** were docked into these refined binding sites (II–V) using the standard precision protocol in Glide [52,53]. The compounds were scored and ranked, and significantly more favorable docking scores were obtained for the active compounds (pEC_{50}>5) using the intersubunit binding site model III, than with the other ones. Furthermore, the model was able to enrich the active compounds based on the receiver operating characteristic (ROC) curves (see in Supplementary Material, in Figure S3.).

2.7. Biological evaluation of the best azetidinemethyl derivative *55*

Compound **55** was selected for further detailed characterization on the basis of its excellent functional activity ($[Ca^{2+}]_i$ EC_{50} of 160 nM) with a robust inhibition of response desensitization (Fig. 8., upper panel) and enhancement of peak current amplitude (EC_{50} = 590 nM) and acceptable metabolic stability (with CL_{int} values between 22 and 58). The efflux ratio (PDR) of **55** was 1.3 (tested at 1 μM) indicating no efflux liability of the compound ($Papp_{A-B}$ value of 55 × 10^{-6} cm s^{-1}). The compound – investigated in a panel of commercially available binding assays of 68 molecular targets– did not show serious off-target liabilities, as >50% ligand displacement was seen only for NET, DAT and 5-HT_{2B} at 10 μM (For further details, see Table S4. in the Supplementary Materials). Furthermore, **55** did not show any mutagenicity in the Ames test and its hERG IC_{50} value remained in the acceptable range (4.6 μM). The compound showed not only *in vitro* activity, but also significant efficacy in rodent spatial memory tests *in vivo*. Following ip. administration, it alleviated the scopolamine-induced amnesia or the natural forgetting in the mouse place recognition vs. the rat novel object recognition tests, respectively (Fig. 8., middle panel) with a minimal effective dose of 1 mg/kg in both species. Analysis of brain and blood samples taken from the experimental animals were also carried out (for results, see Fig. 8., middle panel), where relatively high expositions with favorable B/P ratios were measured in both species. The compound, furthermore, showed significant reversal of the 0.075 mg/kg (sc.) scopolamine-induced amnesia in the rat touch screen visual discrimination test (Fig. 8., lower panel), a cognitive model with high translational value. Based on all the above findings, **55** – fulfilling all lead criteria – was selected to be our lead molecule for future optimization.

3. Conclusions

Summarizing the above results, a promising new chemotype with good physicochemical and *in vitro* parameters was identified by an HTS-based approach. A novel, piperidine centered, oxalic acid diamide α7 nACh receptor positive modulator chemotype (**1**, **2**) was found. A close derivative **4** showed not just improved *in vitro* but also *in vivo* activity (*e.g.* in the mouse place recognition test). During hit expansion, the modification of the central core was investigated (**5**–**18**) and as a result, the saturated piperazine ring-centered **11**, the aromatic, phenyl ring-centered (**16**) and the pyridyl ring-centered (**17**) *in vitro* potent derivatives were highlighted and **11** and **17** demonstrated *in vivo* efficacy in the mouse place recognition test as well. Especially, the less planar compound **11** proved to be a promising derivative having the most balanced physicochemical and pharmacological profiles fulfilling the criteria of an advanced hit molecule.

The focus of the hit-to-lead optimization campaign was put on three synthetic approaches. First, versatile substitution patterns were applied on the indole ring with the aim of identifying derivatives with improved metabolic stability and building blocks possessing no genotoxic liability. Unfortunately, only few active derivatives (**19**–**27**) were found and even in these cases the putative formation of mutagenic metabolites could not be excluded.

Second, replacement of the entire indole moiety was attempted. Diverse non-aromatic and putatively non-genotoxic aromatic amine building block libraries were applied in a parallel synthetic setup. Due to the very steep SAR only two derivatives (**28**–**29**) exhibited significant activity.

Third, the omission of the problematic aromatic-amine (indole-amine) moiety through the modification of the oxalic acid diamide linker was attempted via the synthesis of new compounds (**30**–**38**) and as a result a novel, aminomethylindole compound family (**38**–**55**) emerged, in which the applied benzylic amine building blocks possessed no risk for mutagenicity. In addition to that, detailed docking studies using the recently published open-state alpha-7 nicotinic acetylcholine receptor structure were carried out, revealing four possible allosteric binding sites, among them the intersubunit site seems to be the most probable for our compounds. The most balanced physico-chemical and pharmacological profiles were experienced in case of the azetidinemethyl derivative **55**, which demonstrated favorable cognitive enhancing profile not only in cognitive models involving scopolamine-induced amnesia (place recognition test in mice) but also natural forgetting (novel object recognition test in rats). Compound **55** was, furthermore, active in a cognitive paradigm of higher translational value, namely in the rat touch screen visual discrimination test. Therefore, **55** was selected as a lead compound for further optimization.

Despite the experienced steep SAR, the identified structural elements provided a chance for further optimizing the lead compound. Based on all these considerations, cognitive enhancement through positive modulation of α7 nAChRs using compounds from the above described chemotype may seem a viable approach.

4. Experimental section

4.1. Chemistry and chemical methods

Commercially available reagents and reactants were used without further purification. Solvents and gases were dried according to standard procedures. Organic solvents were evaporated with reduced pressure using a rotary evaporator.

Purity of the final compounds was verified using an Agilent 1200 HPLC system equipped with a diode array detector and with an Agilent 6410 triple quadrupole mass spectrometer (QQQ-MS). Eluent A was 0.1% TFA in water and eluent B was the mixture of acetonitrile and water at 95:5 with 0.1% TFA. The mobile phase flow rate was 1.2 mL/min and the applied linear gradient profile was: 0–4 min 0–100% B, 6 min 100%B, 6.01 min 0% B. Chromatograms were recorded at 220 ± 4 nm and the applied injection volume was 1.0 μL. MassHunter Workstation software (B.03.01) was used for data acquisition and processing. Chromatographic analyses were carried out at 40 °C on an Ascentis Express C18 50 × 3.0 mm, 2.7 μm (Sigma-Aldrich) column. The QQQ-MS operating parameters were the following: scanning in positive ionization (ESI+) mode, drying gas temperature of 350 °C, nitrogen flow rate of 12 L/min, nebulizer pressure of 45 psi, capillary voltage of 4 kV, fragmentor voltage 135 V.

^{1}H NMR and ^{13}C NMR measurements were performed on a Bruker Avance III HDX 400 MHz spectrometer equipped with ^{15}N–$^{31}P\{^{1}H$–$^{19}F\}$ 5 mm CryoProbe Prodigy and a Bruker Avance III HDX 500 MHz NMR spectrometer equipped with ^{1}H $\{^{13}C/^{15}N\}$ 5 mm TCI CryoProbe (Bruker Corporation, Billerica, MA, USA). Chemical shifts are given on the delta scale as parts per million (ppm) relative to tetramethylsilane (TMS) (^{1}H: 0.00 ppm, ^{13}C: 0.0 ppm), coupling constants are given in Hz. All experiments were performed at 298 K. NMR spectra were processed using Bruker

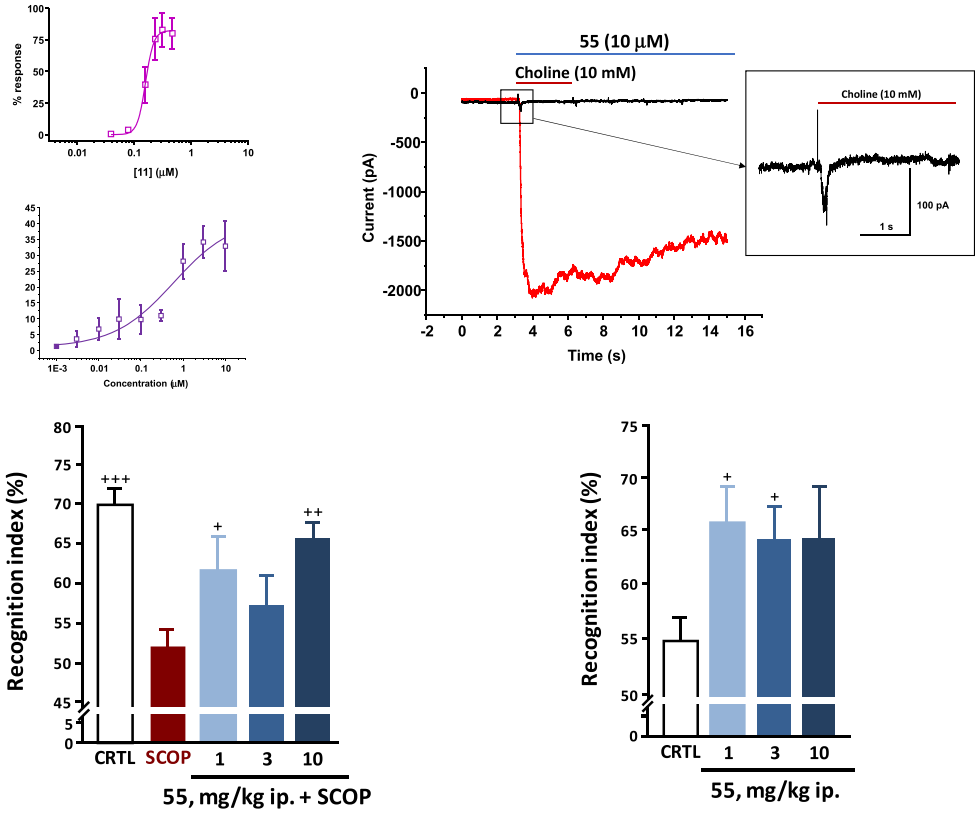

Dose (mg/kg)	55					Dose (mg/kg)	55				
	Brain		Plasma		B/P		Brain		Plasma		B/P
	ng/g	nM	ng/mL	nM			ng/g	nM	ng/mL	nM	
1	271	673	261	647	1.04	**1**	408	1011	301	746	1.43
3	891	2209	914	2268	0.99	**3**	1255	3112	896	2220	1.40
10	4001	9925	3817	9467	1.06	**10**	4491	11132	3235	8019	1.38

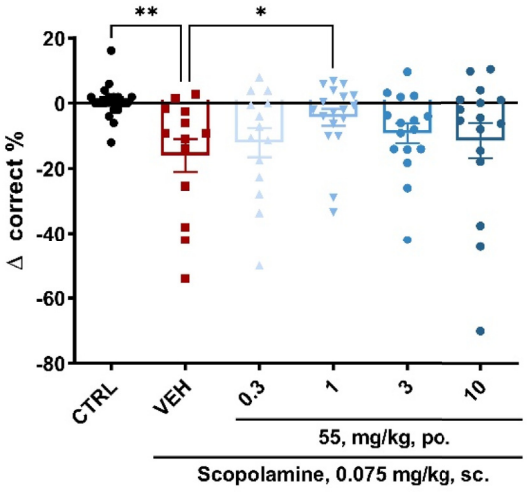

Fig. 8. *Upper panel: In vitro* characterization of the effect of **55**. On the left side, concentration-response curves measured in the $[Ca^{2+}]_i$ assay (upper figure) or in electrophysiological experiments (lower figure) are depicted. On the right side, electrophysiological characterization of the effect of **55** on the choline-induced current is demonstrated. Note the robust potentiation of the small, choline-induced current by **55**. *Middle left panel:* Effect of ip. administration of **55** on the 1 mg/kg (ip.) scopolamine-induced amnesia in the mouse place recognition test. + $p < 0.05$, ++ $p < 0.01$, +++ $p < 0.001$ (ANOVA, followed by post-hoc Dunnett-test). *Middle right panel:* Effect of ip. administration of **55** on the natural forgetting in the rat novel object recognition test. + $p < 0.05$ (ANOVA, followed by post-hoc Dunnett-test). Results of the pilot pharmacokinetic measurements from brain and plasma samples taken from the experimental animals are also included. *Lower panel:* Effect of **55** on the 0.075 mg/kg (sc.) scopolamine-induced amnesia in the rat touch screen visual discrimination test (Δ correct%). *$p < 0.05$ and **$p < 0.01$ represent Dunn's post hoc test results following significant Kruskal-Wallis test ($H = 13.49$, $p < 0.05$).

TopSpin 3.5 pl 7 (Bruker Corporation, Billerica, MA, USA) and ACD/Spectrus Processor version 2017.1.3 (Advanced Chemistry Development, Inc., Toronto, ON, Canada).

Electrospray high-resolution MS measurements (HESI-HRMS) were performed on a Thermo Velos Pro Orbitrap Elite Hybrid Mass spectrometer (Thermo Fisher Scientific, Bremen, Germany). The ionization method was HESI and operated in positive ion mode. The capillary temperature was set at 390 °C. Resolving power of 60,000 (FWHM) at *m/z* 400. Data acquisition and analysis were accomplished with Xcalibur software version 3.0 (Thermo Fisher Scientific Inc.).

4.2. Methods for syntheses and analytical characterization of the final compounds

4.2.1. N-(1H-indol-5-yl)-2-{4-[(4-methylphenyl)methyl]piperidin-1-yl}-2-oxoacetamide (**1**)

The corresponding oxoacetic acid intermediate and the final compound were synthesized in an analogous way as it is described in case of **11**. Yield 43.1%. Mp 86–88 °C. HESI-HRMS: calcd for $C_{23}H_{26}O_2N_3$ $[M+H]^+$: 376.20195; found: 376.20144; delta = −1.37 ppm. ^{1}H NMR (DMSO-d_6, 500 MHz) δ 11.05 (br s, 1H), 10.47 (s, 1H), 7.90 (d, 1H, *J* = 2.0 Hz), 7.3–7.4 (m, 2H), 7.25 (dd, 1H, *J* = 2.0, 8.7 Hz), 7.0–7.1 (m, 4H), 6.39 (ddd, 1H, *J* = 0.8, 2.0, 2.9 Hz), 4.2–4.4 (m, 1H), 3.7–3.8 (m, 1H), 3.0–3.1 (m, 1H), 2.67 (dt, 1H, *J* = 3.0, 12.7 Hz), 2.5–2.5 (m, 2H), 2.26 (s, 3H), 1.7–1.9 (m, 1H), 1.6–1.7 (m, 2H), 1.1–1.2 (m, 2H); ^{13}C NMR (DMSO-d_6, 126 MHz) δ 162.9, 161.9, 136.6, 134.7, 133.0, 129.7, 128.8, 128.7, 127.3, 126.1, 114.8, 111.23, 111.21, 101.1, 45.7, 41.5, 40.6, 37.3, 31.8, 30.9, 20.5.

4.2.2. N-(1H-indol-5-yl)-2-[4-(4-methylphenoxy)piperidin-1-yl]-2-oxoacetamide (**2**)

The oxoacetic acid intermediate and the final compound were synthesized in an analogous way as it is described in case of **11**. Yield 31.9%. Mp 116–118 °C. HESI-HRMS: calcd for $C_{22}H_{24}O_3N_3$ $[M+H]^+$: 378.18122; found: 378.18053; delta = −1.82 ppm. ^{1}H NMR (DMSO-d_6, 500 MHz) δ 11.07 (br s, 1H), 10.52 (s, 1H), 7.92 (d, 1H, *J* = 2.0 Hz), 7.3–7.4 (m, 2H), 7.27 (dd, 1H, *J* = 2.0, 8.7 Hz), 7.09 (d, 2H, *J* = 8.2 Hz), 6.9–6.9 (m, 2H), 6.41 (ddd, 1H, *J* = 0.7, 2.0, 2.9 Hz), 4.62 (tt, 1H, *J* = 3.6, 7.5 Hz), 3.8–3.9 (m, 1H), 3.70 (ddd, 1H, *J* = 3.8, 6.4, 13.4 Hz), 3.4–3.5 (m, 2H), 2.23 (s, 3H), 1.9–2.0 (m, 2H), 1.6–1.7 (m, 2H); ^{13}C NMR (DMSO-d_6, 126 MHz) δ 163.1, 161.7, 154.5, 133.0, 129.8, 129.7, 129.5, 127.3, 126.1, 115.9, 114.8, 111.2, 111.2, 101.1, 71.4, 42.8, 37.8, 30.7, 29.8, 20.0.

4.2.3. N-(2-methyl-1H-indol-5-yl)-2-{4-[(4-methylphenyl)methyl]piperidin-1-yl}-2-oxoacetamide (**3**)

The oxoacetic acid intermediate and the final compound were synthesized in an analogous way as it is described in case of **11**. Mp 132–134 °C. HESI-HRMS: calcd for $C_{24}H_{28}O_2N_3$ $[M+H]^+$: 390.21760; found: 390.21690; delta = −1.80 ppm. ^{1}H NMR (DMSO-d_6, 500 MHz) δ 10.86 (s, 1H), 10.40 (s, 1H), 7.74 (d, 1H, *J* = 1.9 Hz), 7.2–7.2 (m, 1H), 7.1–7.2 (m, 1H), 7.0–7.1 (m, 4H), 6.1–6.1 (m, 1H), 4.3–4.3 (m, 1H), 3.7–3.8 (m, 1H), 3.0–3.1 (m, 1H), 2.6–2.7 (m, 1H), 2.48 (s, 1H), 2.36 (d, 3H, *J* = 0.7 Hz), 2.26 (s, 3H), 1.7–1.8 (m, 1H), 1.6–1.7 (m, 2H), 1.0–1.2 (m, 2H); ^{13}C NMR (DMSO-d_6, 126 MHz) δ 163.0, 161.9, 136.6, 136.4, 134.7, 133.2, 129.5, 128.8, 128.7, 128.3, 113.6, 110.3, 110.2, 99.2, 45.7, 41.5, 40.6, 37.3, 31.8, 30.9, 20.5, 13.3.

4.2.4. N-(1-methyl-1H-indol-5-yl)-2-[4-(4-methylphenoxy)piperidin-1-yl]-2-oxoacetamide (**4**)

The oxoacetic acid intermediate and the final compound were synthesized in an analogous way as it was described in case of **11**. Yield 37.9%. Mp 143–145 °C. HESI-HRMS: calcd for $C_{23}H_{26}O_3N_3$ $[M+H]^+$: 392.19687; found: 392.19613; delta = −1.88 ppm. ^{1}H NMR (DMSO-d_6, 500 MHz) δ 10.55 (s, 1H), 7.9–7.9 (m, 1H), 7.4–7.4 (m, 1H), 7.3–7.3 (m, 2H), 7.1–7.1 (m, 2H), 6.9–6.9 (m, 2H), 6.39 (dd, 1H, *J* = 0.8, 3.1 Hz), 4.62 (tt, 1H, *J* = 3.6, 7.6 Hz), 3.8–3.9 (m, 1H), 3.77 (s, 3H), 3.70 (ddd, 1H, *J* = 4.0, 6.4, 13.5 Hz), 3.4–3.5 (m, 2H), 2.23 (s, 3H), 1.9–2.0 (m, 2H), 1.6–1.7 (m, 2H); ^{13}C NMR (DMSO-d_6, 126 MHz) δ 163.0, 161.7, 154.5, 133.6, 130.4, 129.8 (overlapping peaks), 129.5, 127.7, 115.9, 114.8, 111.4, 109.6, 100.3, 71.4, 42.8, 37.8, 32.4, 30.7, 29.8, 20.0.

4.2.5. N-(1-methyl-1H-indol-5-yl)-2-{3-[(4-methylphenoxy)methyl]azetidin-1-yl}-2-oxoacetamide (**5**)

*Step 1. tert-Butyl 3-{[(methanesulfonyl)oxy]methyl}azetidine-1-carboxylate (**5b**).* *tert*-Butyl 3-(hydroxymethyl)azetidine-1-carboxylate (**5a**, 2.88 g, 15.4 mmol) and Et_3N (4.3 mL, 30.8 mmol, 2 eq) were dissolved in CH_2Cl_2 (130 mL) at room temperature. To the solution was dropwise added methanesulfonyl chloride (2.0 mL, 30 mmol, 1.95 eq), followed by stirring at the same temperature for 2.5 h, then the solvent was removed under reduced pressure. The residue was dissolved in EtOAc and the solution was washed with a saturated aqueous solution of $NaHCO_3$ and with brine, dried over anhydrous Na_2SO_4, filtered and concentrated under reduced pressure to afford **5b** (4.0 g, quant.) as a yellow liquid which was used in the next step without further purification.

*Step 2. tert-Butyl 3-[(4-methylphenoxy)methyl]azetidine-1-carboxylate (**5c**).* A mixture of **5b** (3.8 g, 14 mmol), *p*-cresol (1.95 g, 18 mmol), Cs_2CO_3 (9.85 g, 30.2 mmol) and DMF (100 mL) was stirred at 110 °C overnight. The inorganic solid material was filtered off, the filtrate was concentrated under vacuum. The residue was dissolved in CH_2Cl_2, washed in turn with water, 2 M aqueous NaOH solution and brine. The organic phase was dried over anhydrous Na_2SO_4, filtered and concentrated. The residue was purified by column chromatography on silica gel (eluent: CH_2Cl_2/MeOH = 98:2) to afford **5c** (2.3 g, 58%) as light yellow oil.

*Step 3. 3-[(4-Methylphenoxy)methyl]azetidine (**5d**).* Trifluoroacetic acid (24 mL, 313 mmol) was added to a solution of **5c** (2.3 g, 8.3 mmol) in CH_2Cl_2 (50 mL) cooled to 0 °C in an ice water bath and the solution was stirred for 1 h at this temperature. The solvent was removed under reduced pressure at 40 °C. Ice water was added to the residue and the pH of the mixture was adjusted to 9 by addition of saturated $NaHCO_3$ solution. The mixture was extracted with CH_2Cl_2, the combined organic layer was washed with brine, dried over anhydrous Na_2SO_4 and filtered. The solvent was removed under reduced pressure to afford **5d** (1.37 g, 7.7 mmol, 93%).

*Step 4. N-(1-methyl-1H-indol-5-yl)-2-{3-[(4-methylphenoxy)methyl]azetidin-1-yl}-2-oxoacetamide (**5**).* To a solution of [(1-methyl-1*H*-indol-5-yl)carbamoyl]formic acid (**8b**) (135 mg, 0.8 mmol) in dry CH_2Cl_2 (10 mL) was added *N,N,N′,N′*-tetramethyl-*O*-(1*H*-benzotriazol-1-yl)uronium hexafluorophosphate (HBTU) (304 mg, 0.8 mmol) and Et_3N (335 μL, 2.4 mmol, 3.0 eq) at room temperature under argon. The mixture was stirred for 20 min then 3-[(4-methylphenoxy)methyl]azetidine (**5d**) (213 mg, 0.8 mmol) was added. The mixture was stirred at room temperature overnight. After completion of the reaction (monitored by TLC), the reaction mixture was quenched by addition of saturated $NaHCO_3$ solution (10 mL), the organic layer was washed with water (10 mL), then the organic phase was dried over anhydrous Na_2SO_4, filtered and concentrated *in vacuo*. The residue was purified by column chromatography on silica gel eluting with ethyl acetate: cyclohexane (67:33) to yield 91.5 mg (30%) of the title compound **5.** LC-MS (ESI) *m/z* [M+H]+= 378.1. Mp 185–186 °C. HESI-HRMS: calcd for $C_{22}H_{24}O_3N_3$ $[M+H]^+$: 378.18122; found: 378.18052; delta = −1.85 ppm. ^{1}H NMR (DMSO-d_6, 500 MHz) δ 10.35 (s, 1H), 8.01 (d, 1H, *J* = 2.0 Hz), 7.49 (dd, 1H, *J* = 2.0, 8.8 Hz), 7.37 (d, 1H, *J* = 8.8 Hz), 7.30 (d, 1H, *J* = 3.1 Hz), 7.1–7.1 (m, 2H), 6.8–6.9 (m, 2H), 6.38 (dd, 1H, *J* = 0.8, 3.1 Hz), 4.67 (ddd, 1H, *J* = 0.8, 8.5, 10.6 Hz), 4.37 (ddd, 1H, *J* = 1.0, 5.7, 10.6 Hz), 4.17 (ddd, 1H, *J* = 1.0, 8.5, 10.7

Hz), 4.14 (d, 2H, $J = 6.6$ Hz), 3.86 (dd, 1H, $J = 1.0, 5.4, 10.7$ Hz), 3.76 (s, 3H), 3.0–3.1 (m, 1H), 2.23 (s, 3H); ^{13}C NMR (DMSO-d_6, 126 MHz) δ 159.5, 157.9, 156.3, 133.6, 130.3, 129.7, 129.6, 129.3, 127.5, 115.2, 114.4, 111.8, 109.4, 100.3, 68.9, 55.9, 51.0, 32.4, 28.9, 20.0.

4.2.6. N-(1-methyl-1H-indol-5-yl)-2-[3-(4-methylphenoxy) pyrrolidin-1-yl]-2-oxoacetamide (**6**)

The oxoacetic acid intermediate and the final compound were synthesized in an analogous way as it was depicted in case of **11**. The corresponding pyrrolidine intermediate was synthesized in an analogous way as it is described in case of the azetidinemethyl intermediate **5d**. The amide coupling was achieved in an analogous way as in case of **23**. HESI-HRMS: calcd for $C_{22}H_{24}O_3N_3$ $[M+H]^+$: 378.18122; found: 378.18054; delta = −1.79 ppm. ^{1}H NMR (DMSO-d_6, 500 MHz) δ 10.46 (s, 0.5H), 10.46 (s, 0.5H), 7.99 (d, 0.5H, $J = 2.0$ Hz), 7.96 (d, 0.5H, $J = 2.0$ Hz), 7.4–7.5 (m, 1H), 7.3–7.4 (m, 1H), 7.3–7.3 (m, 1H), 7.1–7.1 (m, 2H), 6.8–6.9 (m, 2H), 6.39 (dd, 0.5H, $J = 0.8, 3.1$ Hz), 6.38 (dd, 0–5H, $J = 0.8, 3.1$ Hz), 5.0–5.1 (m, 1H), 3.9–4.0 (m, 1.5H), 3.8–3.8 (m, 0.5H), 3.77 (s, 1.5H), 3.76 (s, 1.5H), 3.6–3.7 (m, 1.5H), 3.54 (ddd, 0.5H, $J = 7.7, 10.1, 12.0$ Hz), 2.24 (s, 2H), 2.22 (s, 2H), 2.1–2.2 (m, 2H); ^{13}C NMR (DMSO-d_6, 126 MHz) δ 161.2, 160.9, 160.0, 159.8, 154.45, 154.41, 133.6, 130.3, 129.9, 129.82, 129.75, 129.69, 129.63, 127.59, 127.57, 115.43, 115.37, 115.1, 111.7, 109.44, 109.42, 100.3, 76.3, 73.9, 52.8, 51.8, 45.5, 44.6, 32.4, 31.2, 28.6, 19.99, 19.97.

4.2.7. N-(1-methyl-1H-indol-5-yl)-2-[4-(4-methylphenoxy) azepan-1-yl]-2-oxoacetamide (**7**)

The corresponding azepane intermediate was synthesized in an analogous way as it is described in case of the azetidinemethyl intermediate **5d**. The amide coupling was achieved in an analogous way as in case of **23**. Yield 50.0%. Mp 134–138 °C. HESI-HRMS: calcd for $C_{24}H_{28}O_3N_3$ $[M+H]^+$: 406.21252; found: 406.21161; delta = −2.24 ppm. ^{1}H NMR (DMSO-d_6, 500 MHz) δ 10.55 (s, 0.5H), 10.54 (s, 0.5H), 7.9–7.9 (m, 1H), 7.4–7.4 (m, 1H), 7.3–7.4 (m, 2H), 7.0–7.1 (m, 2H), 6.8–6.9 (m, 2H), 6.4–6.4 (m, 1H), 4.5–4.6 (m, 1H), 3.77 (2 × s, 3H), 3.4–3.7 (m, 4H), 2.23 (s, 1.5H), 2.21 (s, 1.5H), 2.0–2.1 (m, 1H), 1.8–2.0 (m, 4H), 1.7–1.8 (m, 1H); ^{13}C NMR (DMSO-d_6, 126 MHz) δ 164.6, 164.5, 162.1, 162.0, 154.71, 154.66, 133.59, 133.57, 130.3, 129.88, 129.84, 129.80, 129.23, 129.19, 127.7, 115.8, 115.7, 114.9, 114.8, 111.55, 111.46, 109.6, 100.3, 75.0, 74.3, 47.1, 44.4, 42.4, 34.2, 32.4, 32.0, 31.3, 30.1, 22.1, 20.7, 20.00, 19.98.

4.2.8. N-(1-methyl-1H-indol-5-yl)-2-[3-(4-methylphenoxy) azetidin-1-yl]-2-oxoacetamide (**8**)

*Step 1. ethyl [(1-methyl-1H-indol-*5-yl*)amino](oxo)acetate (**8a**).* 1-Methyl-1*H*-indol-5-amine (**11d**, 1.18 g, 8.07 mmol) and DIPEA (2.1 mL, 12.06 mmol) were dissolved in CH_2Cl_2 (50 mL) and ethyl oxalyl chloride (0.98 mL, 8.77 mmol) was added dropwise to the resulting reaction mixture at 0 °C. The mixture was stirred for 3 h at room temperature. The reaction mixture was treated with saturated aqueous $NaHCO_3$ solution and the organic phase was washed with water, dried over Na_2SO_4 and evaporated to dryness to result in **8a.** Yield: 1.2 g (61%).

*Step 2. [(1-methyl-1H-indol-*5-yl*)carbamoyl]formic acid (**8b**).* **8a** (1.2 g, 4.87 mmol) was hydrolyzed with 2.1 equivalent of aqueous $LiOH \cdot H_2O$ solution (426 mg, 10.15 mmol in 6 mL of water) in methanol (30 mL). The reaction mixture was stirred for 4 h. The pH of the mixture was adjusted to 3 by addition of 1 M HCl solution (ca. 10 mL) and extracted with EtOAc (40 mLx2). The organic phase was dried over Na_2SO_4 and evaporated to dryness. Yield: 1.5 g of crude **8b.** The synthesis of the corresponding azetidine intermediate was achieved in an analogous way as it was described in case of the azetidinemethyl intermediate **5d.** The amide coupling of **5d** and **8b** was achieved in an analogous way as it is described in case of **5.** Yield 8.0%. Mp 218–219 °C. HESI-HRMS: calcd for $C_{21}H_{22}O_3N_3$ $[M+H]^+$: 364.16557; found: 364.16501; delta = −1.53 ppm. ^{1}H NMR (DMSO-d_6, 500 MHz) δ 10.41 (s, 1H), 8.01 (d, 1H, $J = 2.0$ Hz), 7.49 (dd, 1H, $J = 2.0, 8.8$ Hz), 7.37 (d, 1H, $J = 8.8$ Hz), 7.31 (d, 1H, $J = 3.0$ Hz), 7.1–7.2 (m, 2H), 6.7–6.8 (m, 2H), 6.38 (dd, 1H, $J = 0.7, 3.0$ Hz), 5.0–5.1 (m, 2H), 4.4–4.5 (m, 2H), 3.9–4.0 (m, 1H), 3.76 (s, 3H), 2.24 (s, 3H); ^{13}C NMR (DMSO-d_6, 126 MHz) δ 159.6, 157.7, 154.0, 133.7, 130.3, 130.1, 130.0, 129.6, 127.5, 115.3, 114.4, 111.8, 109.4, 100.3, 66.3, 60.4, 55.6, 32.4, 20.0.

4.2.9. N-(1H-indol-5-yl)-2-[3-(4-methylphenoxy)-8-azabicyclo [3.2.1]octan-8-yl]-2-oxoacetamide (**9**)

*Step 1. tert-butyl 3-phenoxy-8-azabicyclo[3.2.1]octane-8-carboxylate (**9b**).* Under an Ar atmosphere, *N*-BOC-nortropine (**9a**) (4.55 g, 20 mmol) was dissolved in abs. THF, *p*-cresole (2.38 g, 22 mmol) and triphenylphosphine (6.82 g, 26 mmol) were added followed by the dropwise addition of DIAD (diisopropyl azodicarboxylate, 5.26 g, 26 mmol) at room temperature. The mixture was stirred at room temperature for 2 days. After completion, 1 M NaOH solution (12 mL) and 2 × EtOAc (2 × 25 mL) were charged. After separation of the phases, the organic phase was dried over Na_2SO_4, and evaporated to dryness. The crude product was purified with flash chromatography using cyclohexane/EtOAc as the eluent. Yield: 2.65 g (42%).

*Step 2. 3-phenoxy-8-azabicyclo[3.2.1]octane (**9c**).* **9b** (2.55 g, 8.4 mmol) was dissolved in 1,4-dioxane (30 mL), HCl solution in 1,4 dioxane (80 mL) was added and the mixture was stirred at room temperature overnight. The resulting solution was evaporated and the solid crude product **9c** was crystalized from diethyl ether. Yield: 1.01 g (58%).

Step 3–5. The oxoacetic acid intermediate and the final compound **9** were synthesized in an analogous way as it is described in case of **11.** Yield 8.2%. Mp 96–97 °C. HESI-HRMS: calcd for $C_{24}H_{26}O_3N_3$ $[M+H]^+$: 404.19687; found: 404.19594; delta = −2.30 ppm. ^{1}H NMR (DMSO-d_6, 500 MHz) δ 11.06 (br s, 1H), 10.48 (s, 1H), 7.96 (s, 1H), 7.3–7.4 (m, 3H), 7.0–7.1 (m, 2H), 6.9–6.9 (m, 2H), 6.4–6.4 (m, 1H), 4.8–4.9 (m, 1H), 4.7–4.7 (m, 1H), 4.6–4.7 (m, 1H), 2.22 (s, 3H), 2.2–2.2 (m, 2H), 1.8–2.1 (m, 4H), 1.7–1.8 (m, 1H), 1.6–1.6 (m, 1H); ^{13}C NMR (DMSO-d_6, 126 MHz) δ 160.6, 159.0, 154.8, 133.0, 129.8, 129.7, 129.4, 127.3, 126.0, 115.8, 115.1, 111.4, 111.1, 101.1, 68.9, 54.0, 50.9, 38.6, 36.8, 28.0, 26.3, 20.0.

4.2.10. 2-[(2R,5S)-2,5-dimethyl-4-[(4-methylphenyl)methyl] piperazin-1-yl]-N-(1H-indol-5-yl)-2-oxoacetamide (**10**)

*Step 1. tert-Butyl (2S,5R)-2,5-dimethyl-4-[(4-methylphenyl) methyl]piperazine-1-carboxylate (**10b**).* *tert*-Butyl-(2*S*,5*R*)-2,5-dimethylpiperazine-1-carboxylate (**10a**) (829 mg, 3.87 mmol) was dissolved in acetonitrile (20 mL) and of 4-methylbenzylbromide (716 mg, 3.87 mmol) was added. The solution was cooled down to 0 °C, triethylamine (539 μL, 7.34 mmol) was dropwise added and stirred overnight at room temperature. The reaction mixture was evaporated to dryness, water and CH_2Cl_2 were added. After separation the aqueous phase was extracted 3 times with CH_2Cl_2. The organic phase was dried and evaporated. Yield: 1.1 g, (89%).

Step 2. The BOC protecting group was removed according to the method used in case of **9c** to obtain (2*R*,5*S*)-2,5-dimethyl-1-[(4-methylphenyl)methyl]piperazine **10c.**

Step 3–5. The oxoacetic acid intermediate and the final compound **10** were synthesized in an analogous way as it is described in case **11.** Yield 30.3%. Mp 90–92 °C. HESI-HRMS: calcd for $C_{24}H_{29}O_2N_4$ $[M+H]^+$: 405.22850; found: 405.22790; delta = −1.49 ppm. ^{1}H NMR (DMSO-d_6, 500 MHz) δ 11.05 (br s, 1H), 10.52 (s, 0.5H), 10.49 (s, 0.5H), 7.91 (d, 0.5H, $J = 1.8$ Hz), 7.89 (d, 0.5H, $J = 1.9$ Hz), 7.3–7.4 (m, 2H), 7.2–7.3 (m, 3H), 7.1–7.2 (m, 2H), 6.4–6.4 (m, 1H), 4.4–4.5 (m, 0.5H), 4.00 (d, 0.5H, $J = 12.9$ Hz), 3.9–4.0 (m, 0.5H),

3.5−3.6 (m, 1.5H), 3.4−3.5 (m, 1.5H), 3.18 (dd, 0.5H, J = 3.7, 12.9 Hz), 3.0−3.1 (m, 0.5H), 2.9−3.0 (m, 0.5H), 2.69 (dd, 0.5H, J = 4.0, 11.8 Hz), 2.61 (dd, 0.5H, J = 4.3, 12.0 Hz), 2.28 (s, 1.5H), 2.27 (s, 1.5H), 2.2−2.3 (m, 1H), 1.35 (d, 1.5H, J = 6.6 Hz), 1.24 (d, 1.5H, J = 6.8 Hz), 0.98 (d, 1.5H, J = 6.6 Hz), 0.95 (d, 1.5H, J = 6.6 Hz); ^{13}C NMR (DMSO-d_6, 126 MHz) δ 163.9, 163.7, 161.9, 161.7, 135.79, 135.75, 135.73, 133.00, 132.98, 129.72, 129.67, 128.7, 128.14, 128.12, 127.3, 126.1, 114.93, 114.90, 111.32, 111.30, 111.2, 101.1, 57.6, 57.5, 51.3, 51.1, 49.5, 48.6, 47.9, 46.5, 44.0, 41.2, 20.6, 16.8, 15.5, 7.1, 6.8.

4.2.11. N-(1-methyl-1H-indol-5-yl)-2-{4-[(4-methylphenyl)methyl] piperazin-1-yl}-2-oxoacetamide (**11**)

Step 1. Ethyl 2-{4-[(4-methylphenyl)methyl]piperazin-1-yl*}-2-oxoacetate (**11b**).* To a solution of 1-(4-methylbenzyl)piperazine (**11a**, 854 mg, 4.49 mmol) and Et_3N (0.94 mL, 6.7 mmol) in CH_2Cl_2 (25 mL) was added ethyl chlorooxoacetate (0.6 mL, 5.37 mmol) at 0 °C under argon, and the mixture was stirred at room temperature overnight. Dichloromethane (100 mL) was added, and the mixture was washed with water, dried over Na_2SO_4, filtered and concentrated under reduced pressure to give the product **11b** (1.243 g, 95%), as light yellow oil.

Step 2. 2-{4-[(4-Methylphenyl)methyl]piperazin-1-yl*}-2-oxoacetic acid (**11c**).* To a solution of **11b** (3.098 g, 10.67 mmol) in ethanol was added dropwise a solution of NaOH (515 mg, 12.88 mmol, 1.2 eq) in water (5 mL) at 0 °C. The mixture was stirred at room temperature for 2.5 h, and concentrated. The residue was dissolved in water (50 mL) extracted with diethyl ether, acidified with 12.9 mL of 1 M aqueous HCl solution and extracted with CH_2Cl_2. The aqueous layer was freeze dried to afford the crude, title compound (3.546 g) as a white solid containing 1.2 eq of NaCl. **11c** was used in the next step without further purification.

Step 3. N-(1-Methyl-1H-indol-5-yl*)-2-{4-[(4-methylphenyl) methyl]piperazin*-1-yl*}-2-oxoacetamide (**11**).* 500 mg of 2-{4-[(4-methylphenyl)methyl]piperazin-1-yl}-2-oxoacetic acid (**11c**, 1.52 mmol) was dissolved in dry DMF under an argon atmosphere. To this solution 1-hydroxybenzotriazole hydrate ($HOBt \cdot H_2O$) (350 mg, 2.287 mmol, 1.5 eq) and *N*-(3-dimethylaminopropyl)-*N′*-ethyl-carbodiimide hydrochloride (EDC. HCl) (438 mg, 2.287 mmol, 1.5 eq) were added and the mixture was stirred for 15 min under argon atmosphere. Afterwards, 1-methyl-1*H*-indol-5-amine (**11d**) (278 mg, 1.9 mmol, 1.25 eq) and Et_3N (386 mg, 3.81 mmol, 2.5 eq) were added. The resulted reaction mixture was stirred for 24 h at room temperature under argon atmosphere. After the completion of the reaction (monitored by TLC) the mixture was diluted with water (20 mL) and extracted with EtOAc (3 × 20 mL). The combined organic layer was washed with water, dried over anhydrous Na_2SO_4, filtered and concentrated *in vacuo.* The crude product **11** was purified by column chromatography to afford 71 mg (12%) of the title compound. LC-MS (ESI) *m/z* $[M+H]^+$ = 391.2. Mp 125−127 °C. HESI-HRMS: calcd for $C_{23}H_{27}O_2N_4$ $[M+H]^+$: 391.21285; found: 391.21181; delta = −2.67 ppm. ^{1}H NMR (DMSO-d_6, 500 MHz) δ 10.54 (s, 1H), 7.9−7.9 (m, 1H), 7.4−7.4 (m, 1H), 7.3−7.3 (m, 2H), 7.2−7.2 (m, 2H), 7.1−7.2 (m, 2H), 6.38 (dd, 1H, J = 0.8, 3.0 Hz), 3.76 (s, 3H), 3.5−3.6 (m, 4H), 3.48 (s, 2H), 2.4−2.5 (m, 4H), 2.28 (s, 3H); ^{13}C NMR (DMSO-d_6, 126 MHz) δ 162.8, 161.4, 136.0, 134.4, 133.6, 130.3, 129.8, 128.9, 128.7, 127.6, 114.8, 111.5, 109.5, 100.3, 61.4, 52.5, 51.7, 45.6, 40.7, 32.4, 20.6.

4.2.12. N-(1-methyl-1H-indol-5-yl)-2-{1-[(4-methylphenyl)methyl] piperidin-4-yl}-2-oxoacetamide (**12**)

*Step 1. 1-[(4-Methylphenyl)methyl]piperidin-4-one (**12b**).* To a solution of 4-piperidone monohydrate hydrochloride (**12a**, 3.0 g, 19.5 mmol) in DMF (60 mL) was added K_2CO_3 (5.4 g, 39 mmol) and 1-bromomethyl-4-methylbenzene (5.42 g, 29.3 mmol, 1.5 eq) at room temperature under argon. The mixture was stirred overnight under this condition. After the completion of the reaction (monitored by TLC- visualized by iodine - *o*-toluidine) the mixture was poured onto water (80 mL) and extracted with EtOAc (3 × 30 mL). The combined organic layer was washed with brine (3 × 30 mL) dried over anhydrous Na_2SO_4, filtered and concentrated *in vacuo.* The residue was chromatographed on silica gel eluting with a mixture of cyclohexane - EtOAc 1:1 to yield 2.54 g (64%) of **12b.**

*Step 2. Ethyl 2-formamido-2-(1-[4-methylphenyl]methylpiperidin-4-ylidene)acetate (**12c**).* To a stirred suspension of NaH (60% in mineral oil) (751 mg, 18.7 mmol, 1.5 eq) in THF (100 mL) was added a solution of ethyl isocyanoacetate (1.78 mL, 16.25 mmol) in THF (5 mL) over a period of 15 min at 0−5 °C under argon. The mixture was stirred for 40 min under this condition then a solution of **12b** (2.54 g, 12.5 mmol) in THF (45 mL) was added dropwise at 0−5 °C. The temperature allowed to warm to room temperature and the mixture was stirred overnight. After the completion of the reaction (monitored by TLC) the mixture was poured onto water (100 mL) and extracted with EtOAc (2 × 80 mL). The combined organic layer was washed with brine (2 × 30 mL) dried over anhydrous Na_2SO_4, filtered and concentrated *in vacuo* to yield 1.09 g of **12c.** It was used in the next step without further purification.

*Step 3. 2-Oxo-2-(1-[4-methylphenyl]methylpiperidin-4-yl)acetic acid (**12d**).* To a stirred solution of **12c** (1.09 g, 3.43 mmol) in EtOH (21 mL) was added 10% aqueous solution of HCl (21 mL) at 0−5 °C under argon then the mixture was stirred at room temperature overnight. After the completion of the reaction (monitored by TLC) to this mixture was added a solution of KOH (3.79 g, 67.7 mmol) dissolved in EtOH (28 mL) and water (10 mL); (pH = 12). After the completion of the hydrolysis (monitored by TLC) pH of the mixture was adjusted to 6 with 1 N HCl solution. The precipitated solid was removed by filtration, the mother liquor was concentrated *in vacuo* to yield 3.2 g (theor. 0.9 g) of the mixture of **12d** together with KCl. It was used in the next step without further purification.

Step 4. The synthesis of **12** was achieved in an analogous way as it is described in case of **11.** Yield 9.1%. Mp 147−148 °C. HESI-HRMS: calcd for $C_{24}H_{28}O_2N_3$ $[M+H]^+$: 390.21760; found: 390.21716; delta = −1.14 ppm. ^{1}H NMR (DMSO-d_6, 500 MHz) δ 10.34 (s, 1H), 8.03 (d, 1H, J = 2.0 Hz), 7.49 (dd, 1H, J = 2.0, 8.8 Hz), 7.39 (d, 1H, J = 8.8 Hz), 7.31 (d, 1H, J = 3.1 Hz), 7.2−7.2 (m, 2H), 7.1−7.1 (m, 2H), 6.39 (dd, 1H, J = 0.8, 3.1 Hz), 3.77 (s, 3H), 3.42 (s, 2H), 3.28 (tt, 1H, J = 3.8, 11.4 Hz), 2.8−2.9 (m, 2H), 2.28 (s, 3H), 2.02 (dt, 2H, J = 2.1, 11.4 Hz), 1.8−1.9 (m, 2H), 1.4−1.5 (m, 2H); ^{13}C NMR (DMSO-d_6, 126 MHz) δ 201.1, 159.3, 135.8, 135.2, 133.7, 130.3, 129.6, 128.6, 127.6, 115.2, 111.9, 109.5, 100.3, 61.9, 52.2, 41.7, 32.4, 27.0, 20.6.

4.2.13. N-(1-methyl-1H-indol-5-yl)-2-oxo-2-[(1r,4r)-4-[(6-methylpyridin-3-yl)methyl] cyclohexyl]acetamide (**13**)

Step 1. Ethyl (1s,4s)-4-[(6-methylpyridin-3-yl*)oxy]cyclohexane-1-carboxylate (**13c**).* To a solution of 6-methylpyridin-3-ol (**13a**, 400 mg, 3.69 mmol, 1.5 eq) in THF (11 mL) was added ethyl *trans*-4-hydroxycyclohexane-1-carboxylate (**13b**, 0.40 mL, 2.46 mmol) and triphenylphosphine (974 mg, 3.71 mmol, 1.51 eq) under inert conditions at 0 °C and stirred for 8 min. Diisopropyl azodicarboxylate (0.73 mL, 3.69 mmol, 1.5 eq) in THF (1 mL) was then added dropwise (in 20 min). After stirring for 1 h at this temperature, the reaction mixture was allowed to warm to room temperature and stirred for further 4 days. The solvent was evaporated under reduced pressure to obtain a crude oil which was then purified by column chromatography using cyclohexane and ethyl acetate (3:1) to cyclohexane and ethyl acetate (1:2) as an eluent to yield (464 mg, 71.63%) of **13c.**

Step 2. (1s,4s)-4-[(6-methylpyridin-3-yl*)oxy]cyclohexane-1-carboxylic acid (**13d**).* To a solution of **13c** (558 mg, 2.12 mmol) in methanol (15 mL) was added potassium carbonate (586 mg, 4.24 mmol, 2 eq) and water (3.75 mL) then the mixture was heated at 70

°C for 2 h. After the reaction mixture had been allowed to cool to room temperature, 10% HCl solution was added, followed by the addition of CH_2Cl_2 (25 mL) and water (25 mL), and the two phases were separated. The aqueous layer was extracted with CH_2Cl_2 (5 × 15 mL). The combined organic layer was washed with water (20 mL) and brine (20 mL). The aqueous layer was extracted again with CH_2Cl_2 (3 × 15 mL). The combined organic layer was dried over Na_2SO_4 and concentrated and dried at 40 °C for 24 h. Yield: 204 mg (41%).

Step 3. 3-{4-[(6-Methylpyridin-3-yl*)oxy]cyclohexyl}-3-oxo-2-(triphenyl-λ⁵-phosphanylidene) propanenitrile (**13f**).* To a mixture of **13d** (197 mg, 0.837 mmol) in CH_2Cl_2 (14 mL) at 0 °C was added EDC (169 mg, 0.879 mmol, 1.05 eq) and DMAP (12 mg, 0.098 mmol, 0.117 eq) followed by the dropwise addition of a solution of cyano phosphorane **13e** (506 mg, 1.68 mmol, 2 eq) in CH_2Cl_2 (15 mL). After stirring the mixture at 0 °C for 1 h, it was warmed to room temperature and stirred overnight. The reaction mixture was diluted with CH_2Cl_2 and washed with water (30 mL). The aqueous layer was extracted with CH_2Cl_2 (2 × 15 mL). The combined organic layer was washed with water (15 mL) and brine (15 mL), dried over Na_2SO_4 and concentrated. The residue was purified by column chromatography over silica gel, eluting with a mixture of cyclohexane and EtOAc (1:5) to yield 312 mg (72%) of cyanoketo phosphorane **13f.**

Step 4. Methyl 2-{4-[(6-methylpyridin-3-yl*)oxy]cyclohexyl}-2-oxoacetate (**13g**).* Under argon, oxone (880 mg, 1.43 mmol, 2.41 eq) and of cyanoketo phosphorane **13f** (308 mg, 0.594 mmol) was dissolved in a mixture of CH_2Cl_2 (28 mL) and methanol (12 mL) and heated at 40 °C for 7 days. The reaction mixture was filtered and evaporated. The residue was purified by column chromatography over silica gel, eluted with a mixture of cyclohexane and EtOAc (1:5) to cyclohexane and EtOAc (1:1) then CH_2Cl_2 and methanol (10:1) to yield 51 mg (31%) of **13g.**

Step 5–6. The hydrolysis was accomplished in the same way as it is described in case of **11c.** The amide coupling was achieved in an analogous way as it is described in case of **23.** Yield 5%. Mp 176–178 °C. HESI-HRMS: calcd for $C_{23}H_{26}O_3N_3$ $[M+H]^+$: 392.19687; found: 392.19625; delta = −1.58 ppm. ^{1}H NMR (DMSO-d_6, 500 MHz) δ 10.36 (s, 1H), 8.15 (d, 1H, J = 2.9 Hz), 8.04 (d, 1H, J = 2.0 Hz), 7.51 (dd, 1H, J = 2.0, 8.8 Hz), 7.40 (d, 1H, J = 8.8 Hz), 7.33 (dd, 1H, J = 2.9, 8.5 Hz), 7.32 (d, 1H, J = 3.0 Hz), 7.15 (d, 1H, J = 8.5 Hz), 6.40 (dd, 1H, J = 0.8, 3.0 Hz), 4.3–4.4 (m, 1H), 3.77 (s, 3H), 3.3–3.4 (m, 1H), 2.38 (s, 3H), 2.1–2.2 (m, 2H), 2.0–2.0 (m, 2H), 1.4–1.5 (m, 4H); ^{13}C NMR (DMSO-d_6, 126 MHz) δ 201.3, 159.3, 151.3, 149.5, 137.9, 133.7, 130.4, 129.6, 127.6, 123.2, 122.9, 115.2, 111.9, 109.5, 100.3, 74.9, 42.4, 32.4, 30.3, 25.4, 22.9.

*4.2.14. 2-{1-[(4-Chlorophenyl)methyl]-1H-pyrazol-4-yl}-N-(1-methyl-1H-indol-5-yl)-2-oxoacetamide (**14**)*

*Step 1. 1-[(4-Chlorophenyl)methyl]-1H-pyrazole (**14a**).* Pyrazole (3 g, 44 mmol) was dissolved in DMF (25 mL) and the solution was cooled down to 0 °C. Potassium carbonate (7.3 g. 53 mmol) and the *p*-chlorobenzyl bromide (10.84 g, 53 mmol) were added, the mixture was warmed up to 80 °C and stirred for 16 h. The progress of the reaction was monitored by TLC (40% EtOAc/60% petrolether). After completion of the reaction, the reaction mixture was poured into cooled water and extracted with EtOAc (3 × 200 mL). The combined organic layer was washed with brine, dried and evaporated. The **14a** crude product was purified with column chromatography using a mixture of 25%EtOAc and 75% light petroleum as the eluent. Yield: 2.0 g (23%).

Step 2. Ethyl {1-[(4-chlorophenyl)methyl]-1H-pyrazol-4-yl*}(oxo) acetate (**14b**).* To the solution of **14a** (2.0 g, 10.4 mmol) in acetonitrile was added ethyl 2-chloro-2-oxoacetate (2.02 g, 14.8 mmol) at 0 °C. The solution was stirred at 0 °C for 15 min then heated at reflux temperature overnight. The reaction mass was diluted with water and extracted with EtOAc (2 × 20 mL). The combined organic layer was washed with brine and evaporated. The crude product was purified with column chromatography (eluent: 15% EtOAc/petrolether). Yield: 1.2 g (39%).

Step 3–4. The ester hydrolysis was accomplished in an analogous way as it is described in case of **11c.** The amide coupling was achieved in an analogous way as it is described in case of **23.** Mp 154–156 °C. HESI-HRMS: calcd for $C_{21}H_{18}O_2N_4Cl$ $[M+H]^+$: 393.11128; found: 393.11107; delta = −0.53 ppm. ^{1}H NMR (DMSO-d_6, 500 MHz) δ 10.51 (s, 1H), 8.94 (d, 1H, J = 0.5 Hz), 8.21 (d, 1H, J = 0.5 Hz), 8.10 (d, 1H, J = 2.0 Hz), 7.54 (dd, 1H, J = 2.0, 8.8 Hz), 7.4–7.5 (m, 2H), 7.41 (d, 1H, J = 8.8 Hz), 7.3–7.4 (m, 2H), 7.33 (d, 1H, J = 3.1 Hz), 6.41 (dd, 1H, J = 0.8, 3.1 Hz), 5.46 (s, 2H), 3.78 (s, 3H); ^{13}C NMR (DMSO-d_6, 126 MHz) δ 181.5, 160.4, 142.2, 136.6, 135.3, 133.7, 132.6, 130.4, 129.8, 129.7, 128.6, 127.6, 118.7, 115.3, 112.0, 109.5, 100.4, 54.1, 32.5.

*4.2.15. 2-[2-(4-Chlorophenoxy)-1,3-thiazol-5-yl]-N-(1-methyl-1H-indol-5-yl)-2-oxoacetamide (**15**)*

*Step 1. Ethyl 2-bromo-1,3-thiazole-4-carboxylate (**15b**).* 2-Aminothiazole-4-carboxylate (**15a**) (2 g, 11.6 mmol) was dissolved in acetonitrile (20 mL) and to this stirred solution was added copper(II) bromide (2.6 g, 11.6 mmol) at 0 °C. The resulting mixture was stirred for 20 min at room temperature. Then it was cooled to 0 °C and *tert*-butyl nitrite (1.54 g) was added and stirred for further 2 h at room temperature. After the completion of the reaction, the reaction mixture was concentrated under reduced pressure and the residue was purified by column chromatography using a mixture of 20%EtOAc and 80%petrolether as the eluent. Yield: 1.5 g (57%).

*Step 2. Ethyl 2-(4-chlorophenoxy)-1,3-thiazole-4-carboxylate (**15c**)* A stirred solution of 4-chlorophenol (3.78 mL, 38.5 mmol) in THF (50 mL) was cooled to 0 °C and potassium *tert*-butoxide (5.15 g, 45.9 mmol) was portionwise added. The reaction mixture was refluxed for 2 h and the solvent was evaporated. The obtained potassium salt was suspended in DMSO (60 mL), **15b** (9 g, 38.1 mmol) was added and the mixture was heated at 85 °C for 16 h. After completion of the reaction, the reaction mixture was poured into cooled water and extracted with EtOAc (3 × 350 mL). The combined organic phase was washed with brine, dried (Na_2SO_4) and evaporated under reduced pressure to obtain the crude **15c** (6.05 g, 55.4%). It was used without further purification.

*Step 3. 2-(4-Chlorophenoxy)-1,3-thiazole-4-carbaldehyde (**15d**)* To the stirred solution of **15c** (1.5 g, 5.3 mmol) in CH_2Cl_2 (15 mL) cooled to −70 °C was dropwise added DIBAL-H (1 M solution, 8.3 mL, 8.3 mmol) and it was stirred for 3 h at −70 °C. After completion of the reaction, the reaction mixture was quenched with aqueous citric acid solution at −70 °C. The mixture was stirred for 20 min at room temperature, extracted with CH_2Cl_2 (2 × 100 mL) and the combined organic layer was dried over Na_2SO_4 and evaporated to dryness. Yield: 0.95 g (75%).

Step 4. [2-(4-Chlorophenoxy)-1,3-thiazol-4-yl*](hydroxy)acetonitrile (**15e**).* Intermediate **15d** (0.9 g, 3.76 mmol) was solved in CH_2Cl_2 (10 mL) and the mixture was cooled to 0 °C. Methylmorpholine-*N*-oxide (0.13 g, 1.1 mmol) and trimethylsilyl cyanide (TMSCN) (0.7 mL, 5.6 mmol) were added to the solution and it was allowed to warm up to room temperature and stirred for 16 h. After completion of the reaction, the mixture was poured into water, the aqueous phase was extracted with CH_2Cl_2 (2 × 100 mL). The organic phase was dried and evaporated to dryness. Yield: 0.85 g (84%).

Step 5. [2-(4-Chlorophenoxy)-1,3-thiazol-4-yl*](hydroxy)acetic acid (**15f**).* To **15e** (0.85 g, 3.19 mmol) was added cc HCl (5 mL) and the mixture was refluxed for 3 h. It was poured to cooled water and extracted with EtOAc. The organic layer was dried over Na_2SO_4 and

evaporated. Yield: 0.65 g (72%).

*Step 6. Methyl [2-(4-chlorophenoxy)-1,3-thiazol-*4-yl*](hydroxy) acetate (**15g**).* To a stirred and cooled solution of **15f** (0.65 g, 2.27 mmol) in MeOH (10 mL) was added cc. sulfuric acid (1 mL, 18.8 mmol). The reaction mixture was allowed to reach room temperature and was stirred for an hour at this temperature. Methanol was evaporated and the residue was poured into cooled water and extracted with EtOAc. The organic layer was dried over Na_2SO_4 and evaporated. Yield: 0.55 g (81%).

*Step 7. Methyl [2-(4-chlorophenoxy)-1,3-thiazol-*4-yl*](oxo)acetate (**15h**)* To a stirred and cooled solution of **15g (**1 g, 3.33 mmol) in CH_2Cl_2 (10 mL) was added Dess-Martin periodinane (1.7 g, 4 mmol). The reaction mixture was allowed to reach room temperature and stirred for 3 h at this temperature. To the reaction mixture, cold water was added and it was extracted with EtOAc. The organic layer was dried over Na_2SO_4 and evaporated. Yield: 0.5 g (50%).

Step 8–9. The hydrolysis was accomplished in the same way as it is described in case of **11c.** The amide coupling was achieved in an analogous way as it is described in case of **23.** Yield 13.7%. Mp 170–171 °C. HESI-HRMS: calcd for $C_{20}H_{15}O_3N_3ClS$ $[M+H]^+$: 412.05172; found: 412.05132; delta = −0.96 ppm. ^{1}H NMR (DMSO-d_6, 500 MHz) δ 10.66 (s, 1H), 8.63 (s, 1H), 8.0–8.0 (m, 1H), 7.6–7.6 (m, 2H), 7.5–7.5 (m, 2H), 7.4–7.5 (m, 2H), 7.34 (d, 1H, J = 3.1 Hz), 6.42 (d, 1H, J = 3.1 Hz), 3.78 (s, 3H); ^{13}C NMR (DMSO-d_6, 126 MHz) δ 180.6, 172.0, 161.1, 153.2, 144.5, 133.8, 130.46, 130.45, 130.3, 130.1, 129.5, 127.6, 122.3, 115.2, 112.0, 109.6, 100.4, 32.5.

4.2.16. N-(1-methyl-1H-indol-5-yl)-2-[4-(4-methylphenoxy) phenyl]-2-oxoacetamide (*16*)

*Step 1. Ethyl [4-(4-methylphenoxy)phenyl](oxo)acetate (**16b**).* 1-Methyl-4-phenoxybenzene (**16a**, 5.83 g, 31.6 mmol) was dissolved in chloroform (90 mL) and cooled down to 0 °C. To the solution was added ethyl chlorooxoacetate (4 mL, 37.3 mmol), followed by the portionwise addition of $AlCl_3$ (12.66 g, 94.9 mmol). The solution was stirred for an hour at 0 °C, allowed to warm up to room temperature and it was stirred overnight. The reaction mixture was quenched with water, stirred for an hour and extracted with CH_2Cl_2. The organic layer was washed with 5% $NaHCO_3$ solution twice and brine, dried and evaporated. The crude **16b** was purified with column chromatography (eluent: cyclohexane/EtOAc = 95/5). Yield: 2.608 g (29%).

Step 2–3. The hydrolysis was accomplished in the same way as it is described in case of **11c.** The amide coupling was achieved in an analogous way as it is described in case of **23.** Yield 41.2%. Mp 127–128 °C. HESI-HRMS: calcd for $C_{24}H_{21}O_3N_2$ $[M+H]^+$: 385.15467; found: 385.15422; delta = −1.17 ppm. ^{1}H NMR (DMSO-d_6, 500 MHz) δ 10.72 (s, 1H), 8.1–8.1 (m, 2H), 8.0–8.0 (m, 1H), 7.4–7.4 (m, 2H), 7.34 (d, 1H, J = 3.0 Hz), 7.3–7.3 (m, 2H), 7.0–7.1 (m, 4H), 6.42 (d, 1H, J = 3.0 Hz), 3.78 (s, 3H), 2.33 (s, 3H); ^{13}C NMR (DMSO-d_6, 126 MHz) δ 188.3, 163.0, 162.8, 152.1, 134.3, 133.7, 132.6, 130.7, 130.4, 129.7, 127.7, 127.1, 120.2, 116.8, 115.0, 111.8, 109.6, 100.3, 32.5, 20.3.

4.2.17. N-(1-methyl-1H-indol-5-yl)-2-[6-(4-methylphenoxy) pyridin-3-yl]-2-oxoacetamide (*17*)

*Step 1. ethyl 2-[6-(4-methylphenoxy)pyridin-*3-yl*]-2-oxoacetate (**17b**).* Under argon atmosphere, 5-bromo-(4-methylphenoxy)pyridine (**17a**, 610 mg, 2.3 mmol) was dissolved in toluene and cooled down to −78 °C. To the solution, BuLi (2.5 M in hexane, 924 μL, 2.3 mmol) was dropwise added and it was stirred for 40 min. Diethyl oxalate (502 μL, 3.7 mmol) was dropwise added and the reaction mixture was stirred at −78 °C for 8 h. After completion it was quenched with sat. NH_4Cl solution and extracted with EtOAc. The combined organic layer was washed with brine, dried and evaporated. The crude **17b** was purified with column chromatography (eluent: cyclohexane/EtOAc = 8/2). Yield: 0.331 g (50%).

Step 2–3. The hydrolysis was accomplished in the same way as it is described in case of **11c.** The amide coupling was achieved in an analogous way as it is described in case of **11.** Yield 13.0%. Mp 166–168 °C. HESI-HRMS: calcd for $C_{23}H_{20}O_3N_3$ $[M+H]^+$: 386.14992; found: 386.14929; delta = −1.63 ppm. ^{1}H NMR (DMSO-d_6, 500 MHz) δ 10.73 (s, 1H), 8.90 (dd, 1H, J = 0.7, 2.4 Hz), 8.48 (dd, 1H, J = 2.4, 8.7 Hz), 8.05 (dd, 1H, J = 0.5, 1.9 Hz), 7.5–7.5 (m, 1H), 7.4–7.4 (m, 1H), 7.34 (d, 1H, J = 3.1 Hz), 7.2–7.3 (m, 2H), 7.16 (dd, 1H, J = 0.7, 8.7 Hz), 7.1–7.1 (m, 2H), 6.43 (dd, 1H, J = 0.7, 3.1 Hz), 3.78 (s, 3H), 2.34 (s, 3H); ^{13}C NMR (DMSO-d_6, 126 MHz) δ 186.9, 166.3, 161.3, 151.2, 150.5, 141.4, 134.6, 133.8, 130.4, 130.2, 129.5, 127.6, 124.5, 121.3, 115.2, 112.0, 111.1, 109.6, 100.4, 32.5, 20.3.

4.2.18. N-(1-methyl-1H-indol-5-yl)-2-[5-(4-methylphenoxy) pyrazin-2-yl]-2-oxoacetamide (*18*)

*Step 1. 2-Bromo-5-(4-methylphenoxy)pyrazine (**18b**).* A flask was charged with 2,5-dibromopyrazine (**18a**, 2 g, 8.4 mmol), *p*-cresol (0.91 g, 8.4 mmol), potassium carbonate (2.32 g, 16.8 mmol) and DMF (15 mL) and the reaction mixture was refluxed overnight. After completion it was quenched with water and extracted with CH_2Cl_2. The organic layer was washed with brine dried and evaporated. The crude product **18b** was purified with column chromatography (eluent: cyclohexane/EtOAc = 4/1). Yield: 2.15 g (97%).

*Step 2. 1-[5-(4-Methylphenoxy)pyrazin-*2-yl*]ethan-1-one (**18d**).* Argon was bubbled through toluene (43 mL) for 10 min, **18b** (1.45 g, 5.47 mmol), $Pd(PPh_3)_4$ (63.2 mg, 0.05 mmol) and [1-ethoxy-1-(tributhylstannylethylene)] (**18c**, 2.2 mL, 6.5 mmol) were added. The reaction mixture was refluxed overnight. To the mixture was added 1 M HCl solution (37.5 mL) and the mixture was stirred for 2 h at 70 °C. After completion, it was quenched with 2 M NaOH solution and the phases were separated. The organic layer was dried and evaporated. The **18d** crude product was purified with column chromatography (eluent: cyclohexane/EtOAc = 4/1). Yield: 970 mg (77%).

*Step 3. [5-(4-Methylphenoxy)pyrazin-*2-yl*](oxo)acetic acid (**18e**).* A flask was charged with **18d (**355 mg, 1.56 mmol), pyridine (10 mL) and SeO_2 (518 mg, 4.67 mmol) and the mixture was stirred for 2 days at 70 °C. After completion, the reaction mixture was filtered through celite and evaporated. To the residue cold water was added and it was acidified with 50% phosphoric acid to pH = 2. The resulting solution was extracted with EtOAc, the organic layers were combined, dried and evaporated. The **18e** crude product was reacted without any further purification. Yield: 121 mg (30%).

Step 4. The amide coupling was achieved in an analogous way as it is described in case of **11.** Yield 3.0%. Mp 155–157 °C. HESI-HRMS: calcd for $C_{22}H_{19}O_3N_4$ $[M+H]^+$: 387.14517; found: 387.14432; delta = −2.19 ppm. ^{1}H NMR (DMSO-d_6, 500 MHz) δ 10.75 (s, 1H), 8.91 (d, 1H, J = 1.3 Hz), 8.70 (d, 1H, J = 1.3 Hz), 7.98 (d, 1H, J = 2.0 Hz), 7.4–7.4 (m, 1H), 7.4–7.4 (m, 1H), 7.34 (d, 1H, J = 3.0 Hz), 7.3–7.3 (m, 2H), 7.2–7.2 (m, 2H), 6.43 (dd, 1H, J = 0.8, 3.0 Hz), 3.79 (s, 3H), 2.34 (s, 3H); ^{13}C NMR (DMSO-d_6, 126 MHz) δ 188.0, 163.0, 161.5, 149.8, 143.5, 140.2, 135.5, 135.2, 133.7, 130.5, 130.2, 129.8, 127.7, 121.2, 114.7, 111.4, 109.7, 100.4, 32.5, 20.3.

4.2.19. N-(1,3-dimethyl-1H-indol-5-yl)-2-{4-[(4-methylphenyl) methyl]piperazin-1-yl}-2-oxoacetamide (*19*)

The amide coupling was achieved in an analogous way as it is described in case of **11**. Yield 12.4%. Mp 88–91 °C. HESI-HRMS: calcd for $C_{24}H_{29}O_2N_4$ $[M+H]^+$: 405.22850; found: 405.22788; delta = −1.54 ppm. ^{1}H NMR (DMSO-d_6, 500 MHz) δ 10.53 (s, 1H), 7.8–7.9 (m, 1H), 7.3–7.3 (m, 1H), 7.3–7.3 (m, 1H), 7.2–7.2 (m, 2H), 7.1–7.2 (m, 2H), 7.07 (q, 1H, J = 1.0 Hz), 3.69 (s, 3H), 3.5–3.6 (m, 4H), 3.48 (s, 2H), 2.4–2.4 (m, 4H), 2.28 (s, 3H), 2.20 (d, 3H, J = 1.0 Hz); ^{13}C NMR (DMSO-d_6, 126 MHz) δ 162.8, 161.4, 136.0, 134.4, 133.9, 129.3,

128.9, 128.7, 128.0, 127.7, 114.8, 109.7, 109.4, 108.5, 61.4, 52.5, 51.7, 45.6, 40.7, 32.1, 20.6, 9.3.

4.2.20. N-(2,3-dimethyl-1H-indol-5-yl)-2-{4-[(4-methylphenyl) methyl]piperazin-1-yl}-2-oxoacetamide (**20**)

The amide coupling was achieved in an analogous way as it is described in case of **11**. Yield 23.0%. Mp 113–116 °C. HESI-HRMS: calcd for $C_{24}H_{29}O_2N_4$ $[M+H]^+$: 405.22850; found: 405.22766; delta = −2.08 ppm. ^{1}H NMR (DMSO-d_6, 500 MHz) δ 10.63 (s, 1H), 10.44 (s, 1H), 7.7–7.7 (m, 1H), 7.2–7.2 (m, 2H), 7.1–7.2 (m, 4H), 3.4–3.6 (m, 6H), 2.3–2.5 (m, 4H), 2.29 (s, 3H), 2.28 (s, 3H), 2.11 (s, 3H); ^{13}C NMR (DMSO-d_6, 126 MHz) δ 162.9, 161.3, 136.0, 134.4, 132.3, 132.3, 129.0, 128.9, 128.7, 128.5, 113.6, 110.0, 108.8, 105.0, 61.4, 52.5, 51.6, 45.6, 40.6, 20.6, 11.2, 8.3.

4.2.21. N-(3-fluoro-1-methyl-1H-indol-6-yl)-2-{4-[(4-methylphenyl)methyl]piperazin-1-yl}-2-oxoacetamide (**21**)

3-Fluoro-1-methyl-1*H*-indol-6-amine was synthesized in an analogous way as it is described in the following reference [54]. The amide coupling was achieved in an analogous way as it is described in case of **11**. Yield 26.0%. Mp 127–128 °C. HESI-HRMS: calcd for $C_{23}H_{26}O_2N_4F$ $[M+H]^+$: 409.20343; found: 409.20235; delta = −2.64 ppm. ^{1}H NMR (DMSO-d_6, 500 MHz) δ 10.77 (s, 1H), 7.9–8.0 (m, 1H), 7.48 (d, 1H, J = 8.5 Hz), 7.31 (d, 1H, J = 2.7 Hz), 7.2–7.2 (m, 3H), 7.1–7.2 (m, 2H), 3.67 (s, 3H), 3.5–3.6 (m, 4H), 3.48 (s, 2H), 2.4–2.4 (m, 4H), 2.28 (s, 3H); ^{13}C NMR (DMSO-d_6, 126 MHz) δ 162.5, 161.7, 143.0 (d, J = 238.8 Hz), 136.0, 134.4, 133.1, 132.5 (d, J = 5.0 Hz), 128.9, 128.7, 116.4 (d, J = 2.2 Hz), 112.9, 112.8 (d, J = 16.5 Hz), 112.5 (d, J = 26.6 Hz), 100.9, 61.4, 52.5, 51.6, 45.6, 40.8, 32.3, 20.6.

4.2.22. N-(6-fluoro-1-methyl-1H-indol-5-yl)-2-{4-[(4-methylphenyl)methyl]piperazin-1-yl}-2-oxoacetamide (**22**)

*Step 1. 6-Fluoro-5-nitro-1H-indole-2,3-dione (**22b**).* To a solution of $NaNO_3$ (0.5 g, 6.06 mmol) in conc. H_2SO_4 (3.8 mL, 71 mmol) was added dropwise a solution of 6-fluoro-1*H*-indole-2,3-dione (**22a**) (1 g, 6.06 mmol) and conc. H_2SO_4 (10 mL) over a period of 1 h at 0 °C. The reaction mass was then poured to ice water, stirred for 10–15 min, the precipitate was filtered off and dried to get the desired product **22b.** Yield: 1.15 g (90%).

*Step 2. 6-Fluoro-5-nitro-1H-indole (**22c**).* To a solution of **22b** (1.1 g, 5.2 mmol) solved in THF (22 mL) was added borane-THF complex solution (1 M, 12.2 mL, 12.2 mmol) at 0 °C under nitrogen atmosphere. The reaction mixture was allowed to reach room temperature and stirred for 1.5 h 1 M HCl solution was added to reaction mixture and the volatile components were evaporated and the aqueous residue was extracted with EtOAc. The combined organic layer was dried and evaporated, and the residue was purified with column chromatography. Yield: 0.33 g (35%).

*Step 3. 6-Fluoro-1-methyl-5-nitro-1H-indole (**22d**).* NaH (60 m/m % mineral oil suspension, 0.126 g, 3.15 mmol) was added slowly to the solution of **22c** (0.33 g, 1.83 mmol) in DMF (6.6 mL) under nitrogen atmosphere at 0 °C. It was stirred for 0.5 h at 0 °C and then MeI (0.39 g, 2.74 mmol) was slowly added to the reaction mass over 20–25 min at 0 °C. After the completion of the addition the reaction mass allowed to warm up to room temperature and the reaction mixture was stirred for 1 h at this temperature. Ice cold water was added and reaction mixture was extracted with EtOAc. After evaporation of the solvent the desired product **22d** was obtained. Yield: 0.35 g (99%).

*Step 4. 6-Fluoro-1-methyl-1H-indol-5-amine (**22e**).* 6-Fluoro-1-methyl-5-nitro-1*H*-indole (**22d**, 150 mg, 0.77 mmol) was dissolved in MeOH (10 mL). Pd/C (10 mg) was added and the reaction mixture was stirred at room temperature under hydrogen atmosphere overnight. Then the reaction solution was filtered and the filtrate was concentrated to afford **22e**. Yield: 105 mg (83%).

Step 5. The amide coupling was achieved in an analogous way as it is described in case of **23.** Yield 29.0%. Mp 122–124 °C. HESI-HRMS: calcd for $C_{23}H_{26}O_2N_4F$ $[M+H]^+$: 409.20343; found: 409.20245; delta = −2.40 ppm. ^{1}H NMR (DMSO-d_6, 500 MHz) δ 10.35 (s, 1H), 7.73 (d, 1H, J = 7.6 Hz), 7.41 (d, 1H, J = 11.3 Hz), 7.34 (d, 1H, J = 3.1 Hz), 7.2–7.2 (m, 2H), 7.1–7.2 (m, 2H), 6.42 (dd, 1H, J = 0.8, 3.1 Hz), 3.75 (s, 3H), 3.52 (br s, 4H), 3.48 (br s, 2H), 2.4–2.5 (m, 4H), 2.29 (s, 3H); ^{13}C NMR (DMSO-d_6, 126 MHz) δ 162.7, 162.6, 152.2 (d, J = 238.4 Hz), 136.0, 134.4, 133.9 (d, J = 11.8 Hz), 130.7 (d, J = 3.2 Hz), 128.9, 128.7, 123.7, 117.0 (d, J = 1.7 Hz), 116.6 (d, J = 15.4 Hz), 100.5, 96.5 (d, J = 25.0 Hz), 61.4, 52.4, 51.6, 45.5, 40.7, 32.6, 20.6.

4.2.23. N-(3-fluoro-1-methyl-1H-indol-5-yl)-2-{4-[(4-methylphenyl)methyl]piperazin-1-yl}-2-oxoacetamide (**23**)

To a suspension of 2-{4-[(4-methylphenyl)methyl]piperazin-1-yl}-2-oxoacetic acid (**11c**, 39.3 mg, 0.15 mmol) and 3-fluoro-1-methyl-1*H*-indol-5-amine (**23a**, 24.6 mg, 0.15 mmol) in dry DMF (1 mL) was added HATU (57.03 mg, 0.15 mmol, 1 eq) and DIPEA (104 μL, 4 eq) at room temperature. The mixture was shaken at RT overnight. After the completion of the reaction (monitored by TLC) the mixture was diluted with brine and extracted with EtOAc (3 × 20 mL). The combined organic phase was washed with brine (3 × 20 mL), dried over anhydrous Na_2SO_4, filtered and concentrated *in vacuo*. The residue was purified by flash chromatography on silica gel eluting with 40% EtOAc in cyclohexane. The desired product **23** was crystallized from Et_2O as well to yield 18 mg (30%) of the title compound as white solid. LC-MS (ESI) *m/z* $[M+H]^+$ = 408.5. Yield 29.7%. Mp 138–139 °C. HESI-HRMS: calcd for $C_{23}H_{26}O_2N_4F$ $[M+H]^+$: 409.20343; found: 409.20250; delta = −2.27 ppm. ^{1}H NMR (DMSO-d_6, 500 MHz) δ 10.66 (s, 1H), 7.95 (d, 1H, J = 1.9 Hz), 7.4–7.4 (m, 1H), 7.3–7.4 (m, 2H), 7.2–7.2 (m, 2H), 7.1–7.2 (m, 2H), 3.70 (s, 3H), 3.5–3.6 (m, 2H), 3.5–3.5 (m, 2H), 3.48 (s, 2H), 2.4–2.4 (m, 4H), 2.28 (s, 3H); ^{13}C NMR (DMSO-d_6, 126 MHz) δ 162.6, 161.6, 142.9 (d, J = 238.3 Hz), 136.0, 134.4, 130.1, 130.0 (d, J = 5.1 Hz), 128.9, 128.7, 116.0, 115.4 (d, J = 15.4 Hz), 113.3 (d, J = 26.2 Hz), 110.4, 106.7 (d, J = 2.0 Hz), 61.4, 52.5, 51.7, 45.6, 40.8, 32.4, 20.6.

4.2.24. N-(3-chloro-1-methyl-1H-indol-5-yl)-2-{4-[(4-methylphenyl)methyl]piperazin-1-yl}-2-oxoacetamide (**24**)

The synthesis of 3-chloro-1-methyl-1*H*-indol-5-amine is detailed in the following chemical literature [55]. The amide coupling was achieved in an analogous way as it is described in case of **23**. Yield 32.4%. Mp 109–110 °C. HESI-HRMS: calcd for $C_{23}H_{26}O_2N_4Cl$ $[M+H]^+$: 425.17388; found: 425.17322; delta = −1.55 ppm. ^{1}H NMR (DMSO-d_6, 500 MHz) δ 10.70 (s, 1H), 7.97 (d, 1H, J = 2.0 Hz), 7.53 (s, 1H), 7.47 (d, 1H, J = 8.9 Hz), 7.37 (dd, 1H, J = 2.0, 8.9 Hz), 7.2–7.2 (m, 2H), 7.1–7.2 (m, 2H), 3.76 (s, 3H), 3.5–3.6 (m, 2H), 3.5–3.5 (m, 2H), 3.48 (s, 2H), 2.4–2.4 (m, 4H), 2.28 (s, 3H); ^{13}C NMR (DMSO-d_6, 126 MHz) δ 162.6, 161.6, 136.0, 134.4, 132.5, 130.9, 128.9, 128.7, 127.1, 124.4, 115.9, 110.6, 108.0, 101.9, 61.4, 52.5, 51.7, 45.7, 40.8, 32.7, 20.6.

4.2.25. 4-{[(7-Fluoro-1H-indol-5-yl)carbamoyl]carbonyl}-1-[(4-methylphenyl) methyl]piperazin-1-ium acetate (**25**)

The amide coupling was achieved in an analogous way as it is described in case of **23**. Yield 27.8%. Mp 111–113 °C. HESI-HRMS: calcd for $C_{22}H_{24}O_2N_4F$ $[M+H]^+$: 395.18778; found: 395.18678; delta = −2.53 ppm. ^{1}H NMR (DMSO-d_6, 500 MHz) δ 11.96 (br s, 0.5H, A), 11.57 (br s, 1H), 10.66 (s, 1H), 7.70 (d, 1H, J = 1.6 Hz), 7.40 (dd, 1H, J = 2.4, 3.0 Hz), 7.25 (dd, 1H, J = 1.6, 13.0 Hz), 7.2–7.2 (m, 2H), 7.1–7.2 (m, 2H), 6.50 (ddd, 1H, J = 2.0, 3.0, 3.4 Hz), 3.5–3.6 (m, 2H), 3.5–3.5 (m, 2H), 3.48 (s, 2H), 2.40 (q, 4H, J = 5.1 Hz), 2.28 (s, 3H), 1.91 (s, 2H, A); (A: acetic acid); ^{13}C NMR (DMSO-d_6, 126 MHz) δ 172.0 (A), 162.6,

161.5, 148.1 (d, $J = 241.9$ Hz), 136.0, 134.4, 130.8 (d, $J = 6.7$ Hz), 129.8 (d, $J = 8.9$ Hz), 128.9, 128.7, 127.2, 120.7 (d, $J = 13.1$ Hz), 107.0 (d, $J = 3.2$ Hz), 102.2 (d, $J = 1.9$ Hz), 100.1 (d, $J = 20.8$ Hz), 61.4, 52.5, 51.7, 45.6, 40.8, 21.0 (A), 20.6; (A: acetic acid).

4.2.26. N-{1-methyl-1H-pyrrolo[2,3-b]pyridin-5-yl}-2-{4-[(4-methylphenyl)methyl]piperazin-1-yl}-2-oxoacetamide (**26**)

The amide coupling was achieved in an analogous way as it is described in case of **23**. Yield 31.3%. Mp 85–87 °C. HESI-HRMS: calcd for $C_{22}H_{26}O_2N_5$ $[M+H]^+$: 392.20810; found: 392.20764; delta = −1.18 ppm. ^{1}H NMR (DMSO-d_6, 500 MHz) δ 10.80 (s, 1H), 8.41 (d, 1H, $J = 2.3$ Hz), 8.28 (d, 1H, $J = 2.3$ Hz), 7.52 (d, 1H, $J = 3.4$ Hz), 7.2–7.2 (m, 2H), 7.1–7.2 (m, 2H), 6.45 (d, 1H, $J = 3.4$ Hz), 3.80 (s, 3H), 3.5–3.6 (m, 4H), 3.48 (s, 2H), 2.4–2.5 (m, 4H), 2.28 (s, 3H); ^{13}C NMR (DMSO-d_6, 126 MHz) δ 162.4, 161.8, 144.6, 136.0, 136.0, 134.4, 131.0, 128.9, 128.7, 127.4, 119.9, 119.2, 98.7, 61.4, 52.5, 51.7, 45.7, 40.8, 30.8, 20.6.

4.2.27. N-{3-fluoro-1-methyl-1H-pyrrolo[2,3-b]pyridin-5-yl}-2-{4-[(4-methylphenyl)methyl]piperazin-1-yl}-2-oxoacetamide (**27**)

*Step 1. 5-Bromo-3-fluoro-1H-pyrrolo[2,3-b]pyridine (**27b**).* Under an argon atmosphere, 5-bromo-7-azaindole (**27a**) (1.86 g, 9.4 mmol) was dissolved in a mixture of dry acetonitrile (225 mL) and conc. acetic acid (45 mL). The solution was heated to 40 °C, Selectfluor (5 g, 14.1 mmol, 1.5 eq) was added, the resulted mixture was heated to 80 °C and stirred overnight under these conditions. It was evaporated to dryness, the crude product was dissolved in EtOAc (200 mL) and washed twice with water. The organic layer was dried over Na_2SO_4 and evaporated. After flash column chromatography (eluent: CH_2Cl_2/MeOH = 99/1) 362 mg of product was isolated (18%).

*Step 2. 5-Bromo-3-fluoro-1-methyl-1H-pyrrolo[2,3-b]pyridine (**27c**).* A solution of **27b** (300 mg, 1.4 mmol) in dry THF (12 mL) was cooled to 0 °C and NaH (140 mg, 60 m/m% mineral oil suspension, 3.5 mmol, 2.5 eq) was added in portions. Afterwards the solution was allowed to warm up to room temperature (approx. 30 min) and iodomethane (397 mg, 2 eq) was added dropwise and the mixture was stirred overnight. The reaction was quenched by the addition of water. The mixture was extracted three times with EtOAc. The extract was dried over Na_2SO_4, filtered and evaporated to dryness to obtain 320 mg of yellowish brown oil (**27c**), which was used without further purification.

*Step 3. N-benzyl-3-fluoro-1-methyl-1H-pyrrolo[2,3-b]pyridin-5-amine (**27d**).* Compound **27c** (320 mg, 1.4 mmol) was dissolved in dry toluene(15 mL). Argon was streamed through the solution for 20 min. Afterwards, benzylamine (0.305 mL, 2.8 mmol), NaO^{t}Bu (405 mg, 4.2 mmol), RuPhos (66 mg, 0.14 mmol) and $Pd_2(dba)_3$ (65 mg, 0.07 mmol) were added. The reaction mixture was heated to 105 °C overnight. The mixture was allowed to cool to ambient temperature, water was added and the mixture was extracted with EtOAc, dried over Na_2SO_4 and evaporated to dryness. The obtained **27d** was used without further purification.

*Step 4. 3-Fluoro-1-methyl-1H-pyrrolo[2,3-b]pyridin-5-amine (**27e**)* Compound **27d** (96 mg, 0.376 mmol) was hydrogenated in a mixture of methanol (6 mL) and EtOAc (6 mL) with 10% Pd/C (35 mg) at atmospheric pressure for 48 h. The catalyst was filtered off, and the solvent was evaporated. The crude product was purified with flash chromatography, using EtOAc as the eluent to obtain 23 mg of **27e** (37%).

*Step 5. N-{3-Fluoro-1-methyl-1H-pyrrolo[2,3-b]pyridin-5-yl}-2-{4-[(4-methylphenyl)methyl] piperazin-1-yl}-2-oxoacetamide (**27**).* 2-{4-[(4-methylphenyl)methyl]piperazin-1-yl}-2-oxoacetic acid (**11c**, 40 mg, 0.152 mmol) was dissolved in dry DMF (1 mL) under an argon atmosphere. To this solution was added 1-chloro-*N*,*N*,2-trimethyl-1-propenylamine (Ghosez' reagent) (22.4 mg, 23 μL, 0.168 mmol, 1.1 eq) and the mixture was stirred at room temperature for 30 min under argon atmosphere. Afterwards, a solution of 3-fluoro-1-methyl-1*H*-pyrrolo[2,3-*b*]pyridin-5-amine (**27e**) (23 mg, 0.14 mmol, 0.91 eq) and Et_3N (22 μL, 15.5 mg, 0.155 mmol) in DMF (0.5 mL) were added and the reaction mixture was stirred for 4 h at room temperature under argon atmosphere. After the completion of the reaction (monitored by TLC) the mixture was poured onto water (8 mL) and extracted with EtOAc (2 × 15 mL). The organic layer was dried over anhydrous Na_2SO_4, filtered and concentrated *in vacuo*. The residue was chromatographed on silica gel eluting with EtOAc to yield 16 mg (28%) of the title compound **27.** LC-MS (ESI) *m/z* $[M+H]^+ = 410.2$. Mp 129–131 °C. HESI-HRMS: calcd for $C_{22}H_{25}O_2N_5F$ $[M+H]^+$: 410.19868; found: 410.19808; delta = −1.46 ppm. ^{1}H NMR (DMSO-d_6, 500 MHz) δ 10.93 (s, 1H), 8.45 (d, 1H, $J = 2.3$ Hz), 8.34 (d, 1H, $J = 2.3$ Hz), 7.57 (d, 1H, $J = 2.1$ Hz), 7.2–7.2 (m, 2H), 7.1–7.2 (m, 2H), 3.76 (s, 3H), 3.5–3.6 (m, 4H), 3.48 (s, 2H), 2.4–2.4 (m, 4H), 2.28 (s, 3H); ^{13}C NMR (DMSO-d_6, 126 MHz) δ 162.2, 161.9, 139.8 (d, $J = 4.2$ Hz), 140.7 (d, $J = 241.7$ Hz), 137.4, 136.0, 134.3, 128.9, 128.7, 127.6, 115.9 (d, $J = 2.5$ Hz), 113.9 (d, $J = 25.4$ Hz), 107.5 (d, $J = 15.2$ Hz), 61.4, 52.5, 51.6, 45.6, 40.9, 30.5, 20.6.

4.2.28. N-(indolizin-7-yl)-2-{4-[(4-methylphenyl)methyl] piperazin-1-yl}-2-oxoacetamide (**28**)

The amide coupling was achieved in an analogous way as it is described in case of **23**. Yield 48.8%. Mp 181–182 °C. HESI-HRMS: calcd for $C_{22}H_{25}O_2N_4$ $[M+H]^+$: 377.19720; found: 377.19657; delta = −1.68 ppm. ^{1}H NMR (DMSO-d_6, 400 MHz) δ 10.67 (s, 1H), 8.20 (d, 1H, $J = 7.5$ Hz), 7.88 (d, 1H, $J = 2.1$ Hz), 7.44 (ddd, 1H, $J = 0.5$, 1.5, 2.6 Hz), 7.2–7.2 (m, 2H), 7.1–7.2 (m, 2H), 6.69 (dd, 1H, $J = 2.6$, 3.8 Hz), 6.68 (dd, 1H, $J = 2.1$, 7.5 Hz), 6.3–6.3 (m, 1H), 3.5–3.6 (m, 2H), 3.4–3.5 (m, 4H), 2.4–2.4 (m, 4H), 2.28 (s, 3H); ^{13}C NMR (DMSO-d_6, 101 MHz) δ 162.2, 161.7, 136.0, 134.4, 131.2, 128.8, 128.7, 127.8, 126.2, 113.9, 112.4, 106.2, 105.4, 98.4, 61.4, 52.5, 51.6, 45.6, 40.8, 20.6.

4.2.29. N-(1-methyl-2,3-dihydro-1H-indol-5-yl)-2-{4-[(4-methylphenyl)methyl]piperazin-1-yl}-2-oxoacetamide (**29**)

The amide coupling was achieved in an analogous way as it is described in case of **23**. Yield 19.0%. Mp 114–115 °C. HESI-HRMS: calcd for $C_{23}H_{29}O_2N_4$ $[M+H]^+$: 393.22850; found: 393.22753; delta = −2.47 ppm. ^{1}H NMR (DMSO-d_6, 500-MHz) δ 10.36 (s, 1H), 7.3–7.4 (m, 1H), 7.24 (dd, 1H, $J = 2.1$, 8.4 Hz), 7.2–7.2 (m, 2H), 7.1–7.2 (m, 2H), 6.45 (d, 1H, $J = 8.4$ Hz), 3.5–3.5 (m, 2H), 3.4–3.5 (m, 4H), 3.21 (t, 2H, $J = 8.2$ Hz), 2.84 (t, 2H, $J = 8.2$ Hz), 2.66 (s, 3H), 2.3–2.4 (m, 4H), 2.28 (s, 3H); ^{13}C NMR (DMSO-d_6, 126 MHz) δ 162.8, 161.1, 150.2, 136.0, 134.4, 130.2, 128.8, 128.7, 128.4, 119.1, 117.0, 106.5, 61.4, 55.7, 52.5, 51.6, 45.6, 40.7, 36.1, 28.1, 20.6.

4.2.30. N-[(1-methyl-1H-indol-5-yl)methyl]-2-{4-[(4-methylphenyl)methyl]piperazin-1-yl}-2-oxoacetamide (**30**)

The amide coupling was achieved in an analogous way as it is described in case of **23**. Yield 27.0%. Mp 140–141 °C. HESI-HRMS: calcd for $C_{24}H_{29}O_2N_4$ $[M+H]^+$: 405.22850; found: 405.22747; delta = −2.55 ppm. ^{1}H NMR (DMSO-d_6, 400 MHz) δ 9.13 (t, 1H, $J = 6.0$ Hz), 7.42 (d, 1H, $J = 1.6$ Hz), 7.37 (d, 1H, $J = 8.4$ Hz), 7.30 (d, 1H, $J = 3.1$ Hz), 7.2–7.2 (m, 2H), 7.1–7.2 (m, 2H), 7.07 (dd, 1H, $J = 1.6$, 8.4 Hz), 6.37 (dd, 1H, $J = 0.7$, 3.1 Hz), 4.37 (d, 2H, $J = 6.0$ Hz), 3.76 (s, 3H), 3.4–3.5 (m, 6H), 2.3–2.4 (m, 4H), 2.28 (s, 2H); ^{13}C NMR (DMSO-d_6, 101 MHz) δ 163.2, 163.1, 136.0, 135.5, 134.4, 129.8, 128.9, 128.8, 128.7, 127.8, 120.9, 119.1, 109.5, 100.0, 61.4, 52.4, 51.6, 45.4, 42.0, 40.6, 32.4, 20.6.

*4.2.31. 3-(1-Methyl-1H-indol-5-yl)-1-{4-[(4-methylphenyl)methyl] piperazin-1-yl}propane-1,2-dione (**31**)*

Step 1. Intermediate **31a** was synthesized according to the following reference [56].

*Step 2. Ethyl 2-(acetyloxy)-3-(1-methyl-1H-indol-5-yl)prop-2-enoate (**31c**).* A mixture of ethyl 2-acetoxy-3-bromo-2-propenoate (**31a**, 287 mg, 1.2 mmol), 1-methyl-1*H*-indol-5-boronic acid (**31b**, 175 mg, 1 mmol), K_2CO_3 (414 mg, 3 mmol) and $Pd(PPh_3)_4$ (35 mg, 3 mol%) in dioxane (4 mL) was heated at 90 °C for 4 h under an inert atmosphere. After cooling the reaction mixture to room temperature, the solid material was filtered off, the filtrate was concentrated and purified by column chromatography on silica (eluent: EtOAc-cyclohexane, 1:9) to afford **31c** as a yellow oil (180 mg, 63%).

*Step 3. 3-(1-Methyl-1H-indol-5-yl)-2-oxopropanoic acid (**31d**).* A mixture of **31c** (110 mg, 0.38 mmol), ethanol (3 mL), dioxane (1 mL) and saturated aqueous $NaHCO_3$ solution (1 mL) was heated under reflux for 4 h. After cooling to room temperature, the reaction mixture was concentrated and purified by column chromatography on silica (eluent: methanol-CH_2Cl_2, 1:4) to afford **31d** as yellow solid (66 mg, 81%), which was used immediately in the next reaction step.

*Step 4. 3-(1-Methyl-1H-indol-5-yl)-1-{4-[(4-methylphenyl) methyl]piperazin-1-yl}propane-1,2-dione (**31**).* To a suspension of 1-(4-methylbenzyl)piperazine (**11a**, 58 mg, 0.30 mmol) and 3-(1-methyl-1*H*-indol-5-yl)-2-oxopropanoic acid (**31d**, 66 mg, 0.30 mmol) in dry DMF (3 mL) was added HATU (142 mg, 0.375 mmol, 1.25 eq) and DIPEA (105 μL, 2 eq) at room temperature. The mixture was shaken at RT overnight. After the completion of the reaction (monitored by TLC) the mixture was diluted with brine and extracted with EtOAc (3 × 20 mL). The combined organic phase was washed with brine (3 × 20 mL), dried over anhydrous Na_2SO_4, filtered and concentrated *in vacuo*. The residue was purified by flash chromatography on silica gel eluting with 10% EtOAc in CH_2Cl_2. The desired product **31** was crystallized from Et_2O as well to yield 14 mg (12%) of the title compound as white solid. LC-MS (ESI) *m/z* $[M+H]+=$ 389.49. Mp 95–97 °C. HESI-HRMS: calcd for $C_{24}H_{28}O_2N_3$ $[M+H]^+$: 390.21760; found: 390.21680; delta = −2.06 ppm. ^{1}H NMR (DMSO-d_6, 500 MHz) δ 7.4–7.4 (m, 2H), 7.37 (d, 1H, J = 3.0 Hz), 7.1–7.1 (m, 2H), 7.0–7.0 (m, 2H), 7.0–7.0 (m, 1H), 6.40 (dd, 1H, J = 0.7, 3.0 Hz), 4.04 (s, 2H), 3.80 (s, 3H), 3.3–3.4 (m, 2H), 3.11 (s, 2H), 3.0–3.0 (m, 2H), 2.26 (s, 3H), 2.1–2.2 (m, 2H), 1.5–1.6 (m, 2H); ^{13}C NMR (DMSO-d_6, 126 MHz) δ 198.8, 165.3, 136.0, 135.7, 134.3, 130.1, 128.7, 128.7, 128.5, 122.9, 121.7, 121.4, 109.9, 100.1, 61.3, 51.6, 51.6, 46.5, 44.8, 40.5, 32.5, 20.6.

*4.2.32. N-(1-methyl-1H-indole-5-carbonyl)-4-[(4-methylphenyl) methyl]piperidine-1-carboxamide (**32**)*

*Step 1. 1-Methyl-1H-indole-5-carbonitrile (**32b**).* To a solution of l*H*-indole-5-carbonitrile (**32a**, 356 mg, 2.5 mmol) in THF (16 mL) was added NaH (250 mg, 60% in oil, 6.25 mmol) with vigorous stirring at 0 °C under argon atmosphere. The solution was stirred for 30 min, then iodomethane (710 mg, 312 μL, 5 mmol) was added. The reaction mixture was stirred at room temperature for 6 h. The reaction was quenched with water (50 mL) and extracted with EtOAc (3 × 120 mL). The organic layers were combined, washed with water (2 × 30 mL), dried over anhydrous Na_2SO_4, filtered and concentrated *in vacuo* and the residue (390 mg of **32b)** was used in the next step without further purification.

*Step 2. 1-Methyl-1H-indole-5-carboxamide (**32c**).* To a solution of **32b** (390 mg, 2.5 mmol) in DMSO (10 mL) was added K_2CO_3 (120 mg, 0.87 mmol) with vigorous stirring at 10 °C under argon atmosphere then H_2O_2 (270 μL, 2.5 mmol, 30% solution in water) was added. The reaction mixture was stirred at room temperature for 12 h. The reaction was quenched with water (20 mL) and the precipitated material was filtered off and dried to give 330 mg of **31c** that was used in the next step without further purification.

*Step 3. N-[(1-methylindol-5-yl)carbonyl]-4-[(4-methylphenyl) methyl]piperidine-1-carboxamide (**32**).* Oxalyl chloride (343 mg, 228 μL, 2.7 mmol) was added dropwise into a stirred solution of the carboxamide derivative **32c** (314 mg, 1.8 mmol) in dichloroethane (10 mL) at 0 °C. Then, the mixture was heated at reflux for 20–22 h. The solvent was evaporated *in vacuo* to give the respective crude benzoyl isocyanate (**32d**), which was used immediately in the next step without purification. The crude benzoyl isocyanate derivative in dichloroethane (5 mL) was added to a mixture of 4-(4-methylbenzyl)piperidine hydrochloride (607 mg, 2.7 mmol) and triethylamine (365 mg, 502 μL, 3.6 mmol) in dichloroethane (5 mL). It was stirred at room temperature overnight. The reaction was quenched with water (20 mL) and extracted with CH_2Cl_2 (3 × 10 mL). The organic layers were combined, washed with water (2 × 5 mL), dried over anhydrous Na_2SO_4, filtered and concentrated *in vacuo* and the residue was purified by flash chromatography on silica gel (gradient elution: *n*-hexane to *n*-hexane - EtOAc = 50:50), to obtain **32** (17 mg, 25%), as white-off solid. Mp 160–162 °C. HESI-HRMS: calcd for $C_{24}H_{28}O_2N_3$ $[M+H]^+$: 390.21760; found: 390.21697; delta = −1.62 ppm. ^{1}H NMR (DMSO-d_6, 500 MHz) δ 9.92 (s, 1H), 8.17 (d, 1H, J = 1.7 Hz), 7.70 (dd, 1H, J = 1.7, 8.6 Hz), 7.50 (d, 1H, J = 8.6 Hz), 7.43 (d, 1H, J = 3.1 Hz), 7.0–7.1 (m, 4H), 6.55 (dd, 1H, J = 0.8, 3.1 Hz), 3.83 (s, 3H), 3.7–4.2 (br m, 2H), 2.7–3.0 (br m, 2H), 2.5–2.5 (m, 3H), 2.26 (s, 3H), 1.7–1.8 (m, 1H), 1.5–1.6 (m, 2H), 1.1–1.2 (m, 2H); ^{13}C NMR (DMSO-d_6, 126 MHz) δ 166.7, 152.8, 138.2, 136.8, 134.6, 131.2, 128.8, 128.6, 127.2, 124.0, 121.4, 121.1, 109.3, 101.7, 44.8, 41.6, 37.2, 32.6, 31.5, 20.5.

*4.2.33. 1-Methyl-4-(5-{4-[(4-methylphenyl)methyl]piperazine-1-carbonyl}-1,3,4-oxadiazol-2-yl)-1H-indole (**33**)*

Step 1. 1*H*-indole-4-carboxylic acid (**33a**) (5 g, 31 mmol) was dissolved in ethanol (100 mL), conc. sulfuric acid (1 mL) was added and the resulting solution was refluxed for 6 h. The reaction mixture was evaporated to ca. 15 mL and cold water (60 mL) was added and the pH was adjusted to 10 with saturated NaOH solution. The resulting mixture was extracted with CH_2Cl_2 (2 × 75 mL) and the combined organic layer was dried over Na_2SO_4 and was evaporated to dryness. The **33b** crude product was purified with column chromatography (eluent: CH_2Cl_2/MeOH = 99/1). Yield: 2.97 g (51%).

*Step 2. Ethyl 1-methyl-1H-indole-4-carboxylate (**33c**).* A flask was charged with compound **33b** (2.97 g, 15.7 mmol), acetonitrile (60 mL), potassium carbonate (6.51 g, 3 eq) and dimethyl sulphate(2.7 mL, 1.5 eq). The reaction mixture was stirred at 95 °C overnight, then filtered and evaporated to dryness. The residue was dissolved in EtOAc (75 mL) washed with water (2 × 50 mL) and brine (1 × 50 mL), dried over Na_2SO_4 and evaporated. The **33c** crude product was purified by column chromatography with CH_2Cl_2 as the eluent. Yield: 1.94 g (61%).

*Step 3. 1-Methyl-1H-indole-4-carbohydrazide (**33d**).* A solution of **33c** (1.94 g, 9.55 mmol), and hydrazine hydrate (60 mL) in ethanol (96 mL) was refluxed overnight and then it was evaporated to dryness. The residue was taken up in CH_2Cl_2 and washed with water (2 × 50 mL) and brine (50 mL). The organic phase was dried and evaporated. The residue was treated with diethyl ether and the remaining solid **33d** was filtered off and dried. Yield: 1.05 g (58%).

*Step 4. N'-(1-methyl-1H-indole-4-carbonyl)-2-{4-[(4-methylphenyl)methyl]piperazin-1-yl}-2-oxoacetohydrazide (**33e**).* Compound **11b** (0.6 g, 2.2 mmol), CH_2Cl_2 (100 mL), triethylamine (0.8 mL, 2.5 eq) and HBTU (1.04 g, 1.2 eq) were charged into a flask and the solution was stirred for 20 h at room temperature. After that the solution of **33d** (0.54 g, 1.2 eq) in CH_2Cl_2 (70 mL) was added to the reaction mixture and it was stirred for additional 48 h. The resulting reaction mixture was washed with water (2 × 50 mL) and brine (50 mL). The organic layer was dried over Na_2SO_4 and

evaporated to dryness. After column chromatography (eluent: CH_2Cl_2/MeOH = 95/5) the main product was treated with diethyl ether, **33e** was obtained. Yield: 0.22 g (23%).

*Step 5. 1-Methyl-4-(5-{4-[(4-methylphenyl)methyl]piperazine-1-carbonyl}-1,3,4-oxadiazol-2-yl)-1H-indole (**33**).* A flask was charged with compound **33e** (0.22 g, 0.49 mmol), 1,4-dioxane (15 mL) and triethylamine (0.36 mL, 5 eq) and to the mixture was added thionyl chloride (0.08 mL 2 eq). The reaction mixture (after gas formation) was heated to 100 °C for 1.5 h. After completion of the reaction it was evaporated to dryness. The residue was dissolved in CH_2Cl_2 and washed with water (2 × 30 mL) and brine (40 mL). The organic phase was dried over Na_2SO_4 and evaporated. The crude product was crystalized from diethyl ether, the product **33** was filtered off, washed with diethyl ether and dried. Yield: 65 mg (32%). Mp 134–135 °C. HESI-HRMS: calcd for $C_{24}H_{26}O_2N_5$ $[M+H]^+$: 416.20810; found: 416.20714; delta = −2.31 ppm. ^{1}H NMR (DMSO-d_6, 400 MHz) δ 7.8–7.8 (m, 2H), 7.62 (d, 1H, J = 3.1 Hz), 7.3–7.4 (m, 1H), 7.2–7.2 (m, 2H), 7.1–7.2 (m, 2H), 7.06 (dd, 1H, J = 0.7, 3.1 Hz), 3.9–4.0 (m, 2H), 3.90 (s, 3H), 3.7–3.8 (m, 2H), 3.50 (s, 2H), 2.4–2.5 (m, 4H), 2.29 (s, 3H); ^{13}C NMR (DMSO-d_6, 101 MHz) δ 164.8, 157.0, 153.2, 136.9, 136.0, 134.4, 132.4, 128.8, 128.7, 125.1, 120.9, 119.5, 114.4, 113.2, 100.6, 61.3, 52.6, 51.7, 46.5, 42.2, 32.7, 20.6.

*4.2.34. 5-(5-{4-[(4-Chlorophenyl)methyl]piperazine-1-carbonyl}-1-methyl-1H-pyrazol-3-yl)-1H-indole (**34**)*

*Step 1. Ethyl 4-(1H-indol-5-yl)-2,4-dioxobutanoate (**34b**).* In a nitrogen atmosphere dry ethanol (5 mL) was added to a flask and sodium was carefully added (0.202 g, 8.79 mmol). The mixture was cooled to 0–5 °C with an ice bath. Through a septum a solution of diethyl oxalate (1.02 mL, 7.54 mmol), 5-acetylindole (**34a**, 1 g, 6.28 mmol) and ethanol (5 mL) were added slowly, in a drop by drop manner. The resulting solution was stirred in an ice bath for 1 h and it was warmed up to reflux and stirred for further 2 h. After completion of the reaction, water was added (carefully at the beginning) and the mixture was acidified with 1 M HCl. The formed precipitate was filtered off and dried at 40 °C to give **34b.** Yield: 1.353 g (83%).

*Step 2. Ethyl 3-(1H-indol-5-yl) -1-methyl-1H-pyrazole-5-carboxylate (**34c**).* In a nitrogen atmosphere, **34b** (1.353 g, 5.22 mmol) was solved in dry ethanol (15 mL) and methylhydrazine (0.185 mL, 5.74 mmol) was added dropwise. The mixture was refluxed for 3 h. After completion, the reaction mixture was cooled down and evaporated to dryness. The solid residue was dissolved in EtOAc and washed twice with water. The organic phase was dried and evaporated to dryness. The crude product was purified with flash chromatography (eluent: heptane/EtOAc) to result in **34c.** Yield: 520 mg.

*Step 3. 3-(1H-indol-5-yl)-1-methyl-1H-pyrazole-5-carboxylic acid (**34d**).* **34c** (130 mg, 0.483 mmol) was dissolved in a mixture of ethanol (5 mL) and water (0.5 mL). Potassium hydroxide was added (81 mg, 1.448 mmol) and the solution was stirred at room temperature for 3 h. The solvent was evaporated to dryness. Water was added and the solution was acidified (pH = 1) with 1 M HCl. The mixture was extracted 3 times with EtOAc. The combined organic phase was dried and evaporated to dryness. Yield: 135 mg.

*Step 4. 5-(5-{4-[(4-Chlorophenyl)methyl]piperazine-1-carbonyl}-1-methyl-1H-pyrazol-3-yl)-1H-indole (**34**).* In a N_2 atmosphere, a flask was charged with **34d** (116 mg, 0.481 mmol), CH_2Cl_2 (3–5 mL) and triethylamine (0.268 mL, 1.923 mmol). (If not dissolved, few drops of DMF could be added.) 1-(4-chlorobenzyl)piperazine (122 mg, 0.577 mmol) and 1-propanephosphonic acid cyclic anhydride (50% in EtOAc) (0.567 mL, 0.962 mmol) were slowly added. The mixture was stirred at room temperature for 2 h. It was diluted with CH_2Cl_2 and washed with water and dried. The organic phase was evaporated to dryness. The final product **34** was purified with flash chromatography. Yield: 170 mg (81%). Mp 73–75 °C. HESI-HRMS: calcd for $C_{24}H_{25}ON_5Cl$ $[M+H]^+$: 434.17421; found: 434.17311; delta = −2.54 ppm. ^{1}H NMR (DMSO-d_6, 500 MHz) δ 11.12 (br s, 1H), 8.0–8.0 (m, 1H), 7.58 (dd, 1H, J = 1.6, 8.4 Hz), 7.3–7.4 (m, 6H), 6.84 (s, 1H), 6.44 (ddd, 1H, J = 0.8, 2.0, 3.0 Hz), 3.86 (s, 3H), 3.5–3.7 (m, 4H), 3.53 (s, 2H), 2.4–2.5 (m, 4H); ^{13}C NMR (DMSO-d_6, 126 MHz) δ 160.1, 150.1, 136.9, 136.4, 135.6, 131.5, 130.6, 128.1, 127.7, 125.8, 123.6, 118.9, 116.8, 111.4, 102.8, 101.3, 60.7, 52.7, 52.0, 46.9, 41.5, 37.6.

*4.2.35. N-(1-methyl-1H-indol-5-yl)-5-{1-[(4-methylphenyl) methyl]piperidin-4-yl}-1,3,4-oxadiazole-2-carboxamide (**35**)*

*Step 1. Ethyl 1-[(4-methylphenyl)methyl]piperidine-4-carboxylate (**35b**).* In an argon atmosphere, ethyl piperidine-4-carboxylate (**35a**) (10 mL, 64.48 mmol) was dissolved in DMF (80 mL), K_2CO_3 (26.8 g, 3 eq) and 1-(bromomethyl)-4-methylbenzene (14.4 g 1.2 eq) were added. The reaction mixture was stirred at 80 °C overnight. After completion of the reaction, the mixture was filtered and then the filtrate was diluted with water (200 mL) and extracted with CH_2Cl_2 (3 × 50 mL). The combined organic phase was washed with brine, dried and evaporated to dryness. The residue was purified by column chromatography (eluent: CH_2Cl_2/MeOH = 98/2). Yield: 7.9 g (47%).

*Step 2. 1-[(4-Methylphenyl)methyl]piperidine-4-carbohydrazide (**35c**).* A suspension of **35b** (7.9 g, 28.9 mmol) and hydrazine hydrate (40 mL) was heated at 120 °C for 3 h. The reaction mixture was filtered and the resulting solid **35c** was washed with *n*-hexane (3 × 50 mL). Yield: 6.67 g (93%).

*Step 3. Ethyl 5-{1-[(4-methylphenyl)methyl]piperidin-4-yl}-1,3,4-oxadiazole-2-carboxylate (**35d**).* A flask was charged with **35c** (6.55 g, 26.48 mmol), CH_2Cl_2 (106 mL) and triethylamine (6.67 mL, 1.8 eq). The mixture was cooled down on an ice bath and ethyl oxalyl chloride (3.2 mL, 1.08 eq) was added dropwise (gas evolution) and the solution was stirred for 3.5 h at room temperature. The reaction mixture was washed with saturated $NaHCO_3$, dried and evaporated to dryness. The residue was dissolved in toluene (106 mL), pyridine (2.67 mL) and thionyl chloride (6.8 mL, 82.3 mmol, 3 eq) were added (gas evolution) and the reaction mixture was refluxed for 2 h. After ice-water cooling, the precipitated material was filtered off and washed with toluene. The crude product was dissolved in CH_2Cl_2 (200 mL) and the solution was washed with sat. $NaHCO_3$ solution (2 × 75 mL) and water (100 mL). The organic layer was dried and evaporated to dryness. Yield 5.24 g (60%).

Step 4. The hydrolysis of **35d** was accomplished the same way as in case of the preparation of **11c** resulting in **35e.**

*Step 5. N-(1-methyl-1H-indol-5-yl)-5-{1-[(4-methylphenyl)methyl] piperidin-4-yl}-1,3,4-oxadiazole-2-carboxamide (**35**).* To a solution of 1-methyl-1*H*-indol-5-amine (**11d**, 480 mg, 3.3 mmol) of in dry CH_2Cl_2 (130 mL) was added *N,N,N′,N′*-tetramethyl-*O*-(1*H*-benzotriazol-1-yl)uronium hexafluorophosphate (HBTU) (1040 mg, 2.75 mmol) and Et_3N (1920 μL, 5.0 eq) at room temperature under argon. The mixture was stirred for 20 min then was added 5-{1-[(4-methylphenyl)methyl]piperidin-4-yl}-1,3,4-oxadiazole-2-carboxylic acid (**35e**, 2960 mg, 2.75 mmol). The mixture was stirred at room temperature overnight. After the completion of the reaction (monitored by TLC) the reaction mixture was quenched by addition of water (50 mL), the organic layer was washed with saturated NaCl solution (50 mL) then the organic phase was dried over anhydrous Na_2SO_4, filtered and concentrated *in vacuo.* The residue was purified by column chromatography on silica gel eluting with CH_2Cl_2:methanol (95:5) to yield 300 mg (27%) of the title compound. LC-MS (ESI) *m/z* $[M+H]^+$ = 429.51. Mp 153–154 °C. HESI-HRMS: calcd for $C_{25}H_{28}O_2N_5$ $[M+H]^+$: 430.22375; found: 430.22251; delta = −2.89 ppm. ^{1}H NMR (DMSO-d_6, 400 MHz) δ 10.99 (s, 1H), 8.01 (d, 1H, J = 2.0 Hz), 7.5–7.5 (m, 1H), 7.4–7.5 (m, 1H), 7.34 (d, 1H, J = 3.1 Hz), 7.2–7.2

(m, 2H), 7.1–7.2 (m, 2H), 6.43 (d, 1H, $J = 3.1$ Hz), 3.79 (s, 3H), 3.45 (s, 2H), 3.08 (tt, 1H, $J = 3.9, 11.1$ Hz), 2.8–2.9 (m, 2H), 2.28 (s, 3H), 2.1–2.2 (m, 2H), 2.0–2.1 (m, 2H), 1.7–1.9 (m, 2H); ^{13}C NMR (DMSO-d_6, 101 MHz) δ 170.3, 158.8, 151.2, 135.8, 135.1, 133.9, 130.5, 129.4, 128.7, 128.6, 127.5, 115.7, 112.7, 109.5, 100.4, 61.9, 51.8, 32.5, 32.5, 28.8, 20.6.

4.2.36. 3-Methoxy-N-(1-methyl-1H-indol-5-yl)-2-[4-(4-methylphenoxy)piperidin-1-yl]propenamide (**36**)

Step 1. Methyl 3-methoxy-2-[4-(4-methylphenoxy)piperidin-1-yl*] propanoate (**36b**).* Under argon, a mixture of methyl 2-bromo-3-methoxypropanoate (**36a**, 250 mg, 1.3 mmol), 4-(4-methylphenoxy)piperidine hydrochloride (300 mg, 1.3 mmol) and potassium carbonate (360 mg, 2.6 mmol, 2 eq) in DMF (4 mL) was heated at 90 °C for 3 h. The reaction mixture was then cooled to room temperature, diluted with EtOAc (30 mL) and with water (20 mL) then two phases were separated. The aqueous layer was extracted with EtOAc (2 × 15 mL. The combined organic layer was washed with water (3 × 30 mL), dried over Na_2SO_4 and concentrated. The residue was purified by flash column chromatography on silica gel applying gradient elution with a 0–20% EtOAc - CH_2Cl_2 mixture as eluent to yield 246 mg (62%) of **36b.**

Step 2. 3-Methoxy-2-[4-(4-methylphenoxy)piperidin-1-yl*]propanoic acid (**36c**).* To a solution of methyl ester **36b** (237 mg, 0.77 mmol) in methanol (2.3 mL) was added water (2.75 mL) and lithium hydroxide monohydrate (163 mg, 3.88 mmol, 5 eq) and the mixture was stirred at room temperature for 4 h. Then lithium hydroxide monohydrate (40 mg, 0.953 mmol, 5.18 eq) was added again and the mixture stirred for further 90 min at room temperature. After the reaction had been completed, it was neutralized with 10% HCl solution. The mixture was evaporated under reduced pressure to obtain a crude product. It was dried at 40 °C for 24 h. The carboxylic acid **36c** which contains LiCl (393 mg) was used without purification in next step.

Step 3. 3-Methoxy-N-(1-methyl-1H-indol-5-yl*)-2-[4-(4-methylphenoxy)piperidin*-1-yl*]propenamide) (**36**).* To a solution of **36c** (393 mg, 0.77 mmol, contains LiCl) in DMF (12 mL) was added HATU (384 mg, 1 mmol, 1.31 eq) and 1-methyl-1*H*-indol-5-amine (**11d**, 146 mg, 1 mmol, 1.3 eq). The reaction mixture was cooled to 0 °C and then DIPEA (540 μL, 3.1 mmol, 4 eq) was added to the solution. After 1 h the reaction mixture was allowed to reach room temperature and stirred for 2 days. The reaction mixture was diluted with ethyl acetate (60 mL) and water (60 mL) then two phases were separated. The aqueous layer was extracted with ethyl acetate (2 × 20 mL). The combined organic layer was washed with water (5 × 50 mL), dried over Na_2SO_4 and concentrated. The residue was purified by column chromatography over silica gel, eluting with a mixture of cyclohexane and EtOAc (2:1) to get 0.22 g of crude product which was purified again by column chromatography over silica gel eluting with mixture of CH_2Cl_2 and EtOAc (20:1) to yield 70.5 mg (22%) of **36.** Mp 75–78 °C. HESI-HRMS: calcd for $C_{25}H_{32}O_3N_3$ $[M+H]^+$: 422.24382; found: 422.24266; delta = −2.74 ppm. ^{1}H NMR (DMSO-d_6, 400 MHz) δ 9.73 (s, 1H), 7.91 (d, 1H, $J = 2.0$ Hz), 7.3–7.4 (m, 1H), 7.3–7.3 (m, 2H), 7.0–7.1 (m, 2H), 6.8–6.8 (m, 2H), 6.3–6.4 (m, 1H), 4.28 (tt, 1H, $J = 3.7, 8.6$ Hz), 3.76 (s, 3H), 3.7–3.8 (m, 1H), 3.61 (dd, 1H, $J = 5.7, 9.7$ Hz), 3.4–3.4 (m, 1H), 3.27 (s, 3H), 2.9–3.0 (m, 1H), 2.8–2.9 (m, 1H), 2.6–2.7 (m, 1H), 2.4–2.5 (m, 1H), 2.21 (s, 3H), 1.9–2.0 (m, 1H), 1.5–1.7 (m, 2H); ^{13}C NMR (DMSO-d_6, 101 MHz) δ 168.1, 154.8, 133.2, 130.7, 130.1, 129.7, 129.0, 127.7, 115.7, 114.8, 110.9, 109.3, 100.1, 72.3, 70.4, 67.1, 58.2, 47.4, 47.3, 32.4, 31.2, 31.1, 20.0.

4.2.37. 3-(1-Methyl-1H-indol-5-yl)-1-{1-[(4-methylphenyl)methyl] piperidin-4-yl}urea (**37**)

The synthesis of 1-methyl-1*H*-indole-5-carbonyl azide **37a** is described in the following reference [57]. A solution of 1-methyl-1*H*-indole-5-carbonyl azide (**37a**, 425 mg, 2.13 mmol) in toluene (5 mL) was heated under reflux for an hour. A solution of 1-[(4-methylphenyl)methyl]piperidin-4-amine (**37b**, 434 mg, 2.13 mmol) in toluene (5 mL) was added and the heating was continued for 5 more hours. Upon cooling the reaction mixture to room temperature, the crystals separated were filtered off, washed with diethyl ether and dried to yield the title compound **37** (276 mg, 35%). Mp 187–189 °C. HESI-HRMS: calcd for $C_{23}H_{29}ON_4$ $[M+H]^+$: 377.23359; found: 377.23291; delta = −1.80 ppm. ^{1}H NMR (DMSO-d_6, 500 MHz) δ 8.08 (s, 1H), 7.59 (d, 1H, $J = 2.0$ Hz), 7.26 (d, 1H, $J = 8.8$ Hz), 7.22 (d, 1H, $J = 3.0$ Hz), 7.2–7.2 (m, 2H), 7.1–7.1 (m, 2H), 7.05 (dd, 1H, $J = 2.0, 8.8$ Hz), 6.28 (dd, 1H, $J = 0.8, 3.0$ Hz), 5.96 (d, 1H, $J = 7.7$ Hz), 3.72 (s, 3H), 3.4–3.5 (m, 1H), 3.40 (s, 2H), 2.6–2.7 (m, 2H), 2.28 (s, 3H), 2.0–2.1 (m, 2H), 1.7–1.8 (m, 2H), 1.3–1.4 (m, 2H); ^{13}C NMR (DMSO-d_6, 126 MHz) δ 154.9, 135.7, 135.4, 132.5, 132.4, 129.6, 128.7, 128.6, 128.0, 114.1, 109.3, 109.1, 99.7, 61.9, 51.6, 46.0, 32.4, 32.3, 20.6.

4.2.38. N-[(1-methyl-1H-indol-5-yl)methyl]-4-(4-methylphenoxy) benzamide (**38**)

To a solution of (2-methyl-1*H*-indol-5-yl)methanamine (**38a**, 160 mg, 1.0 mmol) in dry CH_2Cl_2 (100 mL) was added *N,N,N′,N′*-tetramethyl-*O*-(1*H*-benzotriazol-1-yl)uronium hexafluorophosphate (HBTU) (460 mg, 1.2 mmol) and Et_3N (360 μL, 2.5 eq) at room temperature under argon. The mixture was stirred for 20 min then was added 4-(4-methylphenoxy)benzoic acid (**38b**, 230 mg, 1.0 mmol). The mixture was stirred at room temperature overnight. After the completion of the reaction (monitored by TLC) the reaction mixture was quenched by addition of water (50 mL), the organic layer was washed with saturated NaCl solution (50 mL) then the organic phase was dried over anhydrous Na_2SO_4, filtered and concentrated *in vacuo*. The residue was purified by column chromatography on silica gel eluting with CH_2Cl_2 - methanol (9:1) to yield (168 mg, 45%) of the title compound. LC-MS (ESI) *m/z* $[M+H]^+ = 370.45$. Mp 139–140 °C. HESI-HRMS: calcd for $C_{24}H_{23}O_2N_2$ $[M+H]^+$: 371.17540; found: 371.17465; delta = −2.03 ppm. ^{1}H NMR (DMSO-d_6, 400 MHz) δ 8.92 (t, 1H, $J = 6.0$ Hz), 7.9–7.9 (m, 2H), 7.46 (d, 1H, $J = 0.7$ Hz), 7.37 (d, 1H, $J = 8.4$ Hz), 7.28 (d, 1H, $J = 3.1$ Hz), 7.2–7.3 (m, 2H), 7.13 (dd, 1H, $J = 1.6, 8.4$ Hz), 6.9–7.0 (m, 4H), 6.37 (dd, 1H, $J = 0.7, 3.1$ Hz), 4.54 (d, 2H, $J = 6.0$ Hz), 3.76 (s, 3H), 2.31 (s, 3H); ^{13}C NMR (DMSO-d_6, 101 MHz) δ 165.1, 159.8, 153.1, 135.4, 133.4, 130.5, 130.1, 129.7, 129.2, 128.8, 127.8, 120.9, 119.5, 118.8, 116.7, 109.3, 100.0, 42.9, 32.4, 20.2.

4.2.39. N-[(1-methyl-1H-indol-5-yl)methyl]-4-(4-methylphenoxy) piperidine-1-carboxamide (**39**)

The amide coupling was achieved in an analogous way as it is described in case of **44**. Yield 19.4%. Mp 132–133 °C. HESI-HRMS: calcd for $C_{23}H_{28}O_2N_3$ $[M+H]^+$: 378.21760; found: 378.21679; delta = −2.15 ppm. ^{1}H NMR (DMSO-d_6, 500 MHz) δ 7.40 (dd, 1H, $J = 0.8, 1.6$ Hz), 7.34 (d, 1H, $J = 8.4$ Hz), 7.27 (d, 1H, $J = 3.1$ Hz), 7.1–7.1 (m, 3H), 7.03 (t, 1H, $J = 5.8$ Hz), 6.8–6.9 (m, 2H), 6.36 (dd, 1H, $J = 0.8, 3.1$ Hz), 4.47 (tt, 1H, $J = 3.6, 8.5$ Hz), 4.31 (d, 2H, $J = 5.8$ Hz), 3.76 (s, 3H), 3.7–3.7 (m, 2H), 3.1–3.2 (m, 2H), 2.22 (s, 3H), 1.8–1.9 (m, 2H), 1.4–1.5 (m, 2H); ^{13}C NMR (DMSO-d_6, 126 MHz) δ 157.3, 154.7, 135.4, 131.4, 129.8, 129.6, 129.2, 127.7, 120.9, 118.6, 115.8, 109.1, 100.0, 72.2, 43.9, 40.9, 32.4, 30.5, 20.0.

4.2.40. N-[(1-methyl-1H-indol-5-yl)methyl]-4-[(4-methylphenyl) methyl]piperazine-1-carboxamide (**40**)

The amide coupling was achieved in an analogous way as it is described in case of **44**. Yield 20.0%. Mp 120–122 °C. HESI-HRMS: calcd for $C_{23}H_{29}ON_4$ $[M+H]^+$: 377.23359; found: 377.23292; delta = −1.77 ppm. ^{1}H NMR (DMSO-d_6, 400 MHz) δ 7.39 (dd, 1H, $J = 0.7, 1.5$ Hz), 7.33 (d, 1H, $J = 8.4$ Hz), 7.27 (d, 1H, $J = 3.1$ Hz), 7.2–7.2 (m, 2H), 7.1–7.2 (m, 2H), 7.06 (dd, 1H, $J = 1.5, 8.4$ Hz), 6.97 (t, 1H,

J = 5.6 Hz), 6.35 (dd, 1H, J = 0.7, 3.1 Hz), 4.29 (d, 2H, J = 5.6 Hz), 3.75 (s, 3H), 3.42 (br s, 2H), 3.2–3.3 (br m, 4H), 2.28 (s, 3H), 2.2–2.4 (br m, 4H); ^{13}C NMR (DMSO-d_6, 101 MHz) δ 157.3, 135.9, 135.4, 134.7, 131.3, 129.6, 128.8, 128.7, 127.7, 120.9, 118.6, 109.1, 99.9, 61.6, 52.3, 43.8, 43.3, 32.4, 20.6.

4.2.41. N-[(1-methyl-1H-indol-5-yl)methyl]-3-(4-methylphenoxy) azetidine-1-carboxamide (**41**)

The amide coupling was achieved in an analogous way as it is described in case of **44**. Yield 47.7%. Mp 141–142 °C. HESI-HRMS: calcd for $C_{21}H_{24}O_2N_3$ $[M+H]^+$: 350.18630; found: 350.18580; delta = −1.44 ppm. ^{1}H NMR (DMSO-d_6, 400 MHz) δ 7.40 (dd, 1H, J = 0.7, 1.6 Hz), 7.35 (d, 1H, J = 8.4 Hz), 7.28 (d, 1H, J = 3.1 Hz), 7.0–7.1 (m, 3H), 6.94 (t, 1H, J = 6.0 Hz), 6.7–6.8 (m, 2H), 6.36 (dd, 1H, J = 0.7, 3.1 Hz), 4.93 (tt, 1H, J = 3.9, 6.3 Hz), 4.2–4.3 (m, 4H), 3.76 (s, 3H), 3.73 (dd, 2H, J = 3.9, 9.5 Hz), 2.23 (s, 3H); ^{13}C NMR (DMSO-d_6, 101 MHz) δ 159.4, 154.1, 135.4, 130.9, 130.0, 129.8, 129.6, 127.8, 120.8, 118.6, 114.3, 109.2, 100.0, 65.4, 56.0, 43.2, 32.4, 20.0.

4.2.42. N-[(1-methyl-1H-indol-5-yl)methyl]-3-(4-methylphenoxy) pyrrolidine-1-carboxamide (**42**)

The amide coupling was achieved in an analogous way as it is described in case of **44**. Yield 57.0%. Mp 123–126 °C. HESI-HRMS: calcd for $C_{22}H_{26}O_2N_3$ $[M+H]^+$: 364.20195; found: 364.20116; delta = −2.18 ppm. ^{1}H NMR (DMSO-d_6, 400 MHz) δ 7.41 (dd, 1H, J = 0.7, 1.6 Hz), 7.33 (d, 1H, J = 8.4 Hz), 7.27 (d, 1H, J = 3.1 Hz), 7.0–7.1 (m, 3H), 6.8–6.9 (m, 2H), 6.69 (t, 1H, J = 6.0 Hz), 6.35 (dd, 1H, J = 0.7, 3.1 Hz), 4.9–5.0 (m, 1H), 4.29 (d, 2H, J = 6.0 Hz), 3.75 (s, 3H), 3.5–3.6 (m, 1H), 3.4–3.5 (m, 2H), 3.3–3.4 (m, 1H), 2.22 (s, 3H), 2.0–2.2 (m, 2H); ^{13}C NMR (DMSO-d_6, 101 MHz) δ 156.4, 154.6, 135.4, 131.4, 129.8, 129.5, 129.4, 127.7, 121.0, 118.6, 115.3, 109.1, 99.9, 75.6, 51.0, 43.6, 43.4, 32.4, 30.5, 20.0.

4.2.43. N-[(1-methyl-1H-indol-5-yl)methyl]-3-[(4-methylphenoxy) methyl]pyrrolidine-1-carboxamide (**43**)

The amide coupling was achieved in an analogous way as it is described in case of **44**. Yield 29.2%. Mp 121–122 °C. HESI-HRMS: calcd for $C_{23}H_{28}O_2N_3$ $[M+H]^+$: 378.21760; found: 378.21681; delta = −2.10 ppm. ^{1}H NMR (DMSO-d_6, 500 MHz) δ 7.41 (dd, 1H, J = 0.8, 1.5 Hz), 7.32 (d, 1H, J = 8.4 Hz), 7.26 (d, 1H, J = 3.1 Hz), 7.0–7.1 (m, 3H), 6.8–6.9 (m, 2H), 6.63 (t, 1H, J = 6.0 Hz), 6.34 (dd, 1H, J = 0.8, 3.1 Hz), 4.29 (d, 2H, J = 6.0 Hz), 3.92 (dd, 1H, J = 6.4, 9.5 Hz), 3.86 (dd, 1H, J = 7.5, 9.5 Hz), 3.75 (s, 3H), 3.49 (dd, 1H, J = 7.4, 10.2 Hz), 3.40 (ddd, 1H, J = 4.7, 8.1, 10.1 Hz), 3.26 (td, 1H, J = 7.6, 10.1 Hz), 3.12 (dd, 1H, J = 7.0, 10.2 Hz), 2.60 (dddddd, 1H, J = 6.4, 6.7, 7.0, 7.4, 7.5, 7.9 Hz), 2.22 (s, 3H), 2.00 (dddd, 1H, J = 4.7, 6.7, 7.6, 12.3 Hz), 1.70 (dddd, 1H, J = 7.6, 7.9, 8.1, 12.3 Hz); ^{13}C NMR (DMSO-d_6, 126 MHz) δ 156.4, 156.3, 135.4, 131.6, 129.7, 129.5, 129.1, 127.7, 121.0, 118.6, 114.2, 109.1, 99.9, 69.1, 48.3, 44.6, 43.5, 37.7, 32.4, 27.6, 20.0.

4.2.44. N-[(1-methyl-1H-indol-5-yl)methyl]-3-[(4-methylphenoxy) methyl]azetidine-1-carboxamide (**44**)

To a solution of (2-methyl-1*H*-indol-5-yl)methanamine (**38a**, 96 mg, 0.6 mmol) in CH_2Cl_2 (6 mL) was added DIPEA (155 mg, 208 μL, 1.2 mmol) and a solution of 4-nitrophenyl chloroformate (121 mg, 0.6 mmol) in CH_2Cl_2 (3 mL) at 0 °C under argon. The mixture was stirred for 1.5 h under these conditions. After the activation period 3-[(4-methylphenoxy)methyl]azetidine (**5d**, 106 mg, 0.6 mmol) in CH_2Cl_2 (3 mL) was added dropwise and the mixture was allowed to warm to room temperature and stirred at this temperature overnight. After the completion of the reaction (monitored by TLC), the mixture was concentrated *in vacuo*. The crude product was chromatographed on silica gel eluting with a mixture of cyclohexane and EtOAc and the resulted product was further purified on preparative TLC to yield 64 mg (26%) of the title compound **44**. LC-MS (ESI) m/z $[M+H]^+$= 418.3. Mp 129–130 °C. HESI-HRMS: calcd for $C_{22}H_{26}O_2N_3$ $[M+H]^+$: 364.20195; found: 364.20115; delta = 2.21 ppm. ^{1}H NMR (DMSO-d_6, 500 MHz) δ 7.40 (dd, 1H, J = 0.8, 1.6 Hz), 7.34 (d, 1H, J = 8.4 Hz), 7.27 (d, 1H, J = 3.0 Hz), 7.0–7.1 (m, 3H), 6.8–6.8 (m, 2H), 6.79 (t, 1H, J = 6.1 Hz), 6.36 (dd, 1H, J = 0.8, 3.0 Hz), 4.26 (d, 2H, J = 6.1 Hz), 4.06 (d, 2H, J = 6.6 Hz), 3.92 (t, 2H, J = 8.2 Hz), 3.76 (s, 3H), 3.63 (dd, 2H, J = 5.4, 8.2 Hz), 2.9–3.0 (m, 1H), 2.22 (s, 3H); ^{13}C NMR (DMSO-d_6, 126 MHz) δ 159.6, 156.3, 135.4, 131.2, 129.7, 129.6, 129.2, 127.8, 120.8, 118.6, 114.3, 109.2, 100.0, 69.4, 51.4, 43.1, 32.4, 27.7, 20.0.

4.2.45. N-[(1-methyl-1H-indol-5-yl)methyl]-1-[(4-methylphenyl) methyl]piperidine-4-carboxamide (**45**)

To a solution of (2-methyl-1*H*-indol-5-yl)methanamine (**38a**, 160 mg, 1.0 mmol) in dry CH_2Cl_2 (100 mL) was added *N,N,N′,N′*-tetramethyl-*O*-(1*H*-benzotriazol-1-yl)uronium hexafluorophosphate (HBTU) (460 mg, 1.2 mmol) and Et_3N (350 μL, 2.5 eq) at room temperature under argon. The mixture was stirred for 20 min then was added 1-[(4-methylphenyl)methyl]piperidine-4-carboxylic acid (260 mg, 1.0 mmol). The mixture was stirred at room temperature overnight. After the completion of the reaction (monitored by TLC) the reaction mixture was quenched by addition of water (50 mL), the organic layer was washed with saturated NaCl solution (50 mL) then the organic phase was dried over anhydrous Na_2SO_4, filtered and concentrated *in vacuo*. The residue was purified by column chromatography on silica gel eluting with CH_2Cl_2 - methanol (9:1) to yield (68 mg 19%) of the title compound. LC-MS (ESI) m/z $[M+H]^+$ = 375.51. Mp 170–172 °C. HESI-HRMS: calcd for $C_{24}H_{30}ON_3$ $[M+H]^+$: 376.23834; found: 376.23761; delta = −1.94 ppm. ^{1}H NMR (DMSO-d_6, 500 MHz) δ 8.19 (t, 1H, J = 5.9 Hz), 7.37 (dd, 1H, J = 0.8, 1.6 Hz), 7.35 (d, 1H, J = 8.4 Hz), 7.28 (d, 1H, J = 3.1 Hz), 7.1–7.2 (m, 2H), 7.1–7.1 (m, 2H), 7.03 (dd, 1H, J = 1.6, 8.4 Hz), 6.36 (dd, 1H, J = 0.8, 3.1 Hz), 4.30 (d, 2H, J = 5.9 Hz), 3.75 (s, 3H), 3.38 (s, 2H), 2.8–2.8 (m, 2H), 2.27 (s, 3H), 2.13 (tt, 1H, J = 4.3, 11.2 Hz), 1.8–1.9 (m, 2H), 1.5–1.7 (m, 4H); ^{13}C NMR (DMSO-d_6, 126 MHz) δ 174.1, 135.7, 135.4, 135.3, 130.0, 129.7, 128.59, 128.62, 127.8, 120.8, 118.7, 109.3, 100.0, 62.0, 52.6, 42.2, 42.0, 32.4, 28.6, 20.6.

4.2.46. (1S,4S)–N-[(1-methyl-1H-indol-5-yl)methyl]-4-(4-methylphenoxy)cyclohexane-1-carboxamide (**46**)

To a suspension of 4-(4-methylphenoxy)cyclohexane-1-carboxylic acid (80 mg, 0.34 mmol) and (2-methyl-1*H*-indol-5-yl) methanamine (**38a**, 56.4 mg, 1.0 mmol) in dry DMF (3 mL) was added HATU (129.6 mg, 0.34 mmol, 1.0 eq) and DIPEA (119 μL, 2 eq) at room temperature. The mixture was shaken at RT overnight. After the completion of the reaction (monitored by TLC) the mixture was diluted with brine and extracted with EtOAc (3 × 20 mL). The combined organic phase was washed with brine (3 × 20 mL), dried over anhydrous Na_2SO_4, filtered and concentrated *in vacuo*. The residue was purified by flash chromatography on silica gel eluting with 10% EtOAc in CH_2Cl_2. The desired product **46** was crystallized from Et_2O as well to yield 93.4 mg (73%) of the title compound as white solid. LC-MS (ESI) m/z $[M+H]^+$ = 376.49. Mp 149–151 °C. HESI-HRMS: calcd for $C_{24}H_{29}O_2N_2$ $[M+H]^+$: 377.22235; found: 377.22170; delta = −1.74 ppm. ^{1}H NMR (DMSO-d_6, 500 MHz) δ 8.19 (t, 1H, J = 5.9 Hz), 7.39 (dd, 1H, J = 0.8, 1.6 Hz), 7.36 (d, 1H, J = 8.4 Hz), 7.28 (d, 1H, J = 3.1 Hz), 7.1–7.1 (m, 2H), 7.04 (dd, 1H, J = 1.6, 8.4 Hz), 6.8–6.8 (m, 2H), 6.36 (dd, 1H, J = 0.8, 3.1 Hz), 4.49 (tt, 1H, J = 2.5, 4.2 Hz), 4.32 (d, 2H, J = 5.9 Hz), 3.76 (s, 3H), 2.27 (tt, 1H, J = 3.3, 11.0 Hz), 1.9–1.9 (m, 2H), 1.7–1.8 (m, 2H), 1.5–1.6 (m, 4H); ^{13}C NMR (DMSO-d_6, 126 MHz) δ 174.4, 154.8, 135.4, 130.1, 129.8, 129.7, 129.0, 127.8, 120.8, 118.7, 115.9, 109.3, 100.0, 70.6, 42.5, 42.2, 32.4, 28.3, 23.6, 20.0.

*4.2.47. N-[(1-methyl-1H-indol-5-yl)methyl]-1-[(4-methylphenyl) methyl]piperidine-3-carboxamide (**47**)*

To a suspension of *N*-benzylpiperidine-4-carboxylic acid (20 mg, 0.38) and of (2-methyl-1*H*-indol-5-yl)methanamine (**38a**, 61.4 mg, 1.0 mmol) in dry DMF (3 mL) was added HATU (145.6 mg, 0.38 mmol, 1.0 eq) and DIPEA (133.4 μL, 2 eq) at room temperature. The mixture was shaken at room temperature overnight. After the completion of the reaction (monitored by TLC) the mixture was diluted with brine and extracted with EtOAc (3 × 20 mL). The combined organic phase was washed with brine (3 × 20 mL), dried over anhydrous Na_2SO_4, filtered and concentrated *in vacuo*. The residue was purified by flash chromatography on silica gel eluting with 10% EtOAc in CH_2Cl_2. The desired product **47** was crystallized from Et_2O as well to yield 65.2 mg (45%) of the title compound as white solid. LC-MS (ESI) *m/z* $[M+H]^+$ = 375.51. Mp 226–228 °C. HESI-HRMS: calcd for $C_{24}H_{30}ON_3$ $[M+H]^+$: 376.23834; found: 376.23746; delta = −2.34 ppm. ^{1}H NMR (DMSO-d_6, 500 MHz) δ 8.2–8.5 (br m, 1H), 7.3–7.4 (m, 2H), 7.29 (d, 1H, *J* = 3.0 Hz), 7.0–7.2 (br m, 4H), 7.01 (dd, 1H, *J* = 1.5, 8.4 Hz), 6.35 (dd, 1H, *J* = 0.8, 3.0 Hz), 4.29 (br d, 2H, *J* = 5.8 Hz), 3.76 (s, 3H), 3.38 (br s, 2H), 2.7–2.8 (br m, 1H), 2.6–2.7 (br m, 1H), 2.3–2.5 (br m, 1H), 2.26 (br s, 3H), 2.0–2.2 (br m, 1H), 1.9–2.0 (br m, 1H), 1.7–1.8 (br m, 1H), 1.5–1.7 (br m, 1H), 1.4–1.5 (br m, 2H); ^{13}C NMR (DMSO-d_6, 126 MHz) δ 173.0, 135.8, 135.5, 135.0, 129.8, 129.7, 128.7, 128.6, 127.8, 120.9, 118.8, 109.4, 100.0, 62.1, 55.6, 53.0, 42.4, 42.3, 32.4, 27.1, 24.0, 20.6.

*4.2.48. 3-[(4-Fluorophenoxy)methyl]-N-[(1-methyl-1H-indol-5-yl) methyl]azetidine-1-carboxamide (**48**)*

Intermediate 3-[(4-fluorophenoxy)methyl]azetidine was synthesized in an analogous way as it was described in case of **5d**. The amide coupling was achieved in an analogous way as it is described in case of **44**. Yield 26.1%. Mp 166–168 °C. HESI-HRMS: calcd for $C_{21}H_{23}O_2N_3F[M+H]^+$: 368.17688; found: 368.17621; delta = −1.82 ppm. ^{1}H NMR (DMSO-d_6, 500 MHz) δ 7.40 (dd, 1H, *J* = 0.8, 1.5 Hz), 7.34 (d, 1H, *J* = 8.4 Hz), 7.27 (d, 1H, *J* = 3.1 Hz), 7.1–7.1 (m, 2H), 7.07 (dd, 1H, *J* = 1.5, 8.4 Hz), 6.9–7.0 (m, 2H), 6.80 (t, 1H, *J* = 6.1 Hz), 6.36 (dd, 1H, *J* = 0.8, 3.1 Hz), 4.27 (d, 2H, *J* = 6.1 Hz), 4.08 (d, 2H, *J* = 6.6 Hz), 3.93 (t, 2H, *J* = 8.2 Hz), 3.76 (s, 3H), 3.64 (dd, 2H, *J* = 5.4, 8.2 Hz), 2.9–3.0 (m, 1H); ^{13}C NMR (DMSO-d_6, 126 MHz) δ 159.6, 156.5 (d, *J* = 235.8 Hz), 154.8 (d, *J* = 1.7 Hz), 135.4, 131.2, 129.6, 127.8, 120.9, 118.6, 115.72 (d, *J* = 22.9 Hz), 115.71 (d, *J* = 8.1 Hz), 109.2, 100.0, 70.0, 51.4, 43.1, 32.4, 27.7.

*4.2.49. 3-[(4-Chlorophenoxy)methyl]-N-[(1-methyl-1H-indol-5-yl) methyl]azetidine-1-carboxamide (**49**)*

Intermediate 3-[(4-chlorophenoxy)methyl]azetidine was synthesized in an analogous way as it was described in case of **5d**. The amide coupling was achieved in an analogous way as it is described in case of **44**. Mp 171–172 °C. HESI-HRMS: calcd for $C_{21}H_{23}O_2N_3Cl$ $[M+H]^+$: 384.14733; found: 384.14687; delta = −1.20 ppm. ^{1}H NMR (DMSO-d_6, 500 MHz) δ 7.40 (dd, 1H, *J* = 0.8, 1.6 Hz), 7.34 (d, 1H, *J* = 8.4 Hz), 7.3–7.3 (m, 2H), 7.28 (d, 1H, *J* = 3.0 Hz), 7.07 (dd, 1H, *J* = 1.6, 8.4 Hz), 6.9–7.0 (m, 2H), 6.80 (t, 1H, *J* = 6.1 Hz), 6.36 (dd, 1H, *J* = 0.8, 3.0 Hz), 4.26 (d, 2H, *J* = 6.1 Hz), 4.10 (d, 2H, *J* = 6.6 Hz), 3.93 (t, 2H, *J* = 8.2 Hz), 3.76 (s, 3H), 3.64 (dd, 2H, *J* = 5.4, 8.2 Hz), 2.9–3.0 (m, 1H); ^{13}C NMR (DMSO-d_6, 126 MHz) δ 159.6, 157.3, 135.4, 131.2, 129.6, 129.1, 127.8, 124.3, 120.9, 118.6, 116.2, 109.2, 100.0, 69.7, 51.4, 43.1, 32.4, 27.6.

*4.2.50. N-[(1-methyl-1H-indol-5-yl)methyl]-3-[(4-methoxyphenoxy)methyl]azetidine-1-carboxamide (**50**)*

Intermediate 3-[(4-methoxyphenoxy)methyl]azetidine was synthesized in an analogous way as it was described in case of **5d**. The amide coupling was achieved in an analogous way as it is described in case of **44**. Yield 42.6%. Mp 118–119 °C. HESI-HRMS: calcd for $C_{22}H_{26}O_3N_3$ $[M+H]^+$: 380.19687; found: 380.19596; delta = −2.39 ppm. ^{1}H NMR (DMSO-d_6, 500 MHz) δ 7.40 (dd, 1H, *J* = 0.8, 1.6 Hz), 7.34 (d, 1H, *J* = 8.4 Hz), 7.27 (d, 1H, *J* = 3.1 Hz), 7.07 (dd, 1H, *J* = 1.6, 8.4 Hz), 6.8–6.9 (m, 4H), 6.79 (t, 1H, *J* = 6.0 Hz), 6.36 (dd, 1H, *J* = 0.8, 3.1 Hz), 4.26 (d, 2H, *J* = 6.0 Hz), 4.03 (d, 2H, *J* = 6.6 Hz), 3.92 (t, 2H, *J* = 8.2 Hz), 3.76 (s, 3H), 3.69 (s, 3H), 3.63 (dd, 2H, *J* = 5.4, 8.2 Hz), 2.9–2.9 (m, 1H); ^{13}C NMR (DMSO-d_6, 126 MHz) δ 159.6, 153.4, 152.5, 135.4, 131.2, 129.6, 127.8, 120.9, 118.6, 115.4, 114.5, 109.2, 100.0, 69.9, 55.3, 51.4, 43.1, 32.4, 27.8.

*4.2.51. N-[(1-methyl-1H-indol-5-yl)methyl]-3-{[4-(trifluoromethoxy)phenoxy]methyl} azetidine-1-carboxamide (**51**)*

Intermediate 3-{[4-(trifluoromethoxy)phenoxy]methyl}azetidine was synthesized in an analogous way as it was described in case of **5d**. The amide coupling was achieved in an analogous way as it is described in case of **44**. Yield 30.9%. Mp 181–182 °C. HESI-HRMS: calcd for $C_{22}H_{23}O_3N_3F_3$ $[M+H]^+$: 434.16860; found: 434.16766; delta = −2.17 ppm. ^{1}H NMR (DMSO-d_6, 500 MHz) δ 7.41 (dd, 1H, *J* = 0.8, 1.5 Hz), 7.34 (d, 1H, *J* = 8.4 Hz), 7.3–7.3 (m, 3H), 7.07 (dd, 1H, *J* = 1.5, 8.4 Hz), 7.0–7.1 (m, 2H), 6.81 (t, 1H, *J* = 6.0 Hz), 6.36 (dd, 1H, *J* = 0.8, 3.1 Hz), 4.27 (d, 2H, *J* = 6.0 Hz), 4.13 (d, 2H, *J* = 6.6 Hz), 3.94 (t, 2H, *J* = 8.2 Hz), 3.76 (s, 3H), 3.65 (dd, 2H, *J* = 5.4, 8.2 Hz), 2.9–3.0 (m, 1H); ^{13}C NMR (DMSO-d_6, 126 MHz) δ 159.6, 157.3, 141.7 (q, *J* = 1.8 Hz), 135.4, 131.2, 129.6, 127.7, 122.4, 120.9, 120.1 (q, *J* = 255.1 Hz), 118.6, 115.6, 109.2, 99.9, 69.8, 51.4, 43.2, 32.4, 27.6.

*4.2.52. N-[(1-methyl-1H-indol-5-yl)methyl]-3-(phenoxymethyl) azetidine-1-carboxamide (**52**)*

Intermediate 3-phenoxymethyl]azetidine was synthesized in an analogous way as it was described in case of **5d**. The amide coupling was achieved in an analogous way as it is described in case of **44**. Yield 17.0%. Mp 143–144 °C. HESI-HRMS: calcd for $C_{21}H_{24}O_2N_3$ $[M+H]^+$: 350.18630; found: 350.18555; delta = −2.15 ppm. ^{1}H NMR (DMSO-d_6, 500 MHz) δ 7.40 (dd, 1H, *J* = 0.8, 1.6 Hz), 7.34 (d, 1H, *J* = 8.4 Hz), 7.3–7.3 (m, 3H), 7.07 (dd, 1H, *J* = 1.6, 8.4 Hz), 6.9–7.0 (m, 3H), 6.80 (t, 1H, *J* = 6.0 Hz), 6.36 (dd, 1H, *J* = 0.8, 3.1 Hz), 4.27 (d, 2H, *J* = 6.1 Hz), 4.10 (d, 2H, *J* = 6.6 Hz), 3.94 (t, 2H, *J* = 8.2 Hz), 3.76 (s, 3H), 3.65 (dd, 2H, *J* = 5.4, 8.2 Hz), 2.9–3.0 (m, 1H); ^{13}C NMR (DMSO-d_6, 126 MHz) δ 159.6, 158.4, 135.4, 131.2, 129.6, 129.4, 127.8, 120.9, 120.6, 118.6, 114.4, 109.2, 100.0, 69.2, 51.4, 43.1, 32.4, 27.7.

*4.2.53. 3-[(4-Cyanophenoxy)methyl]-N-[(1-methyl-1H-indol-5-yl) methyl]azetidine-1-carboxamide (**53**)*

Intermediate 3-[(4-cyanophenoxy)methyl]azetidine was synthesized in an analogous way as it was described in case of **5d**. The amide coupling was achieved in an analogous way as it is described in case of **44**. Yield 11.0%. Mp 184–185 °C. HESI-HRMS: calcd for $C_{22}H_{23}O_2N_4$ $[M+H]^+$: 375.18155; found: 375.18071; delta = −2.25 ppm. ^{1}H NMR (DMSO-d_6, 500 MHz) δ 7.7–7.8 (m, 2H), 7.40 (dd, 1H, *J* = 0.8, 1.5 Hz), 7.34 (d, 1H, *J* = 8.4 Hz), 7.28 (d, 1H, *J* = 3.0 Hz), 7.1–7.1 (m, 2H), 7.07 (dd, 1H, *J* = 1.5, 8.4 Hz), 6.82 (t, 1H, *J* = 6.0 Hz), 6.36 (dd, 1H, *J* = 0.8, 3.0 Hz), 4.27 (d, 2H, *J* = 6.0 Hz), 4.22 (d, 2H, *J* = 6.6 Hz), 3.94 (t, 2H, *J* = 8.2 Hz), 3.76 (s, 3H), 3.65 (dd, 2H, *J* = 5.4, 8.2 Hz), 2.9–3.0 (m, 1H); ^{13}C NMR (DMSO-d_6, 126 MHz) δ 161.9, 159.6, 135.4, 134.1, 131.2, 129.6, 127.8, 120.9, 119.0, 118.6, 115.5, 109.2, 102.8, 100.0, 69.8, 51.3, 43.2, 32.4, 27.5.

*4.2.54. N-[(1-methyl-1H-indol-5-yl)methyl]-3-{[4-(trifluoromethyl)phenoxy]methyl}azetidine-1-carboxamide (**54**)*

Intermediate 3-{[4-(trifluoromethyl)phenoxy]methyl}azetidine was synthesized in an analogous way as it was described in case of **5d**. The amide coupling was achieved in an analogous way as it is described in case of **44**. Yield 25.8%. Mp 218–219 °C. HESI-HRMS: calcd for $C_{22}H_{23}O_2N_3F_3$ $[M+H]^+$: 418.17369; found: 418.17275;

delta = −2.24 ppm. ^{1}H NMR (DMSO-d_6, 500 MHz) δ 7.6–7.7 (m, 2H), 7.41 (dd, 1H, J = 0.8, 1.6 Hz), 7.34 (d, 1H, J = 8.4 Hz), 7.28 (d, 1H, J = 3.1 Hz), 7.1–7.2 (m, 2H), 7.07 (dd, 1H, J = 1.6, 8.4 Hz), 6.82 (t, 1H, J = 6.1 Hz), 6.36 (dd, 1H, J = 0.8, 3.1 Hz), 4.27 (d, 2H, J = 6.0 Hz), 4.21 (d, 2H, J = 6.6 Hz), 3.95 (t, 2H, J = 8.2 Hz), 3.76 (s, 3H), 3.66 (dd, 2H, J = 5.4, 8.2 Hz), 2.9–3.0 (m, 1H); ^{13}C NMR (DMSO-d_6, 126 MHz) δ 161.3, 159.6, 135.4, 131.2, 129.6, 127.8, 126.8 (q, J = 3.8 Hz), 124.5 (q, J = 270.8 Hz), 121.1 (q, J = 32.0 Hz), 120.9, 118.6, 114.9, 109.2, 100.0, 69.7, 51.3, 43.2, 32.4, 27.5.

4.2.55. N-[(1H-indol-5-yl)methyl]-3-{[4-(trifluoromethyl)phenoxy] methyl}azetidine-1-carboxamide (**55**)

Intermediate 3-{[4-(trifluoromethyl)phenoxy]methyl}azetidine was synthesized in an analogous way as it was described in case of **5d**. The amide coupling was achieved in an analogous way as it is described in case of **44**. Yield 39%. Mp 128–130 °C. HESI-HRMS: calcd for $C_{21}H_{21}O_2N_3F_3$ $[M+H]^+$: 404.158040; found: 404.15699; delta = −2.59 ppm. ^{1}H NMR (DMSO-d_6, 500 MHz) δ 10.98 (br s, 1H), 7.6–7.7 (m, 2H), 7.4–7.4 (m, 1H), 7.3–7.3 (m, 2H), 7.1–7.2 (m, 2H), 7.01 (dd, 1H, J = 1.6, 8.4 Hz), 6.80 (t, 1H, J = 6.0 Hz), 6.36 (ddd, 1H, J = 0.9, 2.0, 3.0 Hz), 4.26 (d, 2H, J = 6.0 Hz), 4.21 (d, 2H, J = 6.6 Hz), 3.95 (t, 2H, J = 8.2 Hz), 3.66 (dd, 2H, J = 5.4, 8.2 Hz), 2.9–3.0 (m, 1H); ^{13}C NMR (DMSO-d_6, 126 MHz) δ 161.3, 159.6, 134.8, 131.0, 127.4, 126.8 (q, J = 3.8 Hz), 125.3, 124.5 (q, J = 271.2 Hz), 121.1 (q, J = 31.9 Hz), 120.8, 118.3, 114.9, 110.9, 100.7, 69.7, 51.3, 43.3, 27.5.

4.3. Biological assay methods

Methods used in the present article were already described in detail in our previous paper [41]. Here, only a brief summary is given.

4.3.1. In vitro methods using cells expressing human α7 nACh receptors

4.3.1.1. Cell culture. Generation of the recombinant HEK293-based cell line stably expressing both the target hCHRNA7 protein and the hRIC3 chaperone (α7-nAChR-HEK cells) was already described [41]. Cells were maintained in DMEM (Gibco) supplemented by 10% FBS (Gibco), 2 mM glutamine (Sigma), 50 μg/mL hygromycin B, 400 μg/mL G418 and 1% penicillin-streptomycin antimycotic solution (Sigma/Merck). Cells were split twice a week by trypsinization.

4.3.1.2. Fluorometric $[Ca^{2+}]_i$-assay on cells expressing human α7 nAChR. Orthosteric agonists of the α7 nAChR (*e.g.* PNU-282987) *per se* evoke no Ca^{2+}-influx in most *in vitro* cellular systems, unless they are co-applied with PAMs that concurrently hinder the channel desensitization. However, in the presence of agonists, PAMs with such characteristics result in robust and concentration-dependent Ca^{2+}-influx (it must be noted that the assay is insensitive to PAMs lacking effect on channel desensitization).

Flp-In HEK293 cells stably expressing the human α7 nAChR and the RIC-3 chaperon were cultured in DMEM (Gibco) supplemented by 10% FBS (Gibco), 2 mM glutamine (Sigma), 50 μg/mL hygromycin B, 400 μg/mL G418 and 1% penicillin-streptomycin antimycotic solution (Sigma). Cells were split 1:3–4 twice a week by trypsinization. For the $[Ca^{2+}]_i$ measurements, cells were seeded onto 96-well microplates at a density of 60.000 cells/well and maintained overnight in a tissue culture incubator at 37 °C under an atmosphere of 95% air and 5% CO_2. Before the $[Ca^{2+}]_i$ measurement, 50 μL of the growth medium was aspirated with a cell washer (BioTek Elx405UCVWS, Biotek, Winooski, VT, USA), then 50 μL/well Calcium 5 kit (diluted 2-fold in assay buffer containing 140 mM NaCl, 5 mM KCl, 10 mM HEPES, 2 mM $MgCl_2$, 2 mM $CaCl_2$, 10 mM glucose and 2 mM probenecid; pH = 7.4) was added manually using an 8-channel pipette. After an incubation period of 20 min at 37 °C, 50 μL/well assay buffer containing vehicle (Dimethyl sulfoxide [DMSO], 4% added) or test compounds (4 × of the final concentration) were added. Cells were then incubated for an additional 10 min at 37 °C.

Baseline and agonist-evoked $[Ca^{2+}]_i$-changes were measured with a FlexStation II[96] (Molecular Devices, San Jose, CA). Fluorescence measurements were carried out at 37 °C. The dye was excited at 485 nm, emission was sampled at 525 nm at 1.4-s intervals. Baseline was recorded for 20 s followed by agonist stimulation. 50 μL 4 × concentrated agonist (PNU-282987, 1 μM) solution was added to all wells using the pipettor of FlexStation II and fluorescence was monitored for an additional 20 s. Final DMSO concentration was 1% for all treatments. To achieve this, a series of DMSO stock solutions were prepared from all test compounds. These stocks were stored under 0 °C and were further diluted in assay buffer to obtain the desired final concentration immediately before the measurement. Positive control: PNU-120596, 2.5 μM.

Results were expressed as ΔF/F values using SoftMax Pro software (Molecular Devices), where F was the resting fluorescence preceding agonist application and ΔF was the increase in fluorescence at a given time (ΔF = maximum fluorescence intensity values after stimulation minus average fluorescence intensity values before stimulation). In all experiments, all treatments were measured in multiple wells in parallel, and the mean ΔF/F values were used for analysis. ΔF/F data were converted to corrected % response values by normalizing responses to the control PNU-120596 response. In each individual experiment, the EC_{50} and E_{max} values were determined from 4-parameter sigmoidal concentration-response curves fitted to the corrected response data using SoftMax Pro, with the lower asymptote fixed to zero. EC_{50} and E_{max} values from individual experiments were averaged and presented as mean ± SD.

4.3.1.3. High-throughput screening. The HTS was run on the full Corporate screening library utilizing a FLIPR $[Ca^{2+}]_i$ assay on Flp-In HEK293 cells stably expressing human α7 nAChR and RIC-3. The average Z' for the screen was 0.86 with a statistically derived activity threshold of 7.3% at 10 μM, resulting in 0.3% active rate. Actives were tested for specificity on a HEK-293 cell line expressing TRPM8 receptors and for solution integrity using LC/MS.

4.3.1.4. Patch clamp measurements. Channel physiology of α7 nAChRs was studied by automated whole-cell patch clamp QPatch-HTX, Sophion) in single-cell mode. Whole-cell patch recordings were made from α7-nAChR-HEK cells 2 days after plating at a holding potential of −80 mV at room temperature. Inward currents were evoked by 3-s-long application of 10 mM choline with 2–4 min intervals in the absence, then in the presence of test compounds and recorded at 10 kHz sampling frequency. Solutions containing the test compounds were applied to the cells for 6–10 min. The control solution contained the same concentration of the vehicle (0.1% DMSO) as the solutions of the test compound. Peak amplitudes of current evoked by choline was measured from the baseline current. The fold increase (FI) value was calculated from the ratio of the peak current amplitudes evoked by choline in the presence or in the absence of the test compounds. EC_{50} values were calculated from FI values by testing several concentrations of the test compound.

For electrophysiological measurements using $GABA_A$ receptors, HEK293 cells stably expressing human α1β3γ2 and α5β3γ2 $GABA_A$Rs (Eurofins, CYL3053 and CYL3073) were investigated by whole-cell patch clamp using the QPatch-HTX automated patch clamp system in single-cell mode. Whole-cell patch clamp recordings were made from cells 2–4 days after plating at a holding potential of −80 mV at room temperature. Inward currents were

evoked by 3-s-long application of the agonist 1 μM GABA with 2-4-min intervals in the absence, then and in the presence of test compound. Solutions containing the test compound were applied to the cells for 7–10 min. The control solution contained the same concentration of the vehicle (0.1% DMSO) as the solutions of the test compound. Peak amplitudes of current evoked by GABA was measured from the baseline current. The modulation values were calculated from the comparison of peak currents in the absence and in the presence of the test compound.

For hERG measurement, CHO cells stably expressing Kv11.1 potassium channel (hERG; bSys) were investigated by whole-cell patch clamp using the QPatch-HTX automated patch clamp system in voltage-clamp mode at room temperature. Cells were held at −80 mV and hERG currents were activated by a +20 mV prepulse of 5 s duration followed by a step to −40 mV for 1.5 s. The current traces were recorded, and the peak of the tail current evoked by the −40 mV step was measured as test parameter. Solutions containing the compounds were applied to the cells for 7–10 min. The control solution contained the same concentration of the vehicle (0.1 or 0.3% DMSO) as the solution of the test compounds. The inhibition was calculated from the peak tail currents in the presence and absence of the test compound.

4.3.1.5. Selectivity. Selected compounds were subjected to Eurofins Panlabs Taiwan Ltd. using the Lead Profiling Screen panel comprising binding and enzyme assays for 68 common molecular targets including human recombinant receptors, transporters, enzymes and channels (if a human recombinant target was not available, compounds were tested on the corresponding rodent receptor). Compounds were tested at the nominal test concentration of 10 μM; inhibition values higher than 70% were considered as major.

4.3.1.6. Human, rat and mouse liver microsomal stability assays. *In vitro* metabolic stability was assessed using human (Xenotech, LLC, USA), Wistar rat and NMRI mouse (*In vitro* Metabolism Research, Gedeon Richter Plc, Hungary) liver microsomes. Test compounds were incubated at 1 μM initial test concentration at longest up to 40 min with the liver microsomes (0.5 mg/mL). *In vitro* intrinsic clearance (CL_{int}, μL/min/mg protein) was calculated using the basic concept of clearance prediction [58] according to the following equations: $CL_{int} = V_{max}/K_M$, or if $S \ll K_M$, $CL_{int} = V/S$; V_{max} = maximal rate of enzyme reaction; K_M = affinity constant of substrate concentration; V = actual rate of enzyme reaction under first order conditions, S = substrate concentration in the incubations.

4.3.1.7. Permeability assay. Bi-directional permeability ($Papp_{A-B}$ and $Papp_{B-A}$) and efflux ratio (PDR = $Papp_{B-A}/Papp_{A-B}$) of test compounds were measured using vinblastine-treated Caco-2 (VB-Caco-2) cells [43]. Briefly, the permeability of test compounds (at 1 or 10 μM) were measured in the apical-to-basolateral (A-B) and basolateral-to-apical (B-A) directions in HBSS-HEPES (Hank's Buffered Salt Solution containing 25 mM HEPES) using iso-pH conditions (pH 7.4_A–7.4_B) at 37 °C with moderate shaking (120 rpm). The incubations with test compounds were performed at longest up to 120 min, using appropriate duration of time determined based on preliminary studies for each compound tested. Samples were analyzed using HPLC or UHPLC-MS/MS.

4.3.1.8. Ames test. Mutagenic potential of test compounds was tested by measuring their ability to induce reverse mutations at selected loci of several strains of *Salmonella typhimurium* and *Escherichia coli* by Toxi-Coop Zrt. (Balatonfüred, Hungary). The experiment (a micro-scale Fluctuation Test) was carried out using histidine-requiring auxotroph strains of *Salmonella typhimurium* (*Salmonella typhimurium* TA98, TA100, TA1535 and TA1537), and the tryptophan-requiring auxotroph strain of *Escherichia coli* (*Escherichia coli* WP2 uvrA) in the presence and absence of a metabolic activation system, which is a cofactor-supplemented post-mitochondrial S9 fraction prepared from rat liver.

4.3.2. In vivo methods

4.3.2.1. Place recognition (Y maze) test. Animal maintenance and experiments were conducted in accordance with the National Institute of Health Guide for the Care and Use of Laboratory Animals. All procedures using animals were approved by the local ethics committee (Institutional Animal Welfare Committee of Gedeon Richter Plc. and conformed to the rules and principles of the European Animal Protection Directives (Directive 2010/63/EU).

The task was carried out in a transparent plexiglass Y-maze (each arm has a length of 40 cm, an inner width of 11 cm and a height of 30 cm). Numerous visual cues were placed around the arms and were kept constant during the experiment. The test consisted of two trials (T1 and T2) separated by an intertrial interval of 30 min. Male NMRI mice (Toxicoop, Hungary) were placed in the starting arm (F = familiar arm) of the maze at the beginning of each trial. In T1, one of the symmetric arms of the maze was closed (it will be novel in T2, N = novel arm) and the animals could explore the maze for 5 min (acquisition phase). In T2, mice had free access to all three arms for 2 min (retrieval phase). Test compounds were administered 30 min before T1; scopolamine (1 mg/kg, ip.) was administered after the acquisition trial at a volume of 0.1 mL/10 g. The time spent with exploration in the novel and familiar arms during T2 was measured and recognition index [RI=(N/N+F) × 100)] was calculated for the animals. Differences between the RI values for each group were evaluated by MANOVA, followed by Duncan post hoc test.

4.3.2.2. Novel object recognition (NOR) test. Before testing, male Hannover Wistar rats (Toxicoop, Hungary) were habituated to the apparatus (65 × 45 × 45 cm grey box with sawdust on its floor) in a 3-min session. The test consisted of a sample trial (T1) and a recognition trial (T2), separated by an inter-trial interval of 24 h, during which time rats were replaced into their home cages. In the sample trial (T1), two identical objects were placed in opposite rear corners of the box and could be explored for 3 min. In the recognition trial (T2), one of the identical objects was replaced by a new object. The exploration time for the familiar (F) and the new (N) object was detected in a 3-min session and RI values were calculated as follows: RI=(N/N+F) × 100). Test compounds were administered orally (standard NOR test), 30 min before the sample and recognition trials. Differences between RI values were evaluated by ANOVA, followed by Duncan or LSD post hoc tests. For the comparison of the experimental groups, nonparametric Kruskal-Wallis analysis was used followed by multiple comparisons of mean ranks for all groups as a post hoc test using Statistica 8 software.

4.3.2.3. Rodent touch screen test. Lister Hooded rats (n = 36) were kept in reversed light-dark cycle (lights on from 6:00 p.m. to 6:00 a.m.) and were tested during their active period. At the time of testing they were ca. 8-month-old, weighing 400–500 g. To provide sufficient motivation, food restriction was applied maintaining their 85% of free-feeding body weight. The visual discrimination procedure was carried out in automated Bussey-Saksida touch screen chambers (Campden Instruments Ltd, [59]). Pharmacological testing was preceded by several weeks of learning to perceptually discriminate two images and associating which image is rewarded: Touching the correct stimulus on the screen is rewarded

with food but the incorrect stimulus is non-rewarded, punished with a timeout (5 s) and a flash of light. Incorrect responses are followed by correction trials (re-presentation of the same image-position configuration) until the correct stimulus is chosen. Correction trials do not count towards the session trial limit and the accuracy score. Rats performed the training schedules on daily sessions (50 trials in 30 min; inter trial interval (ITI): 20 s) until stable performance level was reached (50 trials completed with correct % $\geq$ 80%, on two consecutive days). Rats' baseline performance level was recorded one day before pharmacological challenges, when rats were tested under the same experimental conditions as on the treatment day, except for drug administration. Taking account of individual differences in cognitive performance, we applied Δ correct % as the main parameter, which is the difference of correct % on baseline day distracted from the correct % on treatment day of each rat. On the treatment day, each rat received different doses of the test compound (0.3, 1, 3 and 10 mg/kg dissolved in 5% Tween 80) or vehicle orally 45 min before testing, and scopolamine hydrobromide (0.075 mg/kg, corrected for the base, dissolved in saline), or vehicle subcutaneously 20 min before testing. Three testing sessions were carried out allowing 7 days for washing out between them. Between subject design was applied, and rats were not allowed to get into the same treatment group during the sessions. Data were evaluated by non-parametric Kruskal-Wallis test followed by Dunn's post hoc comparisons.

4.3.2.4. Pharmacokinetics. Following the place recognition and the novel object recognition tests, brain and blood samples were taken from the animals (NMRI mice and Wistar rats) participated in the studies for assessment of the test compounds exposure. The compounds were administered intraperitoneally in 5% Tween 80/PBS, the dosing volume was 10 mL/kg to mice and 2 mL/kg to rats. The sampling was done at approx. 1 h (mice) or 35 min (rats). Plasma samples were gained by centrifugation, brain homogenate samples were prepared by homogenizing the whole brain in deionized water (brain: water = 1: 2.5, w/w). Plasma and brain homogenate samples were analyzed after protein precipitation using HPLC-MS/MS method.

Declaration of competing interest

The authors declare that they have no known competing financial interests or personal relationships that could have appeared to influence the work reported in this paper.

Acknowledgements

The whole study was financially supported by Gedeon Richter Plc., Hungary and Orion Corporation, Finland. The authors acknowledge the contribution of Dr. Hugh Chapman in QPatch experiments regarding the measurements in α3β4 nACh-expressing cells.

Appendix A. Supplementary data

Supplementary data to this article can be found online at https://doi.org/10.1016/j.ejmech.2021.113560.

References

[1] A. Karlin, M.H. Akabas, Toward a structural basis for the function of nicotinic acetylcholine receptors and their cousins, Neuron 15 (1995) 1231–1244, https://doi.org/10.1016/0896-6273(95)90004-7.
[2] D. Paterson, A. Nordberg, Neuronal nicotinic receptors in the human brain, Prog. Neurobiol. 61 (2000) 75–111, https://doi.org/10.1016/s0301-0082(99)00045-3.
[3] P.B. Clarke, R.D. Schwartz, S.M. Paul, C.B. Pert, A. Pert, Nicotinic binding in rat brain: autoradiographic comparison of [^{3}H]acetylcholine, [^{3}H]nicotine and [^{125}I]-alpha-bungarotoxin, J. Neurosci. 5 (1985) 1307–1315, https://doi.org/10.1523/JNEUROSCI.05-05-01307.1985.
[4] C. Gotti, M. Zoli, F. Clementi, Brain nicotinic acetylcholine receptors: native subtypes and their relevance, Trends Pharmacol. Sci. 27 (1997) 482–491, https://doi.org/10.1016/j.tips.2006.07.004.
[5] Z. Gil, B.W. Connors, Y. Amitai, Differential regulation of neocortical synapses by neuromodulators and activity, Neuron 19 (1997) 679–686, https://doi.org/10.1016/S0896-6273(00)80380-3.
[6] J.P. Changeux, D. Bertrand, P.J. Corringer, S. Dehaene, S. Edelstein, C. Léna, N. Le Novère, L. Marubio, M. Picciotto, M. Zoli, Brain nicotinic receptors: structure and regulation, role in learning and reinforcement, Brain Res. Rev. 26 (1998) 198–216, https://doi.org/10.1016/s0165-0173(97)00040-4.
[7] C. Gotti, D. Fornasari, F. Clementi, Human neuronal nicotinic receptors, Prog. Neurobiol. 53 (2006) 199–237, https://doi.org/10.1016/s0301-0082(97)00034-8.
[8] O.V. Poisik, J.X. Shen, S. Jones, J.L. Yakel, Functional alpha7-containing nicotinic acetylcholine receptors localize to cell bodies and proximal dendrites in the rat substantia nigra pars reticulata, J. Physiol. 586 (2008) 1365–1378, https://doi.org/10.1113/jphysiol.2007.149963.
[9] E. Tribollet, D. Bertrand, A. Marguerat, M. Raggenbass, Comparative distribution of nicotinic receptor subtypes during development, adulthood and aging: an autoradiographic study in the rat brain, Neuroscience 124 (2004) 405–420, https://doi.org/10.1016/j.neuroscience.2003.09.028.
[10] E.M. Ullian, P.B. Sargent, Pronounced cellular diversity and extrasynaptic location of nicotinic acetylcholine receptor subunit immunereactivities in the chicken pretectum, J. Neurosci. 15 (1995) 7012–7023, https://doi.org/10.1523/JNEUROSCI.15-11-07012.1995.
[11] B. Lendvai, E.S. Vizi, Nonsynaptic chemical transmission through nicotinic acetylcholine receptors, Physiol. Rev. 88 (2008) 333–349, https://doi.org/10.1152/physrev.00040.2006.
[12] R. Fabian-Fine, P. Skehel, M.L. Errington, H.A. Davies, E. Sher, M.G. Stewart, A. Fine, Ultrastructural distribution of the α7 nicotinic acetylcholine receptor subunit in rat hippocampus, J. Neurosci. 21 (2001) 7993–8003, https://doi.org/10.1523/JNEUROSCI.21-20-07993.2001.
[13] J.A. Dani, D. Bertrand, Nicotinic acetylcholine receptors and nicotinic cholinergic mechanisms of the central nervous system, Annu. Rev. Pharmacol. Toxicol. 47 (2007) 699–729, https://doi.org/10.1146/annurev.pharmtox.47.120505.105214.
[14] J.K. Gill, M. Savolainen, G.T. Young, R. Zwart, E. Sher, N.S. Millar, Agonist activation of α7 nicotinic acetylcholine receptors via an allosteric transmembrane site, Proc. Natl. Acad. Sci. U.S.A. 108 (2011) 5867–5872, 10.1073%2Fpnas.1017975108.
[15] O. Delbono, M. Gopalakrishnan, M. Renganathan, L.M. Monteggia, M.L. Messi, J.P. Sullivan, Activation of the recombinant human α7 nicotinic acetylcholine receptor significantly raises intracellular free calcium, J. Pharmacol. Exp. Therapeut. 280 (1997) 428–438, https://doi.org/10.1016/S0014-5793(97)00600-5.
[16] A. Schrattenholz, E.F. Pereira, U. Roth, K.H. Weber, E.X. Albuquerque, A. Maelicke, Agonist responses of neuronal nicotinic acetylcholine receptors are potentiated by a novel class of allosterically acting ligands, Mol. Pharmacol. 49 (1996) 1–6.
[17] N.G. Castro, E.X. Albuquerque, Brief-lifetime, fast-inactivating ion channels account for the α-bungarotoxin-sensitive nicotinic response in hippocampal neurons, Neurosci. Lett. 164 (1993) 137–140, https://doi.org/10.1016/0304-3940(93)90876-M.
[18] M. Alkondon, S. Reinhardt, C. Lobron, B. Hermsen, A. Maelicke, E.X. Albuquerque, Diversity of nicotinic acetylcholine receptors in rat hippocampal neurons. II. The rundown and inward rectification of agonist-elicited whole-cell currents and identification of receptor subunits by in situ hybridization, J. Pharmacol. Exp. Therapeut. 271 (1994) 494–506.
[19] T. Collins, G.T. Young, N.S. Millar, Competitive binding at a nicotinic receptor transmembrane site of two α7-selective positive allosteric modulators with differing effects on agonist-evoked desensitization, Neuropharmacology 61 (2011) 1306–1313, 10.1016%2Fj.neuropharm.2011.07.035.
[20] A.J. Harvey, T.D. Avery, L. Schaeffer, C. Joseph, B.C. Huff, R. Singh, C. Morice, B. Giethlen, A.A. Grishin, C.J. Coles, P. Kolesik, S. Wagner, E. Andriambeloson, B. Huyard, E. Poiraud, D. Paul, S.M. O'Connor, Discovery of BNC375, a potent, selective, and orally available type I positive allosteric modulator of α7 nAChRs, ACS Med. Chem. Lett. 10 (2019) 754–760, https://doi.org/10.1021/acsmedchemlett.9b00001.
[21] J.H. Grønlien, M. Håkerud, H. Ween, K. Thorin-Hagene, C.A. Briggs, M. Gopalakrishnan, J. Malysz, Distinct profiles of alpha7 nAChR positive allosteric modulation revealed by structurally diverse chemotypes, Mol. Pharmacol. 72 (2007) 715–724, https://doi.org/10.1124/mol.107.035410.
[22] M.S. Thomsen, H.H. Hansen, D.B. Timmerman, J.D. Mikkelsen, Cognitive improvement by activation of alpha7 nicotinic acetylcholine receptors: from animal models to human pathophysiology, Curr. Pharmaceut. Des. 16 (2010) 323–343, https://doi.org/10.2174/138161210790170094.
[23] S. Sahdeo, T. Wallace, R. Hirakawa, F. Knoflach, D. Bertrand, H. Maag, D. Misner, G.C. Tombaugh, L. Santarelli, K. Brameld, M.E. Milla, D.C. Button, Characterization of RO5126946, a novel a7 nicotinic acetylcholine receptor–positive allosteric modulator, J. Pharmacol. Exp. Therapeut. 350 (2014) 455–468, https://doi.org/10.1124/jpet.113.210963.

[24] B. Lendvai, F. Kassai, Á. Szájli, Zs Némethy, α7 Nicotinic acetylcholine receptors and their role in cognition, Brain Res. Bull. 93 (2013) 86–96, https://doi.org/10.1016/j.brainresbull.2012.11.003.
[25] A. Nikiforuk, T. Kos, A. Potasiewicz, P. Popik, Positive allosteric modulation of alpha 7 nicotinic acetylcholine receptors enhances recognition memory and cognitive flexibility in rats, Eur. Neuropsychopharmacol 25 (2015) 1300–1313, https://doi.org/10.1016/j.euroneuro.2015.04.018.
[26] P.M. Callahan, E.J. Hutchings, N.J. Kille, J.M. Chapman, A.V. Terry Jr., Positive allosteric modulator of α7 nicotinic-acetylcholine receptors, PNU-120596 augments the effects of donepezil on learning and memory in aged rodents and non-human primates, Neuropharmacology 67 (2013) 201–212, https://doi.org/10.1016/j.neuropharm.2012.10.019.
[27] A.S. Lewis, G.I. van Schalkwyk, M.H. Bloch, Alpha-7 nicotinic agonists for cognitive deficits in neuropsychiatric disorders: a translational meta-analysis of rodent and human studies, Prog. Neuro-Psychopharmacol. Biol. Psychiatry 75 (2017) 45–53, https://doi.org/10.1016/j.pnpbp.2017.01.001.
[28] K. Antonio-Tolentino, C.R. Hopkins, Selective α7 nicotinic receptor agonists and positive allosteric modulators for the treatment of schizophrenia – a review, Expet Opin. Invest. Drugs 29 (2020) 603–610, https://doi.org/10.1080/13543784.2020.1764938.
[29] R.S.E. Keefe, H.A. Meltzer, N. Dgetluck, M. Gawryl, G. Koenig, H.J. Moebius, I. Lombardo, D.C. Hilt, Randomized, double-blind, placebo-controlled study of encenicline, an α7 nicotinic acetylcholine receptor agonist, as a treatment for cognitive impairment in schizophrenia, Neuropsychopharmacology 40 (2015) 3053–3060, https://doi.org/10.1038/npp.2015.176.
[30] T. Dinklo, H. Shaban, J.W. Thuring, H. Lavreysen, K.E. Stevens, L. Zheng, C. Mackie, C. Grantham, I. Vandenberk, G. Meulders, L. Peeters, H. Verachtert, E. De Prins, A.S.J. Lesage, Characterization of 2-[[4-fluoro-3-(trifluoromethyl) phenyl]amino]- 4-(4-pyridinyl)-5-thiazolemethanol (JNJ-1930942), a novel positive allosteric modulator of the α7 nicotinic acetylcholine receptor, J. Pharmacol. Exp. Therapeut. 336 (2011) 560–574, https://doi.org/10.1124/jpet.110.173245.
[31] H.J. Ng, E.R. Whittemore, M.B. Tran, D.J. Hogenkamp, R.S. Broide, T.B. Johnstone, L. Zheng, K.E. Stevens, K.W. Gee, Nootropic α7 nicotinic receptor allosteric modulator derived from GABAA receptor modulators, Proc. Natl. Acad. Sci. U.S.A. 104 (2007) 8059–8064, https://doi.org/10.1073/pnas.0701321104.
[32] R. Faghih, S.M. Gopalakrishnan, J.H. Grønlien, J. Malysz, C.A. Briggs, C. Wetterstrand, H. Ween, M.P. Curtis, K.A. Sarris, G.A. Gfesser, R. El-Kouhen, H.M. Robb, R.J. Radek, K.C. Marsh, W.H. Bunnelle, M. Gopalakrishnan, Discovery of 4-(5-(4-chloro phenyl)-2-methyl-3-propionyl-1H-pyrrol-1-yl)benzenesulfonamide (A-867744) as a novel positive allosteric modulator of the α7 nicotinic acetylcholine receptor, J. Med. Chem. 52 (2009) 3377–3384, https://doi.org/10.1021/jm9003818.
[33] D.B. Timmermann, J.H. Grønlien, K.L. Kohlhaas, E.Ø. Nielsen, E. Dam, T.D. Jørgensen, P.K. Ahring, D. Peters, D. Holst, J.K. Christensen, J. Malysz, C.A. Briggs, M. Gopalakrishnan, G.M. Olsen, An allosteric modulator of the α7 nicotinic acetylcholine receptor possessing cognition-enhancing properties in vivo, J. Pharmacol. Exp. Therapeut. 323 (2007) 294–307, https://doi.org/10.1124/jpet.107.120436.
[34] R.S. Hurst, M. Hajos, M. Raggenbass, T.M. Wall, N.R. Higdon, J.A. Lawson, K.L. Rutherford-Root, M.B. Berkenpas, W.E. Hoffmann, D.W. Piotrowski, V.E. Groppi, G. Allaman, R. Ogier, S. Bertrand, D. Bertrand, S. Arneric, A novel positive allosteric modulator of the α7 neuronal nicotinic acetylcholine receptor: in vitro and in vivo characterization, J. Neurosci. 25 (2005) 4396–4405, https://doi.org/10.1523/JNEUROSCI.5269-04.2005.
[35] R.L. Papke, S. Garai, C. Stokes, N.A. Horenstein, A.D. Zimmerman, K.A. Abboud, G.A. Thakur, Differing activity profiles of the stereoisomers of 2,3,5,6TMP-TQS, a putative silent allosteric modulator of a7 nAChR, Mol. Pharmacol. 98 (2020) 292–302, https://doi.org/10.1124/mol.120.119958.
[36] A. Potasiewicz, M. Hołuj, T. Kos, P. Popik, H.R. Arias, A. Nikiforuk, 3-Furan-2-yl-N-p-tolyl-acrylamide, a positive allosteric modulator of the a7 nicotinic receptor, reverses schizophrenia-like cognitive and social deficits in rats, Neuropharmacology 113 (2017) 188–197, https://doi.org/10.1016/j.neuropharm.2016.10.002.
[37] B. Balsera, J. Mulet, S. Sala, F. Sala, R. Torre-Martínez, S. Gonzalez-Rodríguez, A. Plata, L. Naesens, A. Fernandez-Carvajal, A. Ferrer-Montiel, M. Criado, M.J. Perez de Vega, R. Gonzalez-Muniz, Amino acid and peptide prodrugs of diphenylpropanones positive allosteric modulators of a7 nicotinic receptors with analgesic activity, Eur. J. Med. Chem. 143 (2018) 157–165, https://doi.org/10.1016/j.ejmech.2017.10.083.
[38] B.E. Neilsen, S. Stabile, C. Vitale, C. Bouzat, Design, Synthesis and functional evaluation of a novel series of phosphonate-functionalized 1,2,3-triazoles as positive allosteric modulators of α7 nicotinic acetylchloline receptors, ACS Chem. Neurosci. 11 (2020) 2688–2704, https://doi.org/10.1021/acschemneuro.0c00348.
[39] Y. Li, L. Sun, T. Yang, W. Jiao, J. Tang, X. Huang, Z. Huang, Y. Meng, L. Luo, X. Wang, X. Bian, F. Zhang, K. Wang, Q. Sun, Design and Synthesis of novel positive allosteric modulators of α7 nicotinic acetylcholine receptors with the ability to rescue auditory gating deficit in mice, J. Med. Chem. 62 (2019) 159–173, https://doi.org/10.1021/acs.jmedchem.7b01492.
[40] N. Sinha, N.P. Karche, M.K. Verma, S.S. Walunj, P.B. Nigade, G. Jana, S.P. Kurhade, A.K. Hajare, A.R. Tilekar, G.R. Jadhav, B.R. Thube, J.S. Shaikh, S. Balgude, L.B. Singh, V. Mahimane, S.K. Adurkar, G. Hatnapure, F. Raje, Y. Bhosale, D. Bhanage, S. Sachchidanand, R. Dixit, R. Gupta, A.M. Bokare, M. Dandekar, A. Bharne, M. Chatterjee, S. Desai, S. Koul, D. Modi, M. Mehta, V. Patil, M. Singh, J. Gundu, R.N. Goel, C. Shah, S. Sharma, D. Bakhle, R.K. Kamboj, V.P. Palle, Discovery of novel, potent, brain-permeable, and orally efficacious positive allosteric modulator of α7 nicotinic acetylcholine receptor [4-(5-(4-chlorophenyl)-4-methyl-2-propionylthiophen-3-yl)benzenesulfonamide]: structure–activity relationship and preclinical characterization, J. Med. Chem. 63 (2020) 944–960, https://doi.org/10.1021/acs.jmedchem.9b01569.
[41] I. Ledneczki, P. Tapolcsányi, E. Gábor, A. Visegrády, M. Vass, J. Éles, P. Holm, A. Horváth, A. Pocsai, S. Mahó, I. Greiner, B. Krámos, Z. Béni, J. Kóti, A.E. Káncz, M. Thán, S. Kolok, J. Laszy, O. Balázs, Gy Bugovits, J. Nagy, M. Vastag, Á. Szájli, É. Bozó, Gy Lévay, B. Lendvai, Z. Némethy, Discovery of novel positive allosteric modulators of the α7 nicotinic acetylcholine receptor: scaffold hopping approach, Eur. J. Med. Chem. 214 (2021) 113189, https://doi.org/10.1016/j.ejmech.2021.113189.
[42] Gedeon Richter Plc, Substituted (Aza)indole Derivatives, 2018. WO2020012424A1.
[43] E. Hellinger, M.L. Bakk, P. Pócza, K. Tihanyi, M. Vastag, Drug penetration model of vinblastine-treated Caco-2 cultures, Eur. J. Pharmaceut. Sci. 41 (2010) 96–106, https://doi.org/10.1016/j.ejps.2010.05.015.
[44] R. Benigni, C. Bossa, Mechanisms of chemical carcinogenicity and mutagenicity: a review with implications for predictive toxicology, Chem. Rev. 111 (2011) 2507–2536, https://doi.org/10.1021/cr100222q.
[45] G. Patlewicz, N. Jeliazkova, R.J. Safford, A.P. Worth, B. Aleksiev, An evaluation of the implementation of the Cramer classification scheme in the Toxtree software, SAR QSAR Environ. Res. 19 (2008) 495–524, https://doi.org/10.1080/10629360802083871.
[46] G.T. Young, R. Zwart, A.S. Walker, E. Sher, N.S. Millar, Potentiation of 7 nicotinic acetylcholine receptors via an allosteric transmembrane site, Proc. Natl. Acad. Sci. U.S.A. 105 (2008) 14686–14691, https://doi.org/10.1073/pnas.0804372105.
[47] A. Chatzidaki, J.M. D'Oyley, J.K. Gill-Thind, T.D. Sheppard, N.S. Millar, The influence of allosteric modulators and transmembrane mutations on desensitization and activation of α7 nicotinic acetylcholine receptors, Neuropharmacology 97 (2015) 75–85, https://doi.org/10.1016/j.neuropharm.2015.05.006.
[48] J. Newcombe, A. Chatzidaki, T.D. Sheppard, M. Topf, N.S. Millar, Diversity of nicotinic acetylcholine receptor positive allosteric modulators revealed by mutagenesis and a revised structural model, Mol. Pharmacol. 93 (2017) 128–140, https://doi.org/10.1124/mol.117.110551.
[49] N.A. Horenstein, R.L. Papke, A.R. Kulkarni, G.U. Chaturbhuj, C. Stokes, K. Manther, G.A. Thakur, Critical molecular determinants of α7 nicotinic acetylcholine receptor allosteric activation, J. Biol. Chem. 291 (2016) 5049–5067, https://doi.org/10.1074/jbc.m115.692392.
[50] C.M. Noviello, A. Gharpure, N. Mukhtasimova, R. Cabuco, L. Baxter, D. Borek, S.M. Sine, R.E. Hibbs, Structure and gating mechanism of the α7 nicotinic acetylcholine receptor, Cell 184 (2021) 2121–2134, https://doi.org/10.1016/j.cell.2021.02.049.
[51] W. Sherman, T. Day, M.P. Jacobson, R.A. Friesner, R. Farid, Novel procedure for modeling ligand/receptor induced fit effects, J. Med. Chem. 49 (2006) 534–553, https://doi.org/10.1021/jm050540c.
[52] R.A. Friesner, J.L. Banks, R.B. Murphy, T.A. Halgren, J.J. Klicic, D.T. Mainz, M.P. Repasky, E.H. Knoll, M. Shelley, J.K. Perry, D.E. Shaw, P. Francis, P.S. Shenkin, Glide: a new approach for rapid, accurate docking and scoring. 1. Method and assessment of docking accuracy, J. Med. Chem. 47 (2004) 1739–1749, https://doi.org/10.1021/jm0306430.
[53] T.A. Halgren, R.B. Murphy, R.A. Friesner, H.S. Beard, L.L. Frye, W.T. Pollard, J.L. Banks, Glide: a new approach for rapid, accurate docking and scoring. 2. Enrichment factors in database screening, J. Med. Chem. 47 (2004) 1750–1759, https://doi.org/10.1021/jm030644s.
[54] Crown Biosciences Inc, Cyclopropanecarboxamido-substitute Aromatic Compounds as Anti-tumor Agents, 2014. WO2014/000418A1.
[55] K. Mahal, M. Resch, R. Ficner, R. Schobert, B. Biersack, T. Mueller, ChemMedChem 9 (2014) 847–854, https://doi.org/10.1002/cmdc.20130053.
[56] M.D. Fryzuk, B. Bosnich, Asymmetric Synthesis. Preparation of chiral methyl chiral lactic acid by catalytic asymmetric hydrogenation, J. Am. Chem. Soc. 101 (1979) 3043–3049, https://doi.org/10.1021/ja00505a035.
[57] J.H. Rigby, P.J. Burke, Synthesis of highly substituted indole alkaloid species via [4+1] cyclization of nucleophilic carbenes and indole isocyanates, Heterocycles 67 (2006) 643–653, https://doi.org/10.3987/COM-05-S(T)38.
[58] A. Rane, G.R. Wilkinson, D.G. Shand, Prediction of hepatic extraction ratio from *in vitro* measurement of intrinsic clearance, J. Pharmacol. Exp. Therapeut. 200 (1977) 420–424.
[59] T.J. Bussey, T.L. Padain, E.A. Skillings, B.D. Winters, A.J. Morton, L.M. Saksida, The touchscreen cognitive testing method for rodents: how to get the best out of your rat, Learn. Mem. 15 (2008) 516–523. http://doi:10.1101/lm.987808.